POLITECNICO DI MILANO

Scuola di Ingegneria Industriale e dell'Informazione

Corso di Laurea in Ingegneria Chimica

SYNTHESIS OF 1,3-DIIODO-5,5-DIMETHYLHYDANTOIN. A GREEN AND COST EFFECTIVE CONTINUOUS FLOW PROCESS.

Relatore: Dr. Cristian GAMBAROTTI

Relatore: Prof. Hans-René BJØRSVIK

Tesi di Laurea di:

Marta FERRERI

783522

Anno Accademico 2012 – 2013

Acknowledgements

Dire grazie a tutte le persone che hanno avuto il merito di formare ciò che oggi sono e che hanno collaborato al raggiungimento di questo traguardo, è veramente difficile da fare in così poche righe.

Grazie Prof. Hans Renè Bjorsvik per tutto il tempo che mi ha dedicato, per gli insegnamenti, i consigli e la possibilità di scoprire e vivere Bergen.
Grazie Cristian per le risposte che hai sempre saputo darmi, rassicurandomi in momenti di incertezza, per l'entusiasmo e la positività che mi hai trasmesso quotidianamente.

Grazie genitori per essere certezze nella mia vita. Grazie papi per avermi contagiato con la costanza e l'impegno che hai sempre dimostrato nel voler raggiungere i tuoi traguardi. Grazie mami per vivere le mie gioie e dolori come fossero tuoi e per avermi sempre regalato stabilità tutte le volte che ho perso l'equilibrio. Grazie sorelle, Dania per essere un caldo rifugio, Mati per la tua forza e saggezza che non mi hai mai fatto mancare. Grazie Mara perché mi hai sempre tra i tuoi pensieri, grazie ai miei nonni per i quali rimarrò sempre un passerotto e a tutta la mia famiglia. Vi voglio bene.
Grazie a tutti quelli che mi hanno sopportato e supportato in questi anni.
Fabri, perché appena t'ho conosciuto sono caduta ai tuoi piedi, Ciro, per le risate senza fine che mi hai regalato, Dade, per la poesia che vedi nel mondo e nella gente, Nati, per la tua purezza, Ali, per la tua costante ricerca di meraviglia, Eli, per le esperienze matte che abbiamo condiviso, Sara, per essere stata presente anche se lontana, Lucio, per la colonna sonora, Lollo, Anna, Nena, Giulia, Fra, Ale, Miri, Mauro, Giamma, Giammi, Tommi, perché facendo parte della mia vita mi avete reso speciale.
Grazie Edo per aver dato il giusto pepe alla mie giornate.
Grazie Elvi, per essere basca, Joan, per i nostri tessuti, Maria, Sergii, Audun e gli altri compagni di università, per avermi sempre aiutato e per aver riempito i miei ultimi mesi.
Grazie a tutti le belle persone che mi hanno regalato positività, chi con un sorriso, chi con un unicorno (in ordine sparso e con qualche inevitabile dimenticanza): Michi, Lollo, Carlo, Fede, Loti, Guido, Teo, Miguel, Mari, Samu, Leo, Andre, Angelo, Dave, Ale, Amani, Amedeo, Gudny, Martin, Sebastian, Saskia. Sophie, Ele.

Grazie Bergen, per avere conciliato il mio studio con la sua pioggia e donato la pace con le sue montagne.

Table of Contents

Abstract

1,3-Diiodo-5,5-dimethylhydantoin was recently revealed to be an excellent iodinating reagent that perform an instantaneous iodination of a series of N-heterocycles. The iodination proceeds with high chemoselectivity and yield with an improved environmental profile with respect to the atom economy compared with other halogenating processes.

A green and economical process for the synthesis of this relative high-priced reagent was designed, developed, scaled-up in batch mode and subsequently transferred to continuous flow mode using the multi-jet oscillating disk (MJOD) flow reactor system. The scale-up and optimization of the batch process were performed by mean of multivariate mathematical and statistical methods, methodology also known as chemometrics. The devised optimized batch process was successfully transferred to the MJOD continuous flow platform. The implementation of the batch mode process to a continuous flow mode process resulted in a highly selective and high throughput (47 g h^{-1} corresponding to a reactor residence time of 9 min) process that provides a practical quantitative yield of the desired iodination reagent. The environmental and economical benefits reached by using the MJOD flow reactor rig were benchmarked with the batch-protocol. A final test run of 8 h, provided an isolated yield of 375 g of high quality 1,3-diiodo-5,5-dimethylhydantoin.

Abstract

Recenti studi hanno dimostrato le potenzialità della 1,3-diiodo-5,5-dimetilidantoina (DIH) in iodurazioni ad alta resa, selettività e ridotto impiego di solventi tossici, caratteristiche che la rendono interessante anche nell'ambito della "green chemistry".

Durante il lavoro di Tesi, è stata messa a punto ed ottimizzata una nuova metodologia di sintesi della DIH a basso impatto ambientale ed economicamente conveniente a partire dalla 5,5-dimetilidantoina (DMH). Il processo ha permesso di ottenere in buone rese DIH, prodotto ad elevato valore aggiunto rispetto al substrato di partenza (DMH: 7.32 €/100g vs DIH:1426 €/100g).

Dopo una fase preliminare di progettazione sperimentale tramite metodi statistici (statistical experimental design) che ha coinvolto l'analisi di diverse procedure e la scelta e la definizione dei livelli d'indagine per ciascuna variabile coinvolta nel processo, l'analisi sperimentale è iniziata con l'ottimizzazione di un reattore batch in microscala (<1 g). I modelli multivariati di regressione, utilizzati per determinare le condizioni ottimali durante questa fase, sono stati applicati anche per determinare il punto di funzionamento ottimale del processo decuplicato in volume. La procedura ottimizzata è stata poi trasferita in continuo mediante l'utilizzo di un micro-reattore recentemente brevettato, multi-jet oscillating disk (MJOD) flow reactor. I benefici che si sono potuti ottenere grazie a questa innovativa tecnologia sono stati notevoli. Andando ad ottimizzare fattori cruciali della presente sintesi, quali scambio materiale e termico e tempo di residenza, e successivo work-up del prodotto, il MJOD-reactor ha consentito un ulteriore e significativo miglioramento della resa, della selettività e della produttività del processo (47 g h^{-1}). Durante una singola reazione di 8 ore sono stati filtrati in continuo circa 375 g di 1,3-diiodo-5,5-dimetilidantoina di alta qualità, quantitativo paragonabile alla totalità di prodotto ottenuto durante le indagini in batch (300 g). La qualità e l'attività iodurante della DIH sintetizzata sono state poi testate con successo nella di-iodurazione dell'imidazolo.

1. Introduction

Halogenated organic compounds play a key role in the chemical industry and for a series of application areas in the society. A wide variety of industrial chemicals is created by adding halogens (F, Cl, Br and I) to organic compounds. [1]

Because of their great reactivity, the free halogen elements are not found in nature. The name halogen derives from the Greek roots hal- ("salt") and -gen ("to produce"), because they all produce sodium salts of similar properties. Another important generalization that can be made about the halogen elements is that they are all oxidizing agents.[2] The oxidation in a cellular system leads to the destruction of microorganism in a direct contact mechanism[3] and can be used to inactivate pathogenic micro-organism such as bacteria and virus particles.[4] For this reason halogenated compounds, especially brominated and chlorinated, have been employed as biocides for industrial and recreational water uses for many years. An overview of such halogenated compounds is provided in Chart 1.

Chart 1. Halogenated chemical compounds for different application areas: 1,2-dichloroethane DCA **1**, vinyl chloride monomer VCM **2**, polyvinyl chloride PVC **3**, Chlorine dioxide **4**, Trichloroethylene TCE **5**, Perchloroethylene PCE **6**, chloro benzene **7**, dichlorodiphenyltrichloroethane DDT **8**, PBDEs **9**.

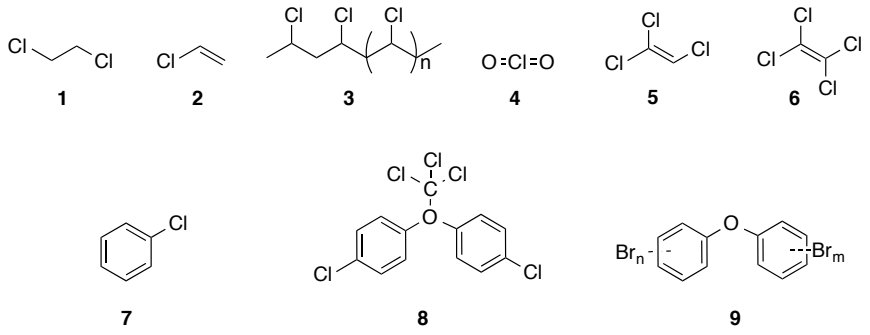

Chlorine controls the majority of water treatment and purification markets (eg Chlorine dioxide **4** as oxidizing agent in the sanitation, food and textile industry, Trichloroethylene TCE **5** and Perchloroethylene PCE **6** as solvents

for industrial cleaning and degreasing application). Several aromatic chloro compounds are used extensively as insecticides,[5] herbicides, fungicides,[6] and bactericides[7]. Example of such compounds includes chloro benzene **7**, which is the starting aryl halide for the synthesis of the now banned insecticide DDT **8**, and for the production of cosmetic products such as soaps and deodorants. The largest industrial application of chlorine is however in production of 1,2-dichloroethane DCA **1**, used to manufacture vinyl chloride monomer VCM **2**, the building block for polyvinyl chloride PVC **3**.[8]

Brominated organic compounds are increasingly becoming popular because of the reduced chemical cost and the higher tolerance to a wider range of pH levels that make them more suitable than chlorinated compounds for treating process water and for avoiding corrosion and algae formation in cooling towers. Bromine as hydrogen bromide is also used to produce purified terephthalic acid, the fumigant methyl bromide, drilling fluids and various plastics. Nevertheless nearly half of industrial consumption of bromine is due to the production of brominated flame retardant (polybrominated diphenylethers PBDEs **9**).[9]

Another important area of application for halogenated compounds is in high value fine and speciality chemicals used to formulate series of pharmaceutical products.[10] Some examples are provided in Chart 2.

Chart 2. Halogenated chemical compounds used as pharmaceutical pruducts: antitumoral 5-fluoracil **10** [11], antibacterial cinafloxacin **11**[12], antimalaric hydroxichloroquine **12**[13].

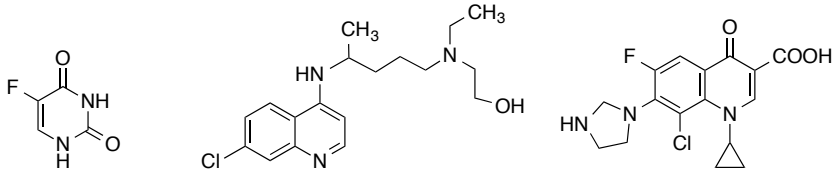

10 **11** **12**

Several amino acids[6] and other biological active compounds used as APIs (active pharmaceutical ingredients) have shown up enhance cytotoxicity if halogenated.[14] In particular, the introduction of a carbon-halogen bond increases the thermal and oxidative stability and the biological membrane permeability[15], fundamental characteristics for a synton.

Furthermore, organic halogenated compounds are of great value in medicinal imaging diagnostics. For example, iodinated aromatic compounds are used as contrast agents for vascular X-ray imaging. Fluorine compounds are used for magnetic resonance imaging (MRI).[16] Radioactive isotopes of fluorine, bromine, and iodine are used as radiotracers for molecular imaging with positron emission tomography (PET) or for single photon emission computed tomography (SPECT)[17], Chart 3.

Chart 3. Halogenated compounds used in medicinal imaging: FIT **13**,[18] Iodixanol **14**.[19]

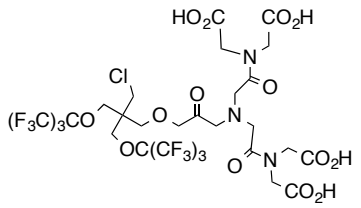

13

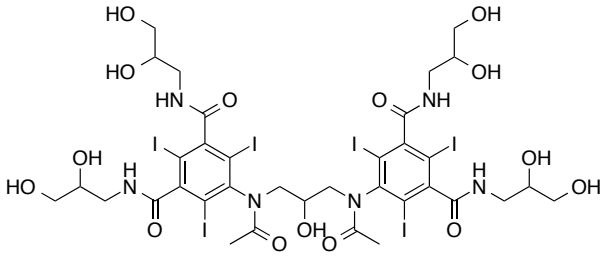

14

Referred to this context, in the past few years, significant progresses have been made in the development of catalytic, asymmetric halogenation reactions. Crucial examples are transition–metal-mediated cross-couplings and nucleophilic substitution reactions and organometallic catalyzed reactions.

In particular, the studies performed have been focused on two areas. First, the development of milder and more sophisticated halogenating reagents that can offer greater chemoselectivity and stereocontrol[20] than the extremely reactive diatomic halides. Secondly, the development of new procedures to perform the halogenation reaction in a more environmental benign way, in order to reduce the hazardous and toxic chemicals usage and to improve the usually poor atom economy of such processes. A growing ecological awareness has corresponded to yearly discoveries of new sources of halogenating organism and enzymes in the marine biosphere and to an increased studying of biological halogenation, as source of inspiration.[15]

Chart 4 provides a selection of reagents used to perform halogenation reactions. These reagents are used both in the research laboratory for organic synthesis and chemical industry, and includes *N*-chlorosuccinimide **15**,[21] *N*-bromosuccinimide **16**,[22] *N*-iodosuccinimide **17**,[23] 1,3-dichloro-5,5-dimethylhydantoin **18**,[24] 1,3-dibromo-5,5-dimethylhydantoin **19**,[25] 1,3-diiodo-5,5-dimethylhydantoin **20**.[26]

Chart 4. Common reagents used for halogenation reactions in organic synthesis and organic processes: *N*-chlorosuccinimide **15**, *N*-bromosuccinimide **16**, *N*-iodosuccinimide **17**, 1,3-Dichloro-5,5-dimethylhydantoin **18**, 1,3-Dibromo-5,5-dimethylhydantoin **19**, 1,3- Diiodo-5,5-dimethylhydantoin **20.**

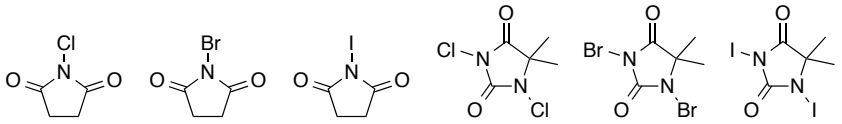

In particular, *N,N'*-dihalo-5,5-dimethylhydantoins have been recently discovered as instantaneous, high-selective and high-yielding reagents for chlorination, bromination and iodination of pyrazoles, indoles and imidazoles. Imidazoles constitute a class of synthetic intermediates of paramount importance in medicinal chemistry,[27] as precursors for NHC ligands[28] in homogenous transition metal catalysis and organocatalysis with different substituents on the backbone and on the ring-N atoms. The process that involves the halo-hydantoin compounds allows operating the halogenation under benign reaction conditions in an efficient, selective and environmental friendly way.[26a] In the context of these investigations, the huge potential of 1,3-diiodo-5,5-dimethylhydantoin **20** as active and versatile iodinating reagent have been disclosed.

Molecular iodine is one of the simplest oxidants currently available, high affordable and with a relatively low toxicity.[29] It has the lowest oxidation potential among all the halides (most readily oxidized) and is the least reactive halogen (the activation of the iodination reaction is usually needed). The iodine atoms of compound **20** are bonded to a more electronegative atom. The

polarization of the iodine-hetero bond reduces the electron density on the iodine atom making it more electrophilic in character,[30] influencing the rate of the electrophilic substitution reactions in the aromatic series and the isomeric composition of the products.[31] Synthetic studies dedicated to 1,3-diiodo-5,5-dimethylhydantoin **20** are extremely limited, although its structure is similar to the *N*-iodosuccinimide **17** but with two N–I bonds. One equivalent of **20** is then expected to have the same oxidative ability as two equivalent of molecular iodine or **17**.[29] An additional advantage of **20** is the high operability of the compound, that is a pale yellow solid, if compared with the instable molecular iodine.[31] One of the drawbacks is the relative high cost of the iodinating reagent **20** especially when compared to the cost of the starting precursor 5,5-dimethylhydantoin **21** (≈200×). (Added value of the research chemicals: **21**=7.32 €/100g→ **20**=1426 €/100g).[32]

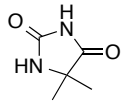

21

The aim of this work was to design, develop, and optimize a cost effective and green synthetic process for the production of the iodination reagent 1,3-diiodo-5,5-dimethylhydantoin **20**. The synthesis, firstly conceived for batch reactor, has been successfully transferred to a continuous flow process. Continuous processing, extensively used in bulk chemical production for large-scale, has been recently disclosed as attractive technique also in fine chemicals and pharmaceutical synthesis. Laboratory-scale flow reactors commonly known as micro-reactors offer several features widely reviewed.[33] Benefits for mixing and heat transfer, a greater surface-volume ratio, enhanced control of the reaction conditions are just few examples of the advantages provided by this technology. Improvements in yield, selectivity and productivity[34] achievable by means of a continuous process influence both the economy and the environmental impact of a synthesis. We expected to optimize the production of the target molecule exploiting the potential of a multi-jet oscillating disk (MJOD) flow reactor, recently devised in our laboratory.[35]

2. Methods and results

1.1. Prior art - Literature overview

Initial literature research revealed rather few previously disclosed processes leading to our target molecule *N,N'*-diiodo-5,5-dimethylhydantoin (DIH) **20**.
Only two articles were identified, namely one that was dating back to 1964, which was disclosed by Orazi, Corral and Bertorello,[36] and the second one from 1975 disclosed by Gottardi.[37] Furthermore, two patents were also disclosed, which both claims novel inventions leading to the iodinated compound **20**, namely by Kodama and collaborator (2002),[38] and Inoue and collaborators (2007).[39] One more patent was disclosed, but this was dedicated to the production of *N*-halogenated in general hydantoins by Hassan and collaborators (2006).[40] We have evaluated these processes and performed some screening experiments in order to assess and decide upon the more suitable procedure for further development and optimization.
At the outset, the process described by Orazi and co-workers was performed by small modifications. Originally this process involved carbon tetrachloride as reaction medium. However, according to the new environmental regulations, carbon tetrachloride is banned because its ozone-depleting[41] and suspected carcinogenic properties.[42] In the place of carbon tetrachloride we used dichloromethane.

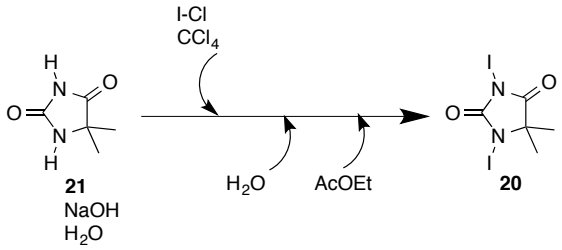

The process we used at the outset was thus: substrate, 5,5-dimethylhydantoin (DMH) **21**, and sodium hydroxide were dissolved in cold water and maintained at 0 ^{o}C using an ice/water bath. To this reaction mixture, a solution of iodine monochloride and dichloromethane was added drop-wise while stirring by means of a magnetic stirrer. After the complete addition of the I-Cl solution, the mixture was stirred for another 15 minutes, filtered and washed with cold

water and sodium thiosulfate (Experimental 4.3.1-DIH synthesis: method 1). The isolated product showed the identical appearance as described by Orazi and co-workers. Further structure or analytical data were not given by Orazi and all.[36] Samples of isolated product were analyzed using HPLC, GC-MS, and ^{1}H NMR, which to our surprise didn't shown our expected compound, but iodoform. Based on this discovery, we realized that it was necessary to redesign the synthetic procedure. The other procedures reported variation in solvent, base, reaction time etc

1.2. Chemometrics and Experimental Design – general concepts[43]

Chemometrics is a science applied to solve descriptive and predictive problems in experimental chemistry.[44] In descriptive applications, the structures of chemical systems are explained by understanding the underlying correlations of their properties. In predictive application, this science allows evaluating the synergies of the variables involved in a process with the intent of removing the redundant or unnecessary information. The major tools involves PCR/PLS (Principal Component Regression/Partial Least Squares),[45] statistical experimental design[46] and multivariate regression and data analysis.[47] The main purpose is to understand how to perform meaningful calculations on data minimizing the number of the experiments.[48] By means of multivariate statistics and mathematical methods, several algorithms implemented in computers programs can be used within all kind of chemistry problems. The potential of chemometrics is huge, ranging from physical chemistry such as kinetics and equilibrium studies, to organic chemistry such as reaction screening and optimization, theoretical chemistry, spectroscopy, chromatography on to applications as varied as industrial process and environmental monitoring, biology, etc. A core area of study in chemometrics is statistical experimental design. Using statistical rules, experimental design is an efficient procedure for planning experiments to obtain an optimized process. Significant variables should be identified to design efficiently the experimental domain in order to achieve the desired response with the least effort in terms of time and cost.

1.3. Pre-experimental design – variables screening

Experimental planning is the starting point of the experimental design. The variables that mostly influence the response of the process should be identified. To approach this goal, an Ishikawa cause-effect (ICE) diagram,[49] originally conceived as tools for quality and productivity management, was slightly modified to fit synthesis experimentation. Going through the previously disclosed procedures for the synthesis of compound **20**, continuous and discrete perturbations generated on the process were recognized. From the outset of the experiment to the measurement of the response, the different variables were noted on a horizontal arrow, defining a time axis. The fish-bones diagram is a useful resource to represent the different correlations between the variables and to graphically classify them as dependent, independent and nuisance, Figure 1.

Figure 1. Ishikawa cause-effect diagram for the **20** synthesis.

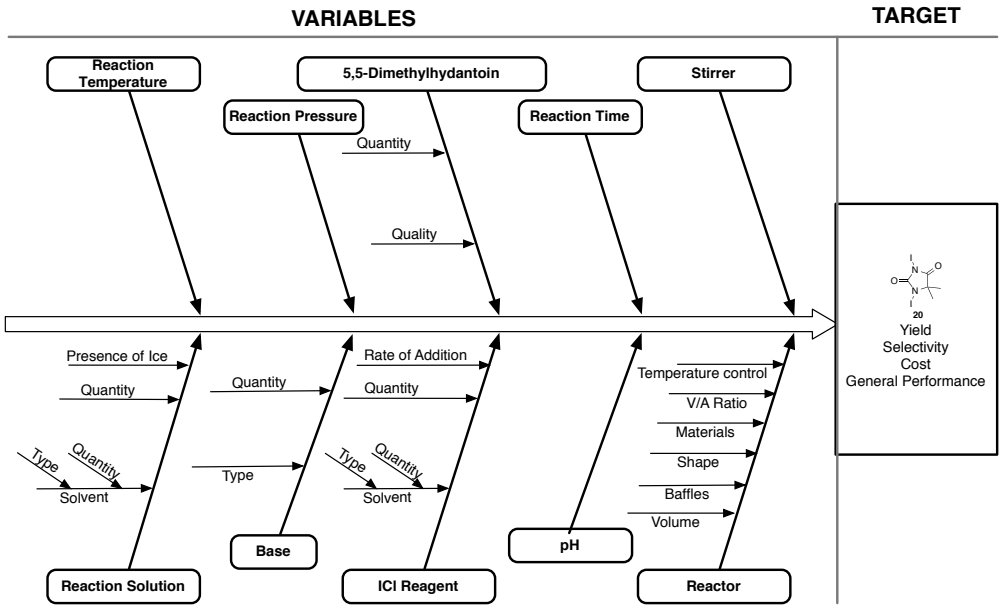

Each independent variable involved in the 1,3-diiodo-5,5-dimethylhydantoin synthesis was examined, performing some screening experiments, and classified according to the influence on the response, Table 1.

Table 1. Identified variables.

#	Name
x_1	K_2CO_3
x_2	ICl
x_3	Addition time
x_4	Reaction time
x_5	Rate of stirring
x_6	Temperature
x_7	pH
x_8	Water
x_9	Ethyl Acetate

A wide variety of inorganic bases were expected to be suitable for the process. Sodium, calcium or potassium, oxide or hydroxide, carbonate or bicarbonate are just few example of water-soluble bases that might be used separately or in a mixture.

Inorganic base K_2CO_3 was chosen after unsuccessful attempts using NaOH and KOH. Potassium carbonate is a milder base than the sodium hydroxide. It is widely used in organic synthesis and in the production of agrochemicals and pharmaceutical. This base in fact facilitates the formation of a required anionic organic nucleophile for coupling with a dissolved electrophile, enhancing the formation of the product.[50] K_2CO_3 is readily soluble in water with the formation of an alkaline solution and does not hydrolyze. Furthermore it is a non-nucleophic base, it means that its steric bulk allows protons attaching the basic atom preventing alkyl groups from doing the same.[51]

The amount of base (x_1) should be at least in the stoichiometric quantity in order to enhance the deprotonation of the nitrogen atoms of the 5,5-dimethylhydantoin. The water, inorganic base and **21** can be feed individually or in a mixture. It is preferable to form the aqueous solution of the inorganic base without the co-presence of the substrate. The heat generation that occurs when a base is dissolved in water might adversely affect the starting molecule **21**.

No halo-organic solvent or co-solvent were required in the process. Introductory experiments using phase-transfer catalyst PTC were performed but any significant improvement of the process response was observed. The application of PTC was thus excluded from our procedure.

The proportion of halogenating agent (x_2) and 5,5-dimethylhydantoin can be varied from the stoichiometric ratio. In literature, the suggested ratio of halogen/nitrogen atom of substrate was 1.8 (value that was accounted during the design).

The time of the reaction can be distinguished between addition time (x_3) and reaction (stirring) time (x_4) after the complete addition of the iodinating reagent.

The rate of stirring (x_5) has a great influence on the yield of the reaction and must be kept at high rate, in order to avoid concentration gradients of halogen or base and to promote the contact between the reacting components.

The reaction was performed in an ice bath in order to maintain the exothermic reacting mixture at approximately 10 °C. During the screening phase, different temperatures (x_6) were attempted. Two experiments at 0 °C and at room temperature (≈ 25°C) were unsuccessful.

The reaction is not an acid-base one then the influence of the pH value (x_7) on the response is negligible.

The amounts of water (x_8) and ethyl acetate (x_9) were kept at fixed levels, in order to change the concentration of the two mixtures varying only the quantity of the base and the iodinating reagent I-Cl.

1.4. Experimental design and multivariate regression: Batch mode

Small Scale Batch Process

The development of the optimize procedure for the production of the target molecule 1,3-diiodo-5,5-dimethylhydantoin **20** was initiated by using a small-scale batch reactor (<1 g). The optimization study was performed by investigate only two variables in a full factorial design (2^k, k=2 experimental variables) with two experiments in the center of the experimental domain. According to finding in pre-experimental design and screening experiments the quantity of base K_2CO_3 (x_1) and the quantity of iodinating reagent I-Cl (x_2) were investigated. The statistical experimental design was performed in random order and reported in standard order with the numerical values of the responses in the right-hand columns of Table 2. The experimental variables and levels are described in the footnotes.

Table 2. Experimental design 2^2+2 for investigation of iodination of 5,5-dimethylhydantoin using I-Cl with water as reaction medium

#	Experimental variables[a,b]		Responses[c]				Iodination of imidazole[d]	
	x_1	x_2	y_1	y_2	y_3	y_4	y_5	y_6
1	-1	-1	1.054	55.47	+	+	0.123	42.25
2	+1	-1	1.301	68.47	+	+	0.155	53.24
3	-1	+1	0.353	18.57	-	-	-	-
4	+1	+1	1.284	67.57	+	+	0.205	70.38
5	0	0	1.555	81.86	+	+	0.179	61.45
6	0	0	1.509	79.42	+	+	0.227	77.93

[a] Synthetic procedure for the iodination of 5,5-dimethylhydantoin: DMH (5 mmol), H_20 (10 mL), ethyl acetate (10 mL). The quantities of base (K_2CO_3) and iodination reagent (I-Cl) are provided in in the table.

[b] Experimental design definition. Experimental variable (x_k) [experimental level: –1, 0, +1]. x_1: mmol of K_2CO_3 [12 , 15 , 18], x_2: mmol of iodinating reagent I-Cl, [12, 15, 18].

[c] Responses and explanations. y_1: weight of isolated product, theoretical yield 1.89 [g]. y_2: yield- of product: y_3: thermal test. y_4: TGA performer (– = no, + = yes), y_5: isolated yield imidazole, theoretical yield 0,291 [g]. y_6: yield-% imidazole.

[d] The isolated DIH was used to di-iodinate the imidazole molecule: Imidazole (11 mmol), DIH (9.1 mmol), H_2O (2 mL), KI (13 mmol), H_2SO_4 97%(1 mL), NaOH (58 mmol), acetic acid. The selectivity ≈95%.

Prior to perform the whole set of experiments provided by the design, objects #1, #4, and #5, namely extremes and central point of the experimental domain, were conducted, Figure 2. The selected levels of the variables have been shown to provide significant variations in the response y_2, yield of the synthesis of the target compound **20** ($y_{2max} - y_{2min}$= 27%).

Figure 2. Yield for the three experiments: #1 where(x_1, x_2) =[-1, -1], #5 where (x_1, x_2)=[0, 0], and #4 where (x_1, x_2)=[1, 1].

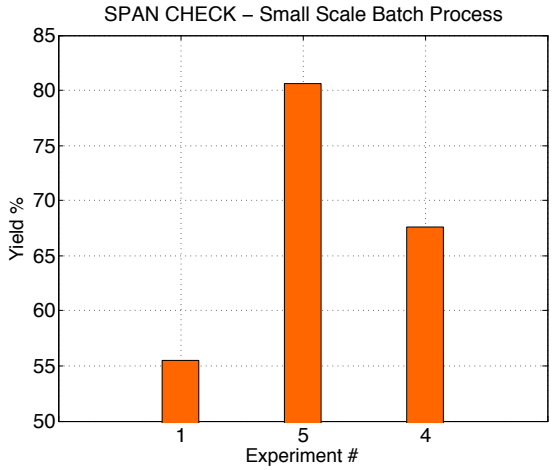

The achieved results of the experimental design are graphically displayed in Figure 3. From the plot, it is possible to observe the accordance between the two measured responses y_2 and y_6: the yield of the **21** iodination follows the same trend of the yield achieved for the imidazole iodination. The quantity of the obtained product appeared to vary accordingly to the quality, measured as iodinating capability. Experiment #3 performed with a slightly basic water solution and a high quantity of I-Cl showed a negligible amount of precipitate that was not the target molecule. The synthetized compound failed both the thermal test (no purple vapours associated to the I_2 release were observed) and the successive imidazole iodination. Central experiments #5 and #6 show similar response values, validating the stability and the reliability of the results (ν= 2.97, std= 1.72). The variation within the entire experimental domain is on the contrary huge, namely in the range 18%-79% yield, showing the relevant influence of the selected variables on the process performances. Statistical factors were estimated and reported in Table 4. The following multivariable regression analysis confirmed and emphasised those qualitative remarks.

Figure 3. Approximate description of the response surface by plotting the experimental data directly: y_2: yield-% of product. y_3: thermal test. y_4: TGA performer (– = no, + = yes), y_6: yield-% imidazole.

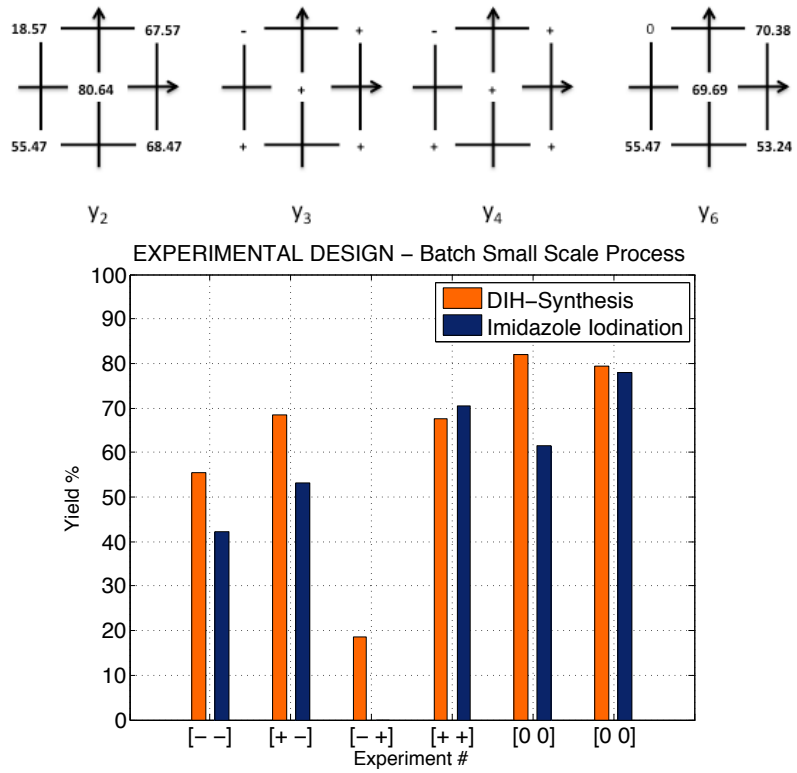

Table 3. Statistical parameters for y_2 responses of the experimental design.

	GM[a]	μ [b]	MAV [c]	Std[d]	v [e]
Central	80.63	80.64	1.22	1.72	2.97
All	56.04	61.89	16.58	23.23	539.99

[a] Geometric Mean: $GM = (\sum_{i=1} y_i)^{1/n}$, i= experiment number: i=4,5 for the central experiments; i=1-5 for all the experiments. n= number of experiments that have been taken into account.

[b] Mean $\mu = \frac{\sum_i y_i}{n}$, i= experiment number: i=4,5 for the central experiments; i=1-5 for all the experiments. n= number of experiments that have been taken into account.

[c] Mean Absolute Variance: $MAV = \frac{\sum_{i=1} y_{max-y_{min}}}{n}$, i= experiment number: i=4,5 for the central experiments; i=1-5 for all the experiments. n= number of experiments that have been taken into account.

[d] Standard deviation: $Std = \sqrt{\frac{\sum_1^i (y_i-\mu)^2}{n-1}}$, i= experiment number: i=4,5 for the central experiments; i=1-5 for all the experiments. n= number of experiments that have been taken into account and μ.

[e] Variance: $v = std^2$

Multivariable regression and model evaluation

Two experimental levels were chosen for each of the variables (x_1 , x_2). Each of the experimental variables was scaled according to equation 1 in order to facilitate the calculation and the comparison of the regression coefficients (β-coefficients). Their numerical value results thus to be a direct measure of how their ranges of variation influence the response in the experimental domain.

$$x_i = \frac{z_i - \left\{z_{i,L} + \frac{1}{2}\left(z_{i,H} - z_{i,L}\right)\right\}}{z_{i,H} - \left\{z_{i,L} + \frac{1}{2}\left(z_{i,H} - z_{i,L}\right)\right\}}, \qquad i = 1,2 \qquad (1)$$

x_i (i= 1, 2) is the experimental variable i given in scaled units, z_i is the experimental variable i given in real units, z_{iL} and z_{iH} are respectively the selected low and high experimental values in real units.

A model matrix $\mathbf{X}_{6 \text{ lines x } 4\text{columns}}$ =[**1 x$_1$ x$_2$ x$_1$x$_2$**] was created on the basis of the design matrix **D**. The model matrix **X** was correlated to the response (percentage yield of the reaction) by means of the MLR (multiple linear regression) method and by using the partial least-squares PLSR.[52] The matrix relation reported in equation 2 summarizes the whole series of experiments of the design.

$$Y = X \cdot \beta + e \qquad (2)$$

A least squares fit of the model is obtained by equation 3:

$$\beta = X^T \cdot X - 1 \cdot X^T \cdot Y \qquad (3)$$

Figure 4 provides the estimated values of the regression coefficients for the iodination of **20**, and the iodination of the imidazole. β_0, the average value of the set of the experiments, was kept outside the graph. β_1 and β_2 are the coefficient related respectively to the variables x_1 and x_2 and β_{12} the interaction coefficient. The cumulative normal probability plot and the adjacent bar plot suggest that the variable x_1 has significant main effect on the response. Indeed the regression coefficient β_1 lies outside the range of the experimental error variation and contributes influencing the response also through the interaction factor.

Figure 4. β-coefficients: DMH iodination, imidazole iodination .

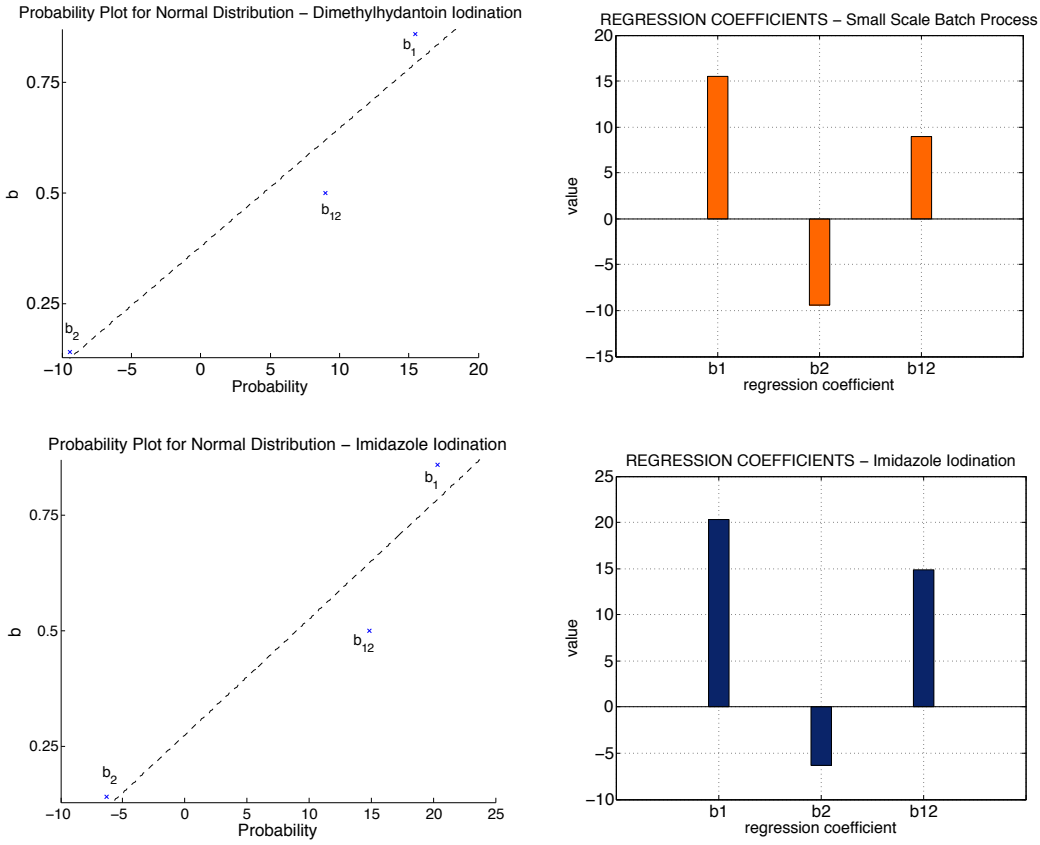

The estimated coefficients were used to create the predictive empirical mathematical model of the response, provided in equation 4. All the regression parameters were considered.

$$y = f(x_1, x_2) = \beta_0 + \sum_{i=1}^{2} \beta_i x_i + \sum_{i=1}^{1} \sum_{j=2}^{2} \beta_{ij} x_i x_j \qquad (4)$$

$$y_2 = f(x_1, x_2) = 61.8933 + 15.5000\, x_1 - 9.4500\, x_2 + 9.0000\, x_1 x_2 \quad (5)$$

$$y_6 = f(x_1, x_2) = 50.8750 + 20.3425\, x_1 - 6.2775\, x_2 + 14.8475\, x_1 x_2 \quad (6)$$

The model was then used to understand the underlying correlation of the property of the process and to determine how the variables might be varied to optimize the procedure. To achieve this aim, a three-dimensional plot of the responses (Figure 5) and an iso-contour map inside of the experimental design domain (Figure 6) were created.

The contour plot, in particular, is a useful resource to display three-dimensional data on a two dimensional chart. Analyzing the iso-responses lines, it was possible to evaluate the optimized conditions for the small-scale batch process within the limit of the experimental design. As expected from the rough overview of the regression β-coefficients, the optimum of the model is reached using a high level of the variable x_1 and a low level of the variable x_2. The responses appeared to be more sensitive to the variation of the iodinating reagent (x_2) than of the base quantity (x_1).

Figure 5. Three-dimensional plot of the model for the DIH synthesis (a) and of the iodination of the imidazole (b)

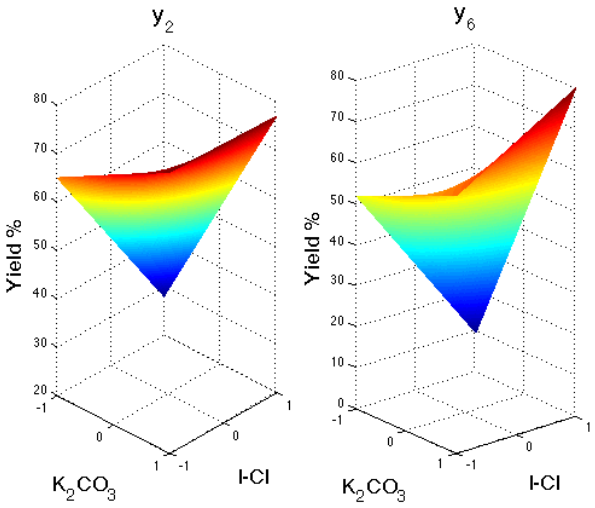

Figure 6. Contour plot inside of the investigation domain: (a) DMH iodination, (b) Imidazole iodination.

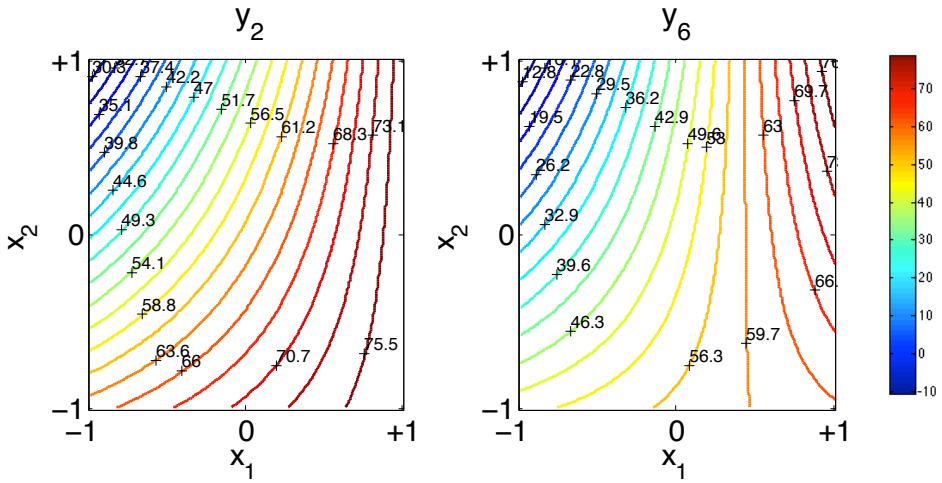

Additional experiments were performed varying the volumes of H_2O and ethyl acetate, *XX m*L and *YY mL* respectively. Experimental variables and responses are summarized in Table 4. Experimental levels and synthetic procedure are reported in the footnotes. As can be pointed out from Figure 7, the response y_2 of these experiments was significantly lower than the mean value of y_2 obtained in the center of the experimental design domain.

Figure 7. Alternative concentration for the central experiment of the experimental design domain.

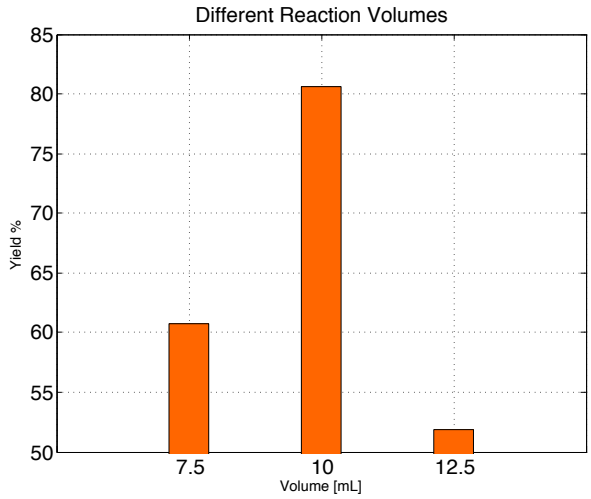

Table 4. Experimental results using different concentration of the reaction mixtures varying the solvents volumes.

#	Experimental variables[a,b]		Responses[c]				Iodination of imidazole[d]	
	XXmL	*YYml*	y_1	y_2	y_3	y_4	y_5	y_6
1	7.5	7.5	0.512	26.95	+	+	0.177	60.77
2	12.5	12.5	1.350	71.07	+	+	0.151	51.84

[a] Synthetic procedure for the iodination of 5,5-dimethylhydantoin: DMH (0.005 mol) K_2CO_3 (2.070 g), I-Cl (2.435 g).
[b]Experimental variable: H_20 (XXmL), ethyl acetate (YYmL). Theoretical yield: 1.89 [g].
[c]Responses and explanations. y_1: weight of isolated product. y_2 : yield-% of product. y_3 : thermal test. y_4: TGA performer (– = no, + = yes), y_5 : isolated yield imidazole: 0,291 [g], y_6 : yield-% imidazole
[d] The isolated diiododimethylhydantoin from iodination experiments of of imidazole: Imidazole (0.011 mol), DIH (0.091 mol), H_2O (2 mL), KI (0.013 mol), H_2SO_4 97% (1 mL), NaOH (0.058 mol), acetic acid. Theoretical yield: 0.291 [g]

An extrapolation of the model was then performed to predict an optimize procedure for the small-scale batch reactor before scaling up the process.

The variables were evaluated at different level outside the experimental domain, coded -2 and +2.

A contour plot was created and reported in Figure 8. Evaluating the iso-response lines, the variables were fixed at (x_1, x_2)=(-2, 0), namely 15 mmol of K_2CO_3 and 11 mmol of I-Cl.

This procedure was tested to validate the accuracy of the model beyond the range investigated during the design.

An improvement of the response leads us to consider the values for the two variables previously described as center point of the experimental design of the up-scaled batch process.

Figure 8. Contour plot extrapolation for the response y_2 of the small-scale batch process

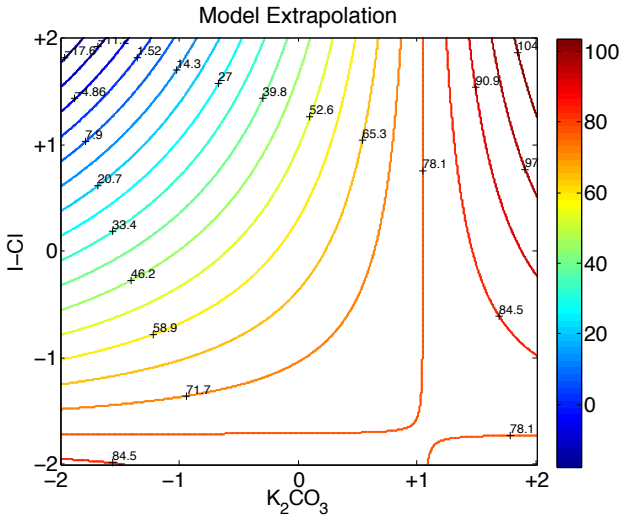

Up-Scaled Batch Process

The next step in the development of the 1,3-diiodo-5,5-dimethylhydantoin synthesis was to perform a scale up of the small scale optimized batch procedure. The aim of this passage was to take into account scale-up effects of the batch mode process before the synthesis was transferred and assessed to continuous flow mode.

In this context, a new experimental design was prepared where the center of the experimental domain was the setting of the optimized small-scale batch procedure. A 10-fold scale-up was performed compared to the original small-scale batch. In this statistical experimental design, three variables were investigated namely quantity of base K_2CO_3 (x_1), quantity of iodinating reagent I-Cl (x_2), and addition time of the I-Cl solution to the reactant mixture of 5,5-dimethylhydantoin and basic water (x_3). The variable x_3 was not investigated in the first small-scale study, but we believed that this variable might influence the performance of the reaction.

A factorial design to 2^k (k=3 experimental variables) including three experiments in the center of the experimental domain was created and performed in random order, with the goal to transform systematic errors into random errors and to minimize time-dependent phenomena. The experimental design (provided in standard order) including the measured numerical values of the responses in the right hand column is reported in Table 5.

The achieved results are graphically presented in Figure 9. According to the bar plot, the variation of the response values within the experimental domain is significant. The experimental design shows a substantial variation in outcome, namely in the range 17%- 63% yield, that shows the relevant influence of the investigated experimental variables on the process performances. In particular, the minimum and maximum results are related respectively to the lowest and the highest values of the addition time x_3 (experiments #1 and #6). The result of the central experiment appears to remain constant throughout the replications #9 #10 and #11. That is confirmed by the estimated statistical factors values, calculated and reported in Table 5. The small standard deviation and the variance values associated to the central experiments validate the

stability and the reproducibility of the synthetic procedure, Table 6. The following multivariate regression analysis confirms and emphasizes the pointed out qualitative observations.

Table 5. Experimental design 2^3+3 for investigation of **20** iodination using I-Cl with water as reaction medium

#	Experimental variables[a,b]					Responses[c]	
	x_1	x_2	x_3	$t_{stirring}$	t_{tot}	y_1	y_2
1	-1	-1	-1	60	120	11.88	62.54
2	+1	-1	-1	60	120	7.83	41.23
3	-1	+1	-1	60	120	9.86	51.92
4	+1	+1	-1	60	120	7.97	41.98
5	-1	-1	+1	60	180	3.96	20.85
6	+1	-1	+1	60	180	3.22	16.94
7	-1	+1	+1	60	180	7.32	38.53
8	+1	+1	+1	60	180	10.54	55.49
9	0	0	0	60	150	10.61	55.88
10	0	0	0	60	150	11.07	58.25
11	0	0	0	60	150	11.31	59.49

[a] Synthetic procedure for the iodination of 5,5-dimethylhydantoin: DMH (50 mmol), H_20 (100 mL), ethyl acetate (100 mL). The quantities of the base (K_2CO_3) , iodination reagent (I-Cl) and the time of addition of the iodination agent are provided in the different experiments 1-5 in the table. All the experiments were conducted in a glass cylinder reactor (7.5 cm) that was immersed in an ice-water bath. The reactor was furnished with a magnetic stirrer and stirrer bar (3.5 cm). All reactions were conducted without daylight.

[b] Definition experimental design. Experimental variable (x_k) [experimental level: -1, 0, +1]. x_1: mmol of K_2CO_3 [140, 150, 160], x_2: mmol of iodination reagent I-Cl, [100, 110, 120], x_3: addition time [60 90 120] [min].

[c] Responses and explanations. y_1: weight of isolated product. Theoretical yield: 18.9 [g]. y_2 : yield-% of product.

Figure 9. Approximate description of the response surface by plotting the experimental data directly: DIH-Yield [%]

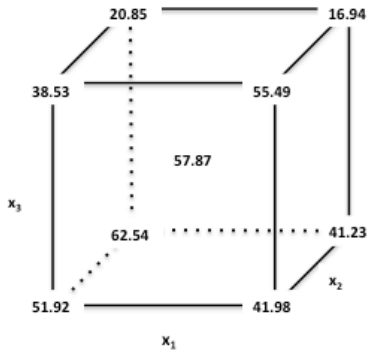

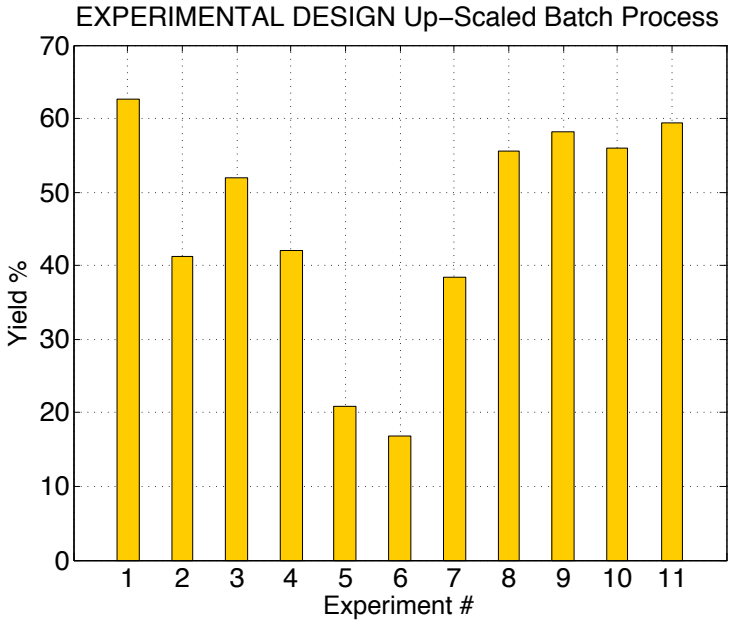

Table 6. Statistical parameters for the yield of the reactions performed in the up-scale batch reactor.

	Geometric Mean[a]	Mean[b]	Mean absolute variation [c]	Std[d]	Variance[e]
Central Values	57.85	57.87	1.3	1.8	3.36
All	12.57	45.73	12.57	15.49	239.9

[a] Geometric Mean: $GM = (\sum_{i=1} y_i)^{1/n}$, *i*= experiment number: *i*=4,5 for the central experiments; i=1-5 for all the experiments. *n*= number of experiments that have been taken into account.

[b] Mean: $\mu = \frac{\sum_i y_i}{n}$, *i*= experiment number: *i*=9, 10, 11 for the central experiments; i=1-11 for all the experiments. *n*= number of experiments that have been taken into account.

[c] Mean absolute variation: $MAV = \frac{\sum_{i=1} y_{max-y_{min}}}{n}$, *i*= experiment number: *i*=9,10,11 for the central experiments; i=1-11 for all the experiments. *n*= number of experiments that have been taken into account.

[d] Standard Variation: $Std = \sqrt{\frac{\sum_1^i (y_i-\mu)^2}{n-1}}$, i= experiment number: *i*=9, 10, 11 for the central experiments; i=1-11 for all the experiments. *n*= number of experiments that have been taken into account and μ, mean value of each set considered.

[e] Variance: $v = std^2$

Multivariate regression and model evaluation

The values of the selected variables x_i reported in the footnotes of Table 5 were scaled according to equation 1, in order to simplify the calculation and the evaluation of the regression coefficients and their influence on the response y.

$$x_i = \frac{z_i - \left\{z_{i,L} + \frac{1}{2}\left(z_{i,H} - z_{i,L}\right)\right\}}{z_{i,H} - \left\{z_{i,L} + \frac{1}{2}\left(z_{i,H} - z_{i,L}\right)\right\}}, \qquad i = 1,2,3 \qquad (1)$$

A model matrix $\mathbf{X}_{11\text{ lines x }8\text{ columns}}$ =[**1 x₁ x₂ x₃ x₁x₂ x₁x₃ x₂x₃ x₁x₂x₃**] was created on the basis of the design matrix **D.** The model matrix **X** was multivariate correlated with the response y_2, percentage yield of the target molecule **20**, using multivariate regression in terms of partial least-squares regression method (PLSR).[52] The regression coefficients that have significant influence on the predictive model were determined by using a cumulative normal probability plot and the adjacent bar plot, Figure 10.

Figure 10. β-coefficients for the synthesis of **20**: cumulative normal probability plot and bar-plot

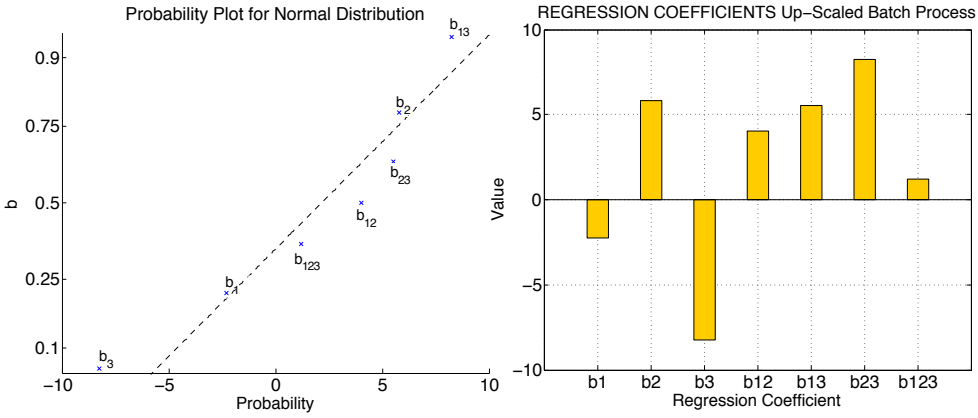

The regression coefficients associated to the variables x_2 and x_3 appear to be larger than the experimental error variation and then have significant main effects. β_1, related to the variable x_1, has influence through interaction effects in combination with the variables that showed significant main effects. In conclusion, all the estimated coefficients were taken into account and used to build the predictive empirical mathematical model of the response, provided in equation 7.

$$y = f(x_1, x_2, x_3) = \beta_0 + \sum_{i=1}^{3} \beta_i x_i + \sum_{i=1}^{2} \sum_{j=2}^{3} \beta_{ij} x_i x_j \qquad (7)$$

$$y_2 = f(x_1, x_2, x_3) = 45.73 - 2.27\, x_1 + 5.79\, x_2 - 8.23 x_3 + 4.03 x_1 x_2 + 5.53 x_1 x_3 + 8.26 x_2 x_3 + 1.18\, x_1 x_2 x_3 \qquad (8)$$

The final model, equation 8, was then used to point out which variables had significant influence on the response and how they might be varied to optimize the synthetic procedure. Three-dimensional plots of the fitted surfaces are shown in Figure 11 and iso-contour maps of the responses within the limits of the experimental design are displayed in Figure 12. Both charts confirm the high sensitivity of the response to the variable x_3, addition time, and to the variable x_1, quantity of base. The curtailed areas of Figure 12 related to a high yield of the target molecule **20** are situated at the lowest values for the variables x_1 and x_3. Variable x_2, I-Cl quantity, doesn't affect equivalently the results of the experiments.

Figure 11. Three-dimensional plots of the model for the production of DIH: (a) x_1 _ x_2, (b) x_1 _ x_3, (c) x_2 _ x_3

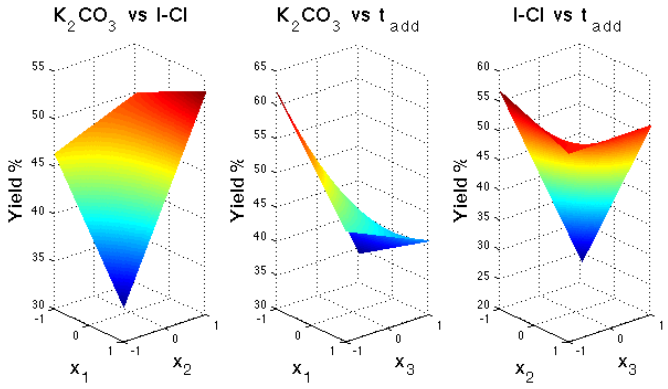

Figure 12. Contour plot inside of the investigation domain.

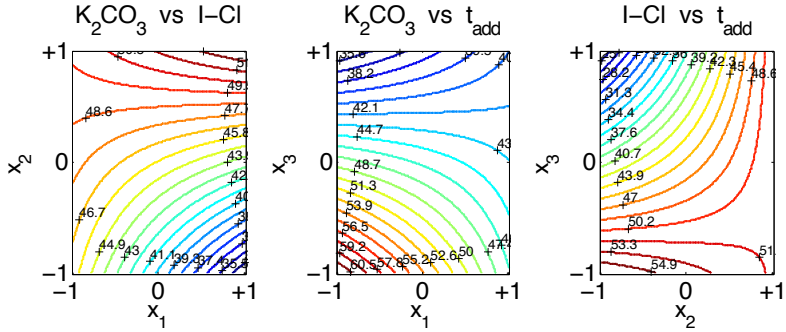

To optimize the procedure an extrapolation of the model was performed and discussed. Iso-contour map projections of the response surface outside the experimental domain were created to predict he optimal conditions for the reaction, Figure 13. Evaluating the plots, the scaled values of the assessed variables were fixed as (x_1, x_2, x_3)=(-1, 0, -2), with a $t_{stirring}$ = 60 [min]. Experiment #5 of Table 7 was performed to confirm the prediction of the model. The setted optimal conditions led to an improvement of the yield. The value of the response was not the predicted one but was higher than the mean value of the responses provided by the design. Additional experiments were designed to refine the optimized synthetic protocol predicted by the model.

Figure 13. Contour plot extrapolation

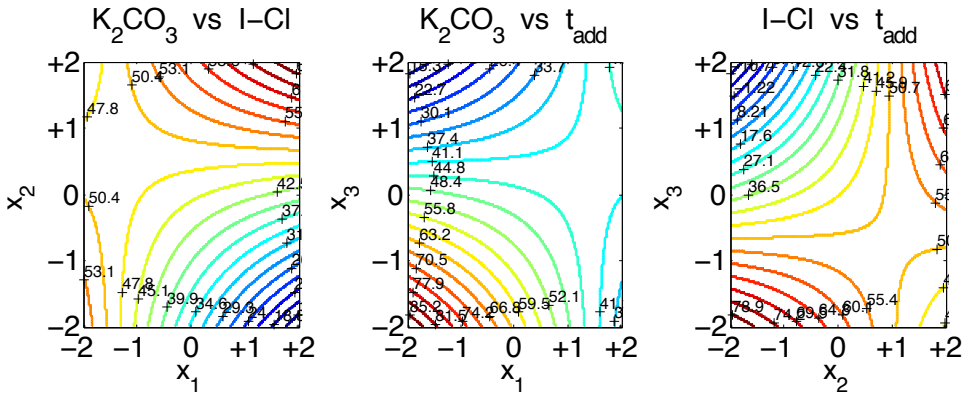

The addiction time x_3 was identified as an important variable for the present reaction. This fact spurred us to perform further investigations related to the reaction time (reactor residence time).

The optimized procedure was used to identify the optimized stirring time x_4 after the complete addition of the iodinating reagent. Reaction details and experimental results are reported in Table 7 and displayed in Figure 14. The curve trend reaches a peak at x_4 of 15 minutes before considerably dropping off, while increasing the stirring time. The experiment #2, the one with the best yield, has been repeated to evaluate the reliability of the result.

The reaction requires a minimum time to start as confirmed by the low value of the first experiment. The gradually decrease of the yield of the target molecule suggests a degradation of the product with a prolonged residence time.

Table 7. Stirring time effect

#	Experimental variables[a,b]		Responses[c]	
	x_4	t_{tot}	y_1	y_2
1	1	31	11.75	61.85
2	15	45	12.74	67.04
3	15	45	12.03	63.34
4	30	60	11.98	63.05
5	60	90	11.67	61.78
6	90	120	9.95	52.37
7	180	210	8.93	47.01
8	270	300	8.08	42.53

[a] Synthetic procedure for the iodination of 5,5-dimethylhydantoin: DMH (50 mmol), H_20 (100 mL), ethyl acetate (100 mL). The quantities of the base (K_2CO_3) x_1, iodination reagent (I-Cl) x_2 and the time of addition of the iodination reagent x_3 are fixed at [-1, 0, -2]=[140 mmol , 110 mmol, 30 min]
[b] x_4: the stirring time after the complete addition of the iodination agent [min] and $t_{tot} = t_{addition} + t_{stirring}$ [min]
[c] Responses and explanations. y_1: weight of isolated product. Theoretical yield: 18.9 [g]. y_2 : yield-% of product.

Figure 14. Stirring time effect

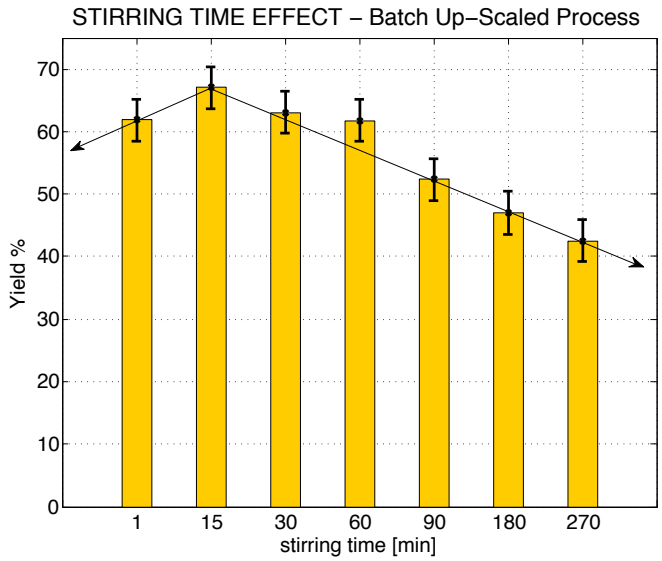

A further extrapolation of the model was performed. Different combination of quantity of iodinating reagent I-Cl and addition time were tested to evaluate those new projections of the response, Figure 15. Reaction condition and results are summarized in Table 8; the predictions of the model were not respected outside the short-range extrapolation domain. The yield of the target molecule didn't increase as predicted by the model then the previously

optimized procedure was not modified. The result of the optimization of the up-scaled batch process was the procedure with a level for the assessed variables as follows: (*x1*, *x2*, *x3*)=(-1, 0, -2), namely 140 mmol of K_2CO_3, 110 mmol of I-Cl added in 30 [min] with a $t_{stirring}$ = 15 min after the complete addition.

Figure 15. Further extrapolation of the model

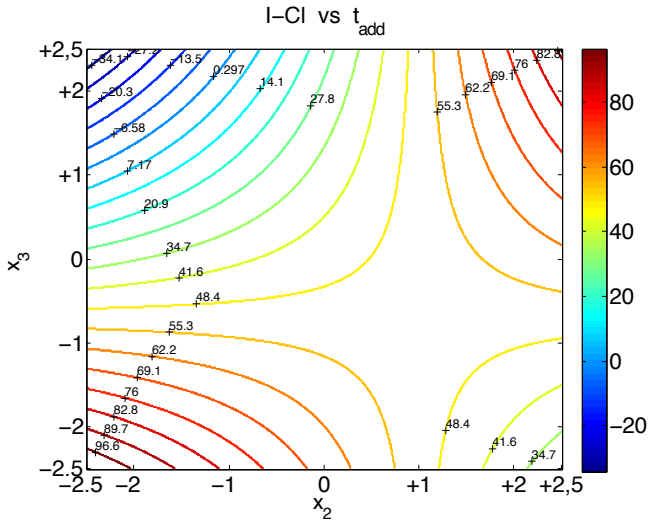

Table 8. Additional experiments based on the optimized procedure.

#	Experimental variables[a,b]				Responses[c]	
	x_2	x_3	$t_{stirring}$	t_{tot}	y_1	y_2
1	-1	-2	15	45	12.12	63.82
2	-1	-2	15	45	11.13	58.49
3	0	-2.5	15	30	11.24	59.15
4	0	-2.5	30	45	10.38	54.65

[a] Synthetic procedure for the iodination of 5,5-dimethylhydantoin: DMH (50 mol), H_20 (100 mL), ethyl acetate (100 mL), x_1: 140 mmol of K_2CO_3.The quantity of iodinating reagent (I-Cl) and the time of addition of the iodinating reagent x_3 are provided in the different experiments 1-4 in the table.

[b]Experimental design definition: Experimental variable x_2: mmoles of iodination reagent I-Cl, [experimental level: -1 0]=[100 110], x_3: addition time [experimental level: -2.5, -2] [15, 30] [min]. x_4: stirring time [min]

[c] Responses and explanations. y_1: weight of isolated product, theoretical yield: 18.9 [g]. y_2 : yield-% of product.

1.5. Multi-jet oscillating disk (MJOD) Flow reactor

Traditionally organic synthesis has been performed batchwise.[53] The increasing economic and environmental pressures have enhanced the researches in continuous processes and continuous manufacturing.[54]

Flow chemistry provides a series of advantages compared with the batch processing methodology. Exquisite control over reaction conditions (temperature, pressure and reaction time), high degree of automation, incorporate continuous separations, in-line recycling of reagents are just few examples of the benefits that make this technology so attractive. Flow micro-reactor chemistry allows improving the energy efficiency of a process increasing heat and mass transferring performance and reducing reaction volumes. These aspects consent to obtain target molecules in high yields and selectivity and to minimize the production of effluents and the usage of hazardous reagents.[35]

In addition the scale up of a reaction can be achieved rapidly with little or no process development work, by either changing the reactor volume or by running several reactors in parallel.[33]

Micro-reactors are made of miniaturized channels of glass,[55] silicon,[56] polymers or stainless steel,[55] depending upon the kind of reagents and conditions involved in the reaction of interest. The micro-channels, however, if from one side enhance the heat and mass transfer, from another present the weakness to be easily occluded if the reaction involves slurry mixture or solid products. Alternative approaches have been investigated to solve this disadvantage. Conventional plug flow reactors and oscillatory flow mixing reactor[57] are two possible options, even if both have serious drawbacks compared to the micro-reactor.

For this reason in our laboratories a novel continuous flow reactor system, MJOD (multi-jet oscillating disk) reactor has been developed and optimized.

This new chemistry platform allows maintaining the advantages, fixing some lacks of the micro-reactors. Additional details and technical description of the MJOD reactor used during all the flow experiments of this thesis are provided in Experimental 4.2.7.

Introductory experiments

The conclusive phase of the development of the synthesis of the target molecule **20** was to adapt and optimize the batch protocol or the application with the multi-jet oscillating disk (MJOD) flow reactor.

At the outset, some screening experiments involving different reaction volumes and different work-up procedures were performed. We were not able to isolate the product **20** after quenching (cold water) the collected post reaction mixture from the flow reactor. In the place of the method involving quenching of the post reaction mixture we introduced a direct paper filtration. The filter funnel was placed at the MJOD reactor output position. Filtration experiments revealed an isolated product of relative good quality (high purity) but the recovery (isolated yield) was rather scares. The paper filter was then substituted with a Buchner filter equipped with a sintered glass dish (D=55 mm, Pyrex porosity grade 3). The semi-continuous filtration of the product on the glass-sinter funnel represented a breakthrough for the investigation. By means of this technique we could collect the majority of the synthetized compound. Reaction details and results of these introductory experiments are reported in Table 9 and Figure 16.

Figure 16. Yield of isolated product **20** obtained with different work-up of the post reaction mixture. Q= quenching. PF=paper filtration. GF= glass-sinter funnel filtration.

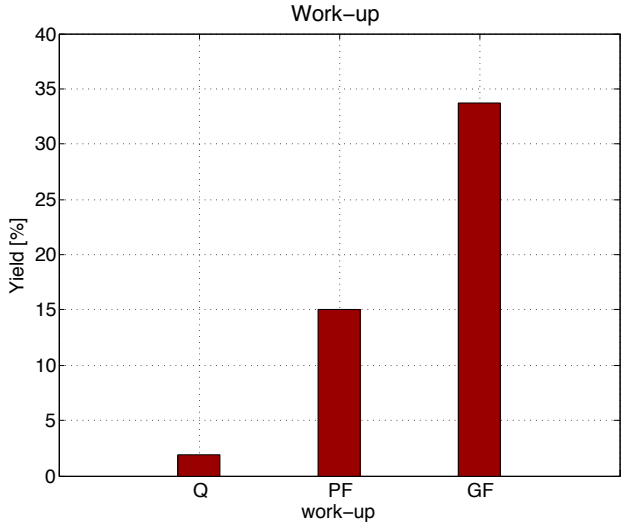

Table 9. Transfer of batch protocol to the multi-jet oscillating disk (MJOD) flow reactor rig. Adaption and optimizing of the transferred flow process. Introductory experiments.

#	DMH [mmol]	K_2CO_3 [mmol]	H_2O [ml]	ICl [mmol]	EtOAc [ml]	Time [min]	Quantity [g]	yield [%]	Work up
1	150	420	300	330	300	10	1.099	1.93	Q[a]
2	100	280	400	220	200	20	-	-	Q[a]
3	100	280	200	220	100	20	0.304	0.80	Q[a]
4	50	140	100	110	50	4	2.869	15.10	PF[b]
5	50	140	100	110	50	4	6.407	33.72	GF[c]

[a] Q = quench with cold water
[b] PF= filtration on a paper filter
[c] GF = filtration on a glass-sinter funnel

The reaction time was disclosed to be a fundamental parameter for the present synthesis performed in batch reactor. Different residence times were then attempted adjusting the pump speeds. The numerical values of the responses are summarized in the right hand column of Table 10, reaction details are described in the footnotes. A graphical overview of the results over the assessed residence time is presented in Figure 17. The reaction yield reaches a peak of 58.72% with a residence time of 9 minutes before starting to decrease. The reaction showed the same behavior observed during the batch process. A minimum starting time is required, as confirmed by the low value of the first experiment. The gradually decrease of the yield suggests a degradation of the product prolonging the residence time.

Figure 17. Residence time variation analysis.

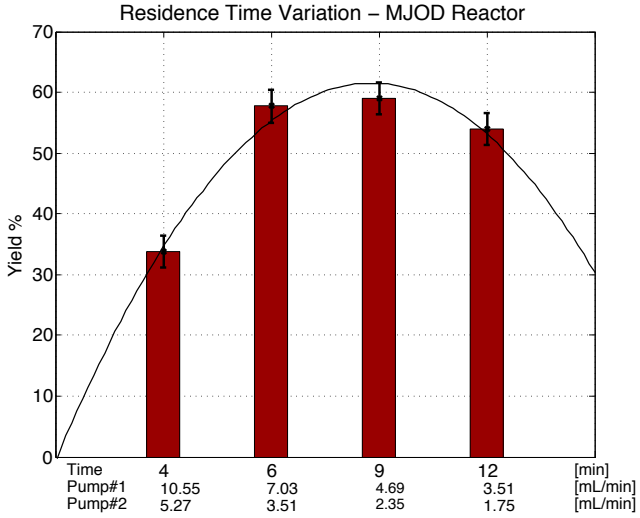

Table 10. Residence time analysis.[a]

#	Pump#1[b] rate [mL/min]	Pump#2[c] rate [mL/min]	Residence Time [min]	Product Amount [d] [g]	Yield [%]
1	10.55	5.27	4	6,407	33,72
2	7.03	3.51	6	10,963	57,71
3	4.69	2.35	9	11,098	58,72
4	3.51	1.75	12	10,257	53,99

[a] The reaction was performed contacting a mixture of 50 mmol of 5,5-dimethylhydantoin, 140 mmol of K_2CO_3 in water 100 mL (reservoir # 1) and a mixture of 110 mmol of I-Cl in Ethyl Acetate 50 mL (reservoir #2)
[b] rate of the pump connected to the reservoir # 1 containing the substrate mixture
[c] rate of the pump connected to the reservoir # 2 containing the iodinating reagent mixture
[d] Weight of the dried product: theoretical yield 18.9 [g].

Replications of the reaction with residence time of 9 minutes were executed to evaluate the stability and the reliability of the results, reported in Table 11. Statistical parameters were calculated and reported in Table 12.

Table 11. Central experiment replications: 50 mmol DMH, 140 mmol K_2CO_3, 110 mmol ICl, 100 mL H_2O, 50 mL EtOAc, t_R=9 min

#	weight [g]	yield [%]
1	11.098	58.72
2	11.305	59.51
3	11.640	61.27
4	10.779	56.74
5	11.199	58.95

Table 12. Statistical parameters for the yield of the reactions performed in the MJOD reactor with a residence time of 9 min.

Geometric Mean[a]	Mean [b]	Min	Max	MAV[c]	Std[d]	Var[e]
59.02	59.04	56.74	61.27	1.08	1.627	2.65

[a] $GM = (\sum_{i=1} y_i)^{1/n}$, *i*= experiment number: *i*=1-5 Table 11
[b] $\mu = \frac{\sum_i y_i}{n}$, *i*= experiment number: *i*=1-5 Table11
[c] $MAV = \frac{\sum_{i=1} y_{max} - y_{min}}{n}$, mean absolute variation, *i*= 1-5 Table11. *n*= 5.
[d] $Std = \sqrt{\frac{\sum_1^i (y_i - \mu)^2}{n-1}}$, i= experiment number: =*i*1-5 Table11 *n*= 5.
[e] $v = std^2$

Additional experiments were performed in order to evaluate the model, centred on the best value of the screening phase (reference experiment: residence time 9 min). Experimental conditions and results are reported in Table 13.

During the screening phase the variation between the different residence time was of three minutes. We observed that this slightly variation of the residence time influenced significantly the response. For this reason, additional experiments (#1 and #2) with residence time of 7.5 minutes were performed.

The aim of this passage was to verify the presence of a maximum between 6 and 9 minutes of residence time. Figure 18 shows that the yields reached with the intermediate time value of 7.5 min are lower than the reference experiment response (mean value).

Figure 18. Residence time effect. Comparison between reference experiment and experiment #1 #2 of Table 13.

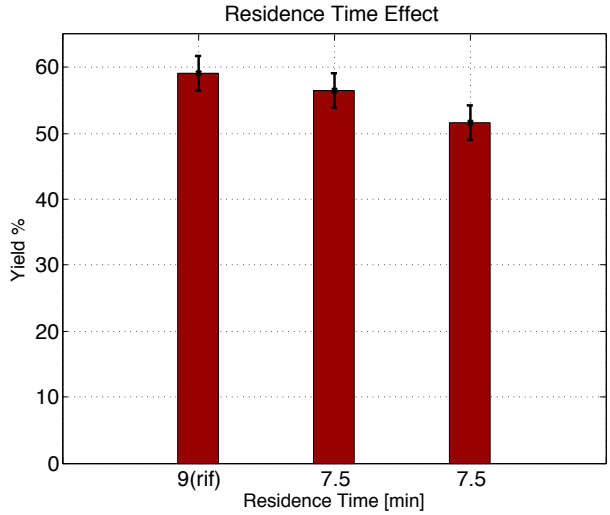

Experiments at room temperature and with different quality of I-Cl were performed, confirming the reference experiment as the best one. In particular, the higher purity I-Cl provided a result comparable with the reference response that didn't justify the usage of a more expensive reagent.

The reaction was run also using a double volume of ethyl acetate for the mixture of the iodinating reagent. The better result of this procedure was confirmed by the replication of the experiment. Figure 19 graphically represents the achieved results.

Figure 19. Temperature effect: experiment #3. I-Cl quality effect: experiment #5. Volume of Ethyl Acetate effect: experiment #6 #7. Comparison with the mean value of the reference experiment.

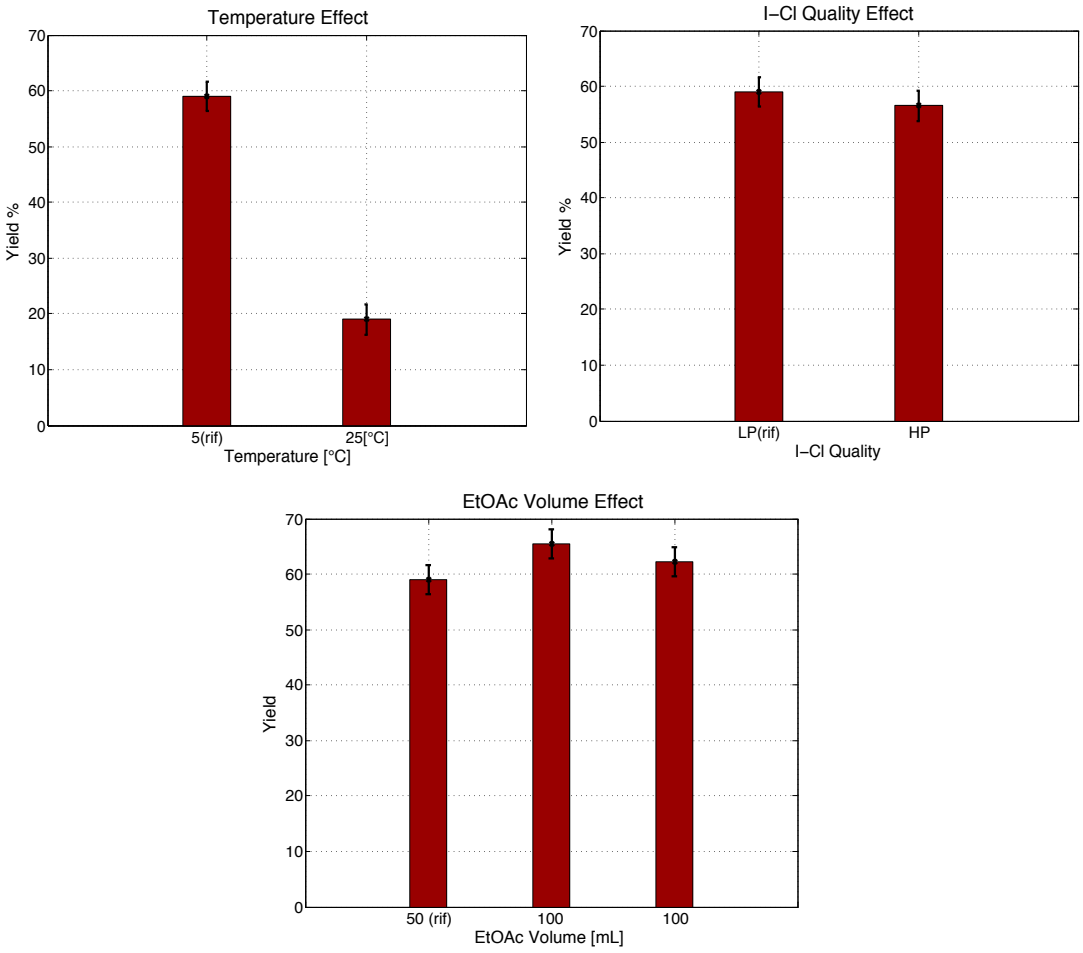

A last set of experiments was performed varying the piston speed. The influence of this variable on the response is significant.

The effects on the yield are graphically represented in Figure 20. The bar-graph displays a low of 9.84% for the experiment with no agitation.

The response increased rapidly starting slightly the piston and remained stable throughout the series of the experimented reactions.

A huge peak of 74.33% for the experiment run with an oscillation speed of 100 rpm can be observed.

The unexpected result was verified not to be an outlier repeating the experiment.

Figure 20. Oscillating frequencies: experiment #13-#17.

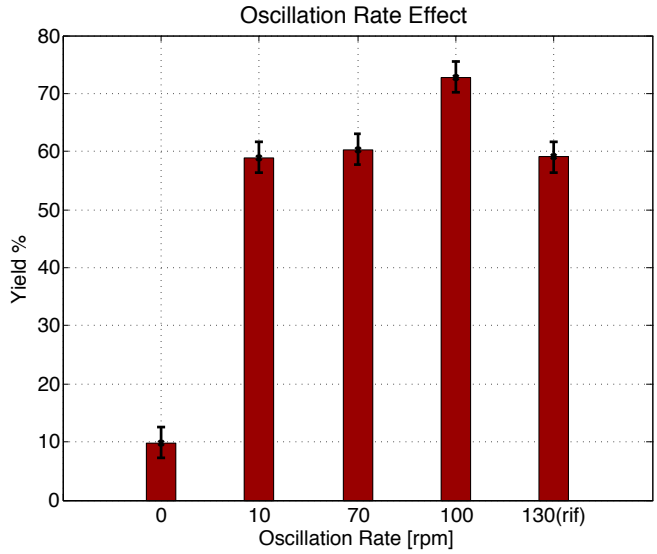

Table 13. Model evaluation experiments and additional experiments

#	DMH [mmol]	K_2CO_3 [mmol]	H_2O [ml]	ICl [mmol]	EtOAc [ml]	time [min]	Rate [rpm]	weight [g]	yield [%]
Residence Time = 7.5 min									
1	50	140	100	110	50	7.5	130	9.814	51.66
2	50	140	100	110	50	7.5	130	10.731	56.49
Room Temperature[a]									
3	50	140	100	110	50	9	130	3.606	18,98
Higher Purity I-Cl [b]									
4	50	140	100	110	50	9	130	6.169	32.47
5	50	140	100	110	50	9	130	10.733	56.50
Higher dilution[c]									
6	50	140	100	110	100	9	130	12.431	65.45
7	50	140	100	110	100	9	130	11.811	62.18
Oscillation Rate[d]									
8	50	140	100	110	50	9	0	1.869	9.84
9	50	140	100	110	50	9	10	11.21	59.01
10	50	140	100	110	50	9	70	11.46	60.32
11	50	140	100	110	50	9	100	14.121	74.33
12	50	140	100	110	50	9	100	13.523	71.19

[a] Temperature=25 °C
[b] 99.998% trace metals basis I-Cl (SigmaAldrich)
[c] Higher dilution for the mixture of the iodinating reagent 100mL instead of 50 mL
[d] Varied changing the voltage of the power supply [0 , 5 , 10, 15, 20] [V]

Long-run time reaction

Predictions

The achieved results of the introductory experiments confirmed that the enhanced mixing and the temperature control provided by the MJOD-flow reactor improve the efficiency of the process, in terms of yield and reduced reaction time. To understand concretely the benefits of the continuous flow process, a long-time run experiment was performed. By conduct such an experiment we expected to minimize the product loss and the uncertainties associated to the critical start-up and shut down operations.

The results of the preliminary tests were used to select the conditions for each variable involved in the continuous process. Different combinations of solvent volume (ethyl acetate: 50 mL or 100 mL) and oscillation rates (130 rpm or 100 rpm) were considered to predict a theoretical production of **20** during three different long-time runs (6 h, 8 h or 10 h). Numerical values of the variables with the estimated response are reported in the right hand column of Table 14. Details and explanations are described in the footnotes of the Table.

Table 14. Predictions estimate for long run time reaction experiments

#	Volume [mL]			t[a] [min]	N[b]			Oscillation Rate [rpm]	Predicted Product Quantity [g]		
	V_{EtOAC}	V_{H2O}	V_{TOT}[d]		6h	8h	10h		6h	8h	10h
1	50	100	150	21	16	22	28	130	188	251	314
2	100	100	200	28	12	16	21	130	153	204	254
3	50	100	150	21	16	22	28	100	232	310	387
4[c]	100	100	200	28	12	16	21	100	187	250	313

[a] time for throughput the whole reaction volume V_{TOT} *:* $t = \frac{V_{TOT}}{\text{Flow rate}}$, where $\text{Flow rate} = \frac{V_{REACTOR}}{\text{Residence time}}$,
with $V_{REACTOR}$=63.33 mL and Residence time=9 min.

[b] number of single reaction that can be performed consecutively in a fixed time t_{TOT}, [6 8 10] [h] $N = t_{TOT} \cdot \text{Flow Rate} \cdot \frac{1}{V_{TOT}}$

[c] prediction with a higher amount of solvent and an higher oscillation rate considering a benefit on the yield proportional to the one reached in the reaction #15 and #16 of the evaluation of the process.

[d] see Table 15 (a) and (b) for details of reaction mixture composition.

Table 15. Details of reaction mixture composition: (a) V_{TOT} 150 mL, (b) V_{TOT} 200 mL

(a)

V_{TOT}=150 mL				
Compound	**Time[h]**			
	6	**8**	**10**	
DMH	108	140	180	g
I-Cl	300	392	501	g
K_2CO_3	326	425	543	g
EtOAc	844	1100	1407	mL
H_2O	1688	2200	2814	mL

(b)

V_{TOT}=200 mL				
Compound	**Time[h]**			
	6	**8**	**10**	
DMH	81	108	135	g
I-Cl	225	300	375	g
K_2CO_3	244	326	407	g
EtOAc	1266	1688	2111	mL
H_2O	1266	1688	2111	mL

Results

The set of conditions #3 was selected to perform the long-time run experiment. We decided to utilize the improvement of the yield obtained by the low ethyl acetate volume and by the slower oscillation rate, disclosed during the screening phase. In particular, a lower amount of solvent allows running consecutively a higher number of reactions, which results in a higher quantity of product in a fixed total time for the experiment. Performing the run for 8 hours resulted to a 22-fold scale-up of the screening experiment. The expected result (310 g) was estimated according to the yield (71%) of the short-run time reaction (Theoretical weight: 418 g).

About 375 g (≈90% yield, about 20% of improvement above the predicted value) of product were collected during the 8-hours run experiment by means of a semi-continuous vacuum filtration (14 batches of filtered product were collected).

1.6. DIH characterization

Literature researches revealed nor information neither spectra to check the quality of the product obtained during the reactions. This lack of information is mainly due to the low thermal stability of the target molecule **21**. The pure solid 1,3-diiodo-5,5-dimethylhydantoin begins to decompose at 180-200 °C , according to the literature[58], and the decomposition rate strongly increases in solution already at room temperature. Several techniques have been tested to perform an analysis of the product. Positive and negative Electrospray Ionizations ESI analyses have been performed without, however, leading to any results. Moreover, because the decomposition take place instead of vaporisation, also Gas-Chromatography/Mass (GC/MS), revealed to be a useless analytical technique.

Thermal Gravimetric analysis TGA and Qualitative thermal tests confirmed that the product obtained was the desired one. The shape TG curve shows that the thermal decomposition occurs in three steps, Figure 21.

Figure 21. TGA profile of sample DIH #5 where (x_1, x_2)=[0,0]

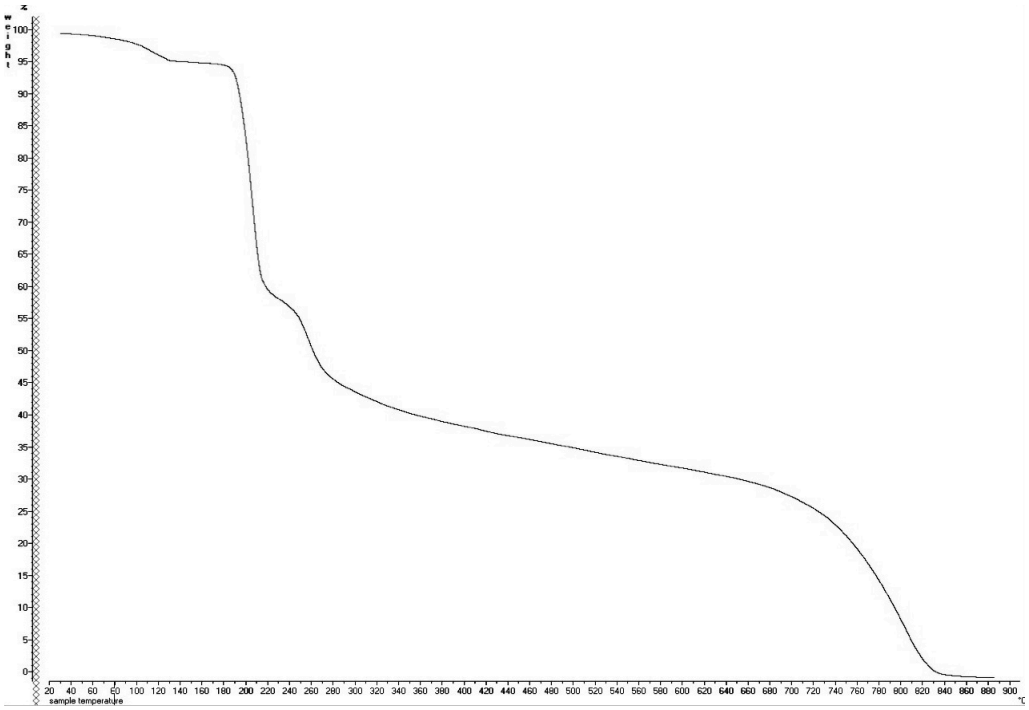

The slightly mass loss (5%) between 100 °C and 200 °C is associated to the small amount of residual water present in the sample. Around 180 °C, the curve shows a weight loss of approximately 35% corresponding to the loss of one of the iodine atom (MW iodine = 126.9, MW DIH = 379.5). Another mass loss of 35%, associated with the loss of the second iodine atom, take place above 220 °C and slowly keeps on until 700 °C. Then the residue completely decomposes.

To qualitative verify the release of gaseous iodine, 200 mg of product have been placed in a round bottom flask and slowly heated by means of a heat gun, providing the expected purple vapours, due to the presence of the iodine atom. At the end of the decomposition, the residue was about the 35% of the initial weight, in complete agreement with the TGA data.

A Fourier Transform Infrared FT-IR spectrometry analysis of the powder has been performed, Figure 22.

Figure 22. IR spectra of sample DIH

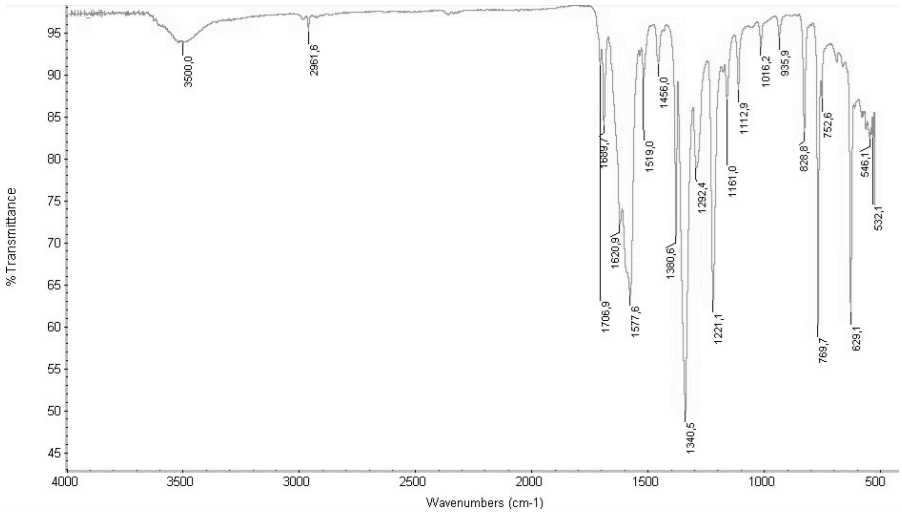

Figure 23 shows the differences between the product and the starting material. It is important to point out that the signal at 3200 present in the spectra of DMH related to the presence of the N-H group disappears in the one of the DIH.

The spectrum of **21** shows instead a signal at higher wavenumber associated to the humidity present in the sample, confirmed also by the NMR analysis.

Similarities between the spectra of the product obtained during the diverse phases of the development are displayed in Figure 24.

Figure 23. IR spectra of sample: comparison between (a)DMH_ Aldrich **21**, (b) DIH produced **20**

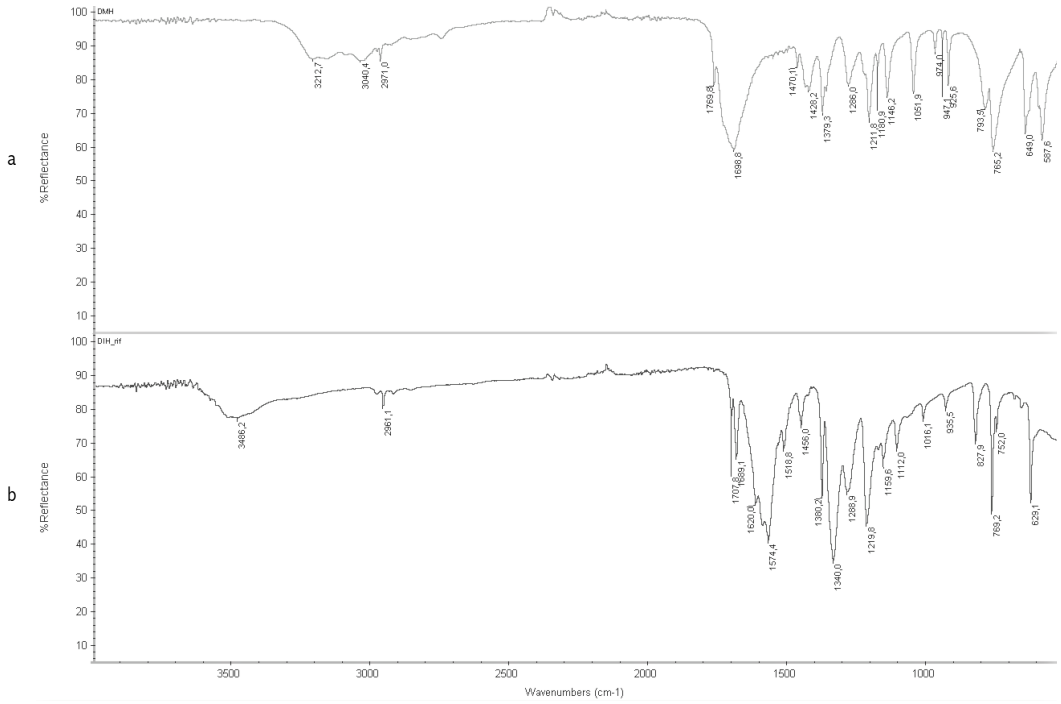

Figure 24. IR spectra of sample: comparison between (a) DIH_batch reactor_small scale, (b) DIH_batch reactor_upscaled, (c) DIH_MJOD

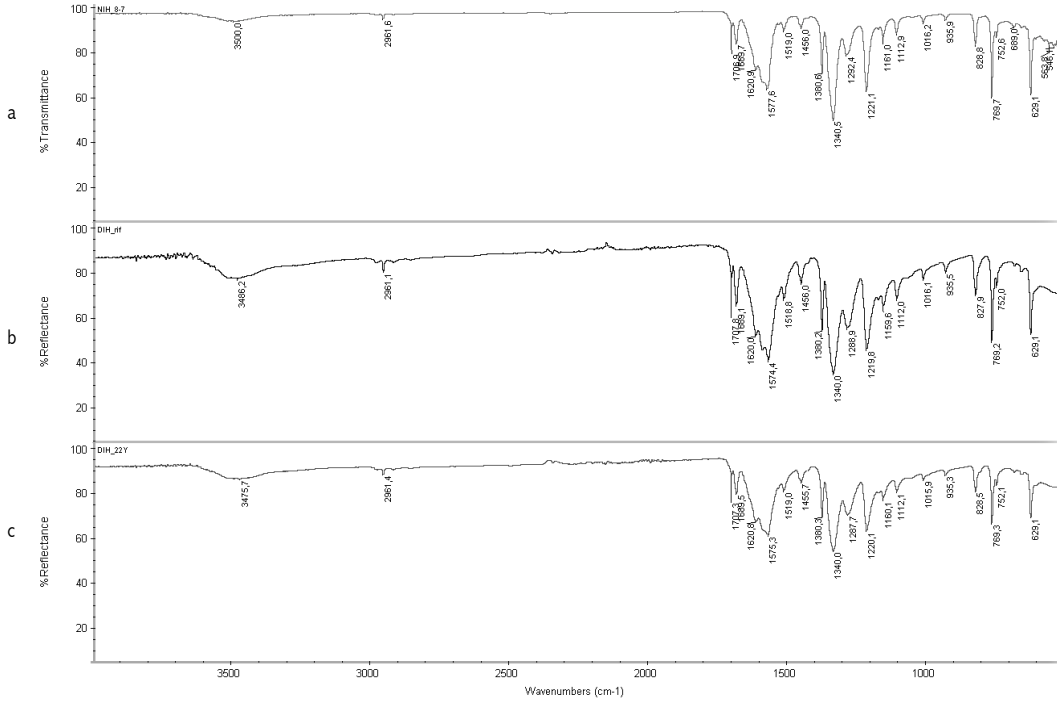

The product of the same reaction performed with the MJOD platform is analysed. The first sample is of the product collected during the first minute after the starting of the reaction, the other is the one collected at the end of the reaction, after being exposed to a consistent amount of solvent. The solvent flow changes the colour of the sample from yellow to white but doesn't change the IR spectrum, as shown in Figure 25.

Figure 25. IR spectra of sample: comparison between (a) DIH , (b) DIH after light and room temperature exposure.

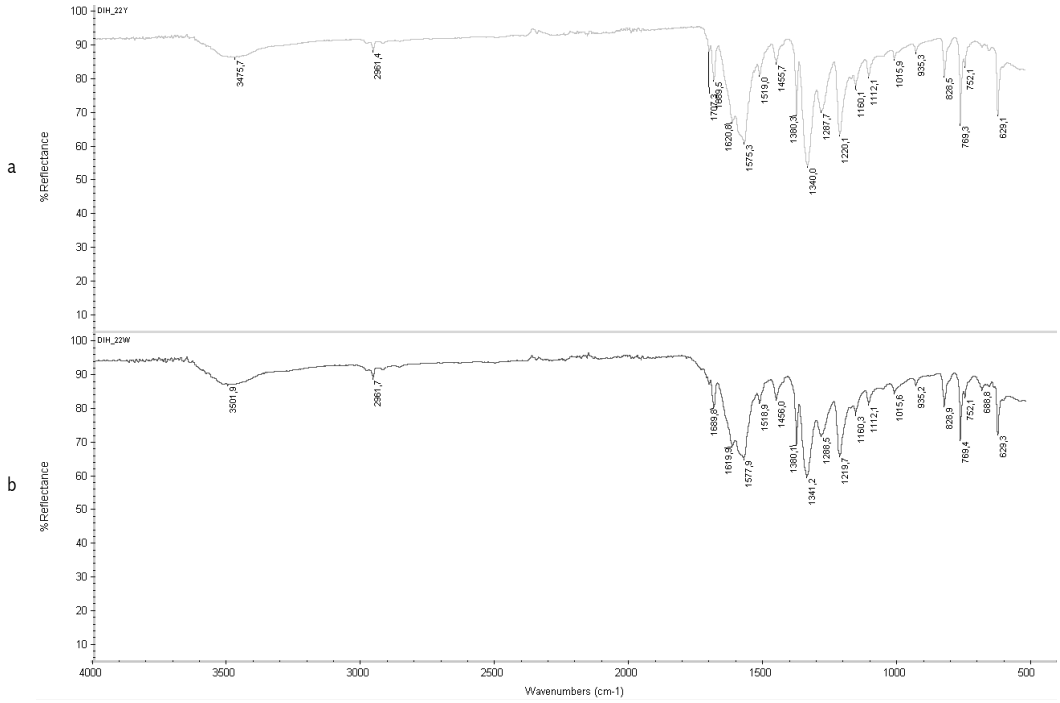

The Proton Nuclear Magnetic Resonance ^{1}H-NMR of the starting precursor 5,5-dimethylhydantoin and of the target molecule **20** has been executed, Figure 26. The area under each pattern is obtained from the integration of the function that defines the signal and is proportional to the number of hydrogen nuclei whose resonance is giving rise to the pattern. Measuring or integrating the different NMR resonances, information regarding the relative numbers of chemically distinct hydrogens can be found. The spectrum of the reagent **21** shows three different peaks because there are three different environments for the hydrogen atoms in the moiety, as expected. Calculating the relative intensities, proportional to the number of hydrogens that are accountable for

the signal, it is possible determine the ratio between the different peaks 1:1:6. The two broad singlets at 9.5 and 7.0 ppm correspond respectively to the imidic and amidic nitrogen atoms, and the singlet at 1.4 ppm is related to the two equivalent methyl groups. Comparing the spectrum of the starting material with the one of the target molecule **20** , it is possible to notice that the signals of the hydrogens bounded to the nitrogen atoms are disappeared because of the substitution by iodine atoms, while the methyl one is still present slightly shifted towards lower frequencies.

Figure 26. NMR spectra comparison between (a) SigmaAldrich **21**, (b) obtained **20** (δ are referred to internal TMS)

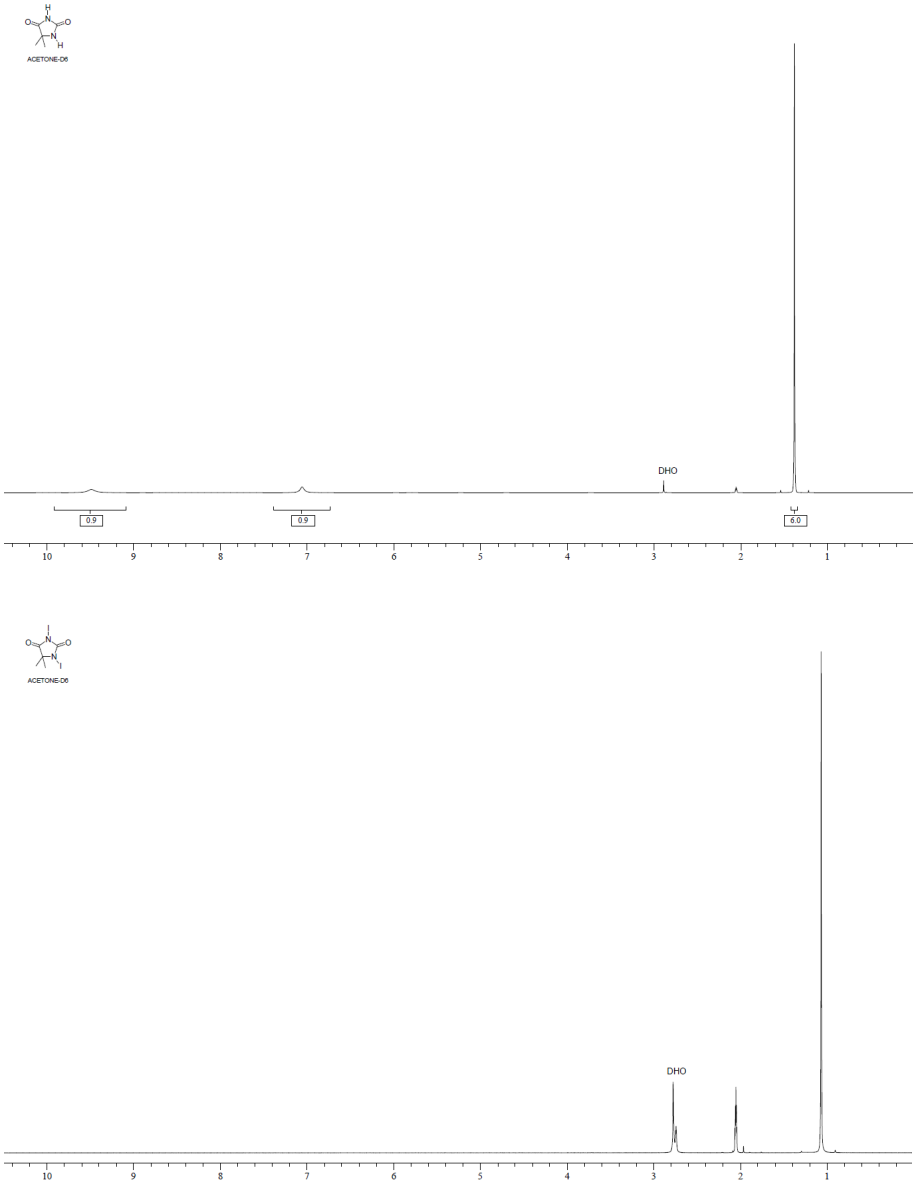

The target molecule **20** was also characterized using an electron spray ionization mass spectrometry (ESI-MS), Figure 27.

The spectrum shows the peak associated to the expected mass of the compound (379.5 g mol^{-1}) and two other signals due to the fragmentation of the molecule. In particular, the signal 254.96 corresponds to the radical cation, associated to the loss of the iodine atom and the addition of H^+.

Figure 27. ESI+ MS spectrum of target molecule 20.

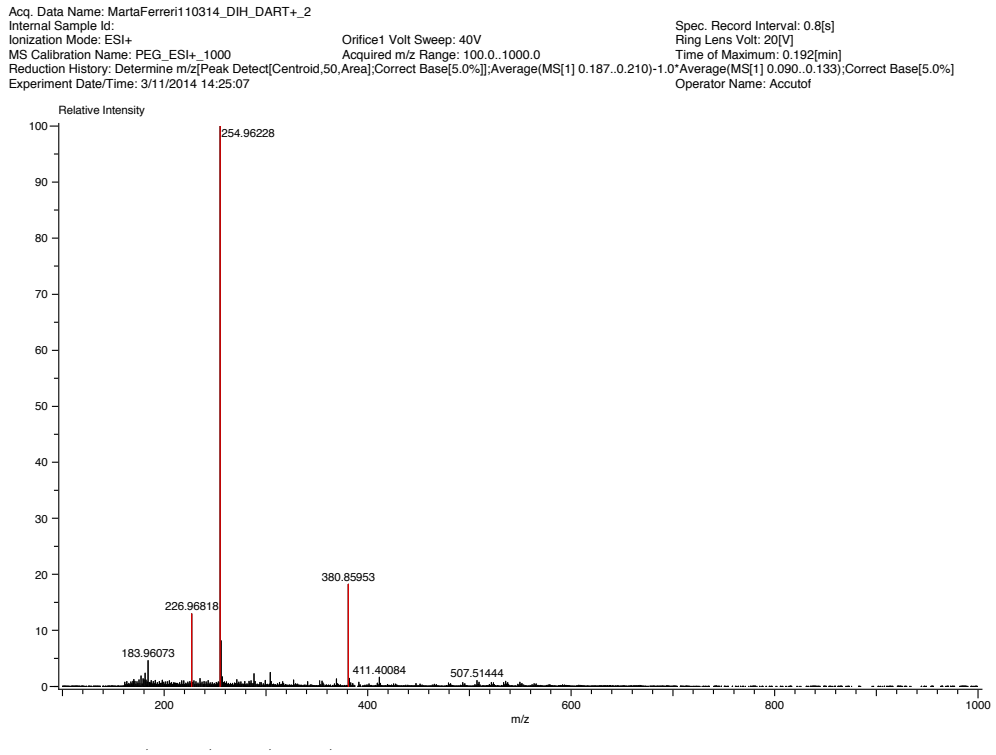

Mass	Intensity	Calc. Mass	Mass Difference (mmu)	Possible Formula	^{12}C	^{1}H	^{127}I	^{14}N	^{16}O	Unsaturation Number
226.96818	103637.25	226.96813	0.05	$^{12}C_4{}^{1}H_8{}^{127}I_1{}^{14}N_2{}^{16}O_1$	4	8	1	2	1	1.5
254.96228	802974.75	254.96304	-0.76	$^{12}C_5{}^{1}H_8{}^{127}I_1{}^{14}N_2{}^{16}O_2$	5	8	1	2	2	2.5
380.85953	146036.75	380.85969	-0.16	$^{12}C_5{}^{1}H_7{}^{127}I_2{}^{14}N_2{}^{16}O_2$	5	7	2	2	2	2.5

MS molecular peak: *m/z* 380.86 [M]+•

3. Environmental Issues and process economy

3.1. Environmental Analysis

Green Chemistry, also referred to as Sustainable Chemistry[59], is a philosophy of chemical and engineering research that promotes the design and the development of processes that minimize or eliminate the use and the generation of hazardous substances leading to significant environmental benefits, innovation and a strengthened economy[60]. This discipline has a different approach to the challenge of reducing the risks posed by chemical processes than the traditional one, based on limiting exposure by controlling circumstantial factors (the use, handling, treatment and post-treatment of chemicals). Indeed, Green Chemistry seeks to minimize the risk by minimizing the hazards[61], regulating the intrinsic factors of a synthesis[62] (selection of chemicals devised to preserve efficacy with reduced toxicity, use of safer auxiliary substances, design of different reaction pathways in order to reduce by-products and unnecessary derivatization, to prevent pollution and waste at the molecular level, to maximize the incorporation of all the materials used into the final product and to increase the energy efficiency[63]).

The areas in which green chemistry has its most immediate impact are fine chemicals and pharmaceutical industries. Those sectors, producing a wide range of chemicals on a small scale, offer more diverse opportunities for introducing new technology than the bulk chemicals sector, furthermore the scale up of the laboratory procedure to plant is less daunting.

Sustainability, by definition, is the capability of a system to be productive integrating optimization and targeting tools for process design and operation. There are several green metrics that can be use to evaluate the environmental impact of a process[64], for instance Trost's atom economy **AE**, reagent relative excess $\boldsymbol{\phi}$, reaction yield **Y**, reaction mass efficiency **RME**, process mass intensity **PMI**, mass productivity **MP**, Sheldon's environmental impact factor $\mathbf{E_{factor}}$, , amongst others[65]. Energy consumption, toxicities of materials and hazard of the process are not included in this dissertation about the green aspects of the 1,3-diiodo-5,5-dimethylhydantoin synthesis.

Preliminary Reaction-Level measures

The balanced reaction for the present iodination is:

$$\mathrm{DMH} + 2 \cdot \mathrm{ICl} + \mathrm{H_2O} + \mathrm{EtOAc} + \mathrm{K_2CO_3} = \mathrm{DIH} + \mathrm{W}$$

When developing chemical processes, chemists focus mainly on maximising selectivity and yield. In recent years, atom economy started to be considered a variable of paramount importance. Atom economy of a process is defined as ratio between the molecular weight of the desired product ($\mathrm{MW_{output}}$) and the total reactants molecular weight ($\mathrm{MW_{input}}$). It is a highly theoretical value that gives a crude indication of how much of the reactants remains in the final product. It is based entirely on the theoretical stoichiometry (ν_o, ν_i=stoichiometric coefficient) of the balanced chemical equation, without taking into account any other reaction detail such as yield, molar excess of reactants, side reaction, solvents, etc.

$$\mathrm{AE} = \frac{\sum \nu_o \cdot \mathrm{MW_{output}}}{\sum \nu_i \cdot \mathrm{MW_{input}}} \cdot 100\% = \frac{\mathrm{DIH}}{\mathrm{DMH} + 2 \cdot \mathrm{ICl}} \cdot 100\%$$

Considering thereafter the present iodination, it is run under non-stoichiometric condition, such that I-Cl is used in a slightly excess and DMH is the limiting reagent. It is possible to define the relative excess of I-Cl involved, taking into account the excess of iodinating reagent **E** and the total mass **TM** of the inputs.

$$\phi = \frac{\mathrm{Excess\ Mass}}{\mathrm{Utilized\ Mass}} \cdot 100\% = \frac{\mathrm{E}}{\mathrm{TM} - \mathrm{E}} \cdot 100\%$$

Using this value, the experimental atom economy of the process $\mathbf{AE_{exp}}$, might be estimated. This parameter takes into account the amounts of reactant atoms that will not be utilized in any products because they are in excess. The $\mathbf{AE_{exp}}$ can be less than or equal to the atom economy because the excess mass is always greater than or equal to zero.

$$\mathrm{AE_{exp}} = \frac{\mathrm{AE}}{(1 + \phi)} \cdot 100\%$$

Post-Process Reaction-Level Green Measures

The percent yield of the reaction **Y**, is given by the ratio between the moles effectively produced of the target molecule DIH ($\mathrm{DIH}_{e,mol}$) and the one theoretically expected from the stoichiometric reaction ($\mathrm{DIH}_{s,mol}$). The reaction yield does not include poor reaction mass efficiencies and correspondingly significant waste of resources (mass or energy). It should be noted that wasted resource might be expensive from both a direct materials cost and a more comprehensive life cycle costing perspective.

$$\mathrm{Y} = \frac{\mathrm{DIH}_{e,mol}}{\mathrm{DIH}_{s,mol}} \cdot 100\%$$

Using this parameter it is possible to estimate the reaction mass efficiency of the process **RME**, a measure of the efficiency of the reactant mass to end up in the desired product. Catalysts, solvents or other reagents not involved in the balanced chemical equation for the process are not taken into account in the calculation[66]. Reaction mass efficiency relates the total reactant mass, yield and atom economy. This combined metric is probably the most significant measure of the environmental impact of the process.

$$\mathrm{RME} = \mathrm{AE}_{\mathrm{exp}} \cdot \mathrm{Y} = \frac{\mathrm{DIH}_{e,mol}}{\mathrm{TM}} \cdot 100\%$$

Final Process-Level Green Measures

It is necessary to consider also the non stoichiometric aspects of the chemical reaction such as kind and amount of solvents and other reagents, that often play a major role in a full green chemistry analysis.

In the pharmaceutical area, the prefer metric to benchmark the greenness of processes is Process Mass Intensity **PMI**, as selected by the American Chemical Society Institute Pharmaceutical Roundtable[67]. **PMI** is defined as the total mass of materials (reactants, reagents, solvents and catayst) used to produce a specified mass of product. This metric is adopted as mass-based parameter to drive greater efficiency and innovation. From a business point of

view, it has the advantage over waste-focused metric such as $\mathbf{E_{factor}}$, of communicating sustainability in terms of adding value (increasing productivity) instead of managing cost (reducing waste), focusing on the inputs instead of on the outputs of the process. Maximizing the value and the efficiency of a pharmaceutical production comprises a waste reduction as one of the benefits. Mass intensity is a value that relates yield of product ($\mathrm{DIH}_{s,g}$), stoichiometry, solvent, and other reagents used in the reaction mixture, and expresses their interaction as a weight/weight ratio. In the ideal situation, **PMI** would approach 1.

$$\mathrm{PMI} = \frac{\mathrm{TM} + \mathrm{SM} + \mathrm{ORM}}{\mathrm{DIH}_{s,g}}$$

To highlight the resource utilization, the mass productivity of the process **MP** can be calculated as percentage of the process mass intensity reciprocal.

$$\mathrm{MP} = \frac{1}{\mathrm{PMI}} \cdot 100\%$$

The environmental impact $\mathbf{E_{factor}}$, as previously discussed, expresses the ratio of total waste mass **W** over the theoretical mass of the desired product.

$$\mathrm{E_{factor}} = \frac{\mathrm{W}}{\mathrm{DIH}_{s,g}} = \mathrm{PMI} - 1$$

An ideal $\mathbf{E_{factor}}$ of 0 is almost achieved in petroleum refining, while the production of bulk and fine chemicals gives $\mathbf{E_{factor}}$ of between 1 and 50. Typical $\mathbf{E_{factor}}$ for the production of pharmaceuticals lies between 25 and 100. While water is not included, inorganic and organic wastes diluted in the aqueous stream must be considered. Toxicities and hazardous of the wastes are considered introducing a correction factor Q (<1 if the waste can be recycled and >1 if the wastes are toxic or hazardous). It might be difficult to use this metric as green parameter because of the lack of clarity associated to the concept of waste.

Estimation of the environmental parameters

Table 16 reports the quantity of each compound and the calculation of the total amount of reagents **TM**, solvents **SM**, other reactants and waste **W** in the different phases of the development of the process. Total mass includes everything that is used in the process with the exception of water. Total mass also includes all mass used in acid, base, salt and organic solvent for washing, extractions, crystallizations, or switching. Water has been excluded from mass calculations since it skews mass data in many processes and does not constitute a significant environmental impact *per se*.

Table 17 displays the calculation of the mass excess **E** of the iodinating reagent, I-Cl, above the stoichiometry of the reaction. Table 18 show the environmental parameters calculated using the equations previously discussed.

Table 16. (a) Reagents, (b) Solvents and Other reagents.

(a)

		Batch small scale				Batch up-scaled process				MJOD-reactor			
Name	**MW**	**Moles [mmol]**		**Mass [g]**		**Moles [mmol]**		**Mass [g]**		**Moles [mmol]**		**Mass [g]**	
	[g/mol]	**s[a]**	**e[b]**	**s[a]**	**e[b]**	**s[a]**	**e[b]**	**s[a]**	**e[b]**	**s[a]**	**e[b]**	**s[a]**	**e[b]**
DMH	128.1	5	5	0.64	0.64	50	50	6.47	6.47	50	50	6.47	6.47
ICl	162.3	10	15	1.62	2.43	100	110	16.2	17.8	100	110	16.2	17.8
Total Mass TM				**2.26**	**3.07**			**22.6**	**24.2**			**22.6**	**24.2**
DIH	379.5	5	4	**1.89**	**1.53**	50	33	**19.2**	**12.3**	50	37	**19.2**	**17.5**

[a] stoichiometric amount

[b] effective experimental amount

(b)

		Batch small scale		Batch up-scaled process		MJOD-reactor	
Name	**MW g/mol**	**mL**	**g**	**mL**	**g**	**mL**	**g**
EtOAc	88.11	10	8.95	100	89.5	50	44.75
Solvent Mass SM			**8.95**		**89.5**		**44.75**
K_2CO_3	138.20		2.070		19.32		19.32
Other Reagents Mass ORM			**2.070**		**19.32**		**19.32**
Waste Mass W[a]			**12.56**		**120.70**		**74.51**

[a] The waste mass is calculated without taking into account the water involved in the process because it doesn't have a significant environmental impact. $W = TM + SM + ORM - DIH_{e,g}$

Table 17. Excess calculation

	Batch small scale				Batch up-scaled process/MJOD-reactor			
Name	**mol**	**Mole ratio**	**Mole equivalents**	**Excess g**	**mol**	**Mole ratio**	**Mole equivalents**	**Excess g**
DMH	0.005	1	1	0	0.0505	1	1	0
I-Cl	0.015	3	1.5	0.816	0.11	2.17	1.09	1.40
			Excess E	**0.816**			**Excess E**	**1.40**

Table 18. Environmental parameters results

Preliminary Reaction-Level measures				
Parameter		**Batch Small scale**	**Batch up-scaled process**	**MJOD-reactor**
AE	Atom Economy	83.81%	83.81%	83.81%
Φ	Relative Excess	35.85%	7.17%	7.17%
AE_{exp}	Experimental Atom Economy	61.69%	78.20%	78.20%
Post-Process Reaction-Level Green Measures				
Parameter		**Batch Small scale**	**Batch up-scaled process**	**MJOD-reactor**
Y	Yield	80.64%	65.27%	89.76%
RME	Reaction Mass Efficiency	49.8%	51.04%	70.27%
Final Process-Level Green Measures				
Parameter		**Batch Small scale**	**Batch up-scaled process**	**MJOD-reactor**
PMI	Process Mass Intensity	7.42	7.01	4.65
MP	Mass Productivity	13.46%	14.25%	21.48%
E_{factor}	Environmental-Impact Factor	6.42	6.01	3.65

As expected, the atom economy is the same for the three phases of the development. It is a parameter based only on the stoichiometry of the balanced chemical reaction. The higher relative excess of iodinating reagent used in the laboratory-scale process, leads to a lower level of experimental atom economy and consequently to a lower reaction mass efficiency. In spite of the higher yield, the small-scale batch process results as attractive as the up-scaled batch one, comparing the values of the process mass intensity (≈7), mass productivity (≈14%) and the $\mathbf{E_{factor}}$ (≈6). The great improvement on the environmental impact of the synthesis can be remarked observing the results referred to the

multi-jet oscillating disk (MJOD) reactor. This reactor enhances significantly the performances of the process. The enhanced yield leads to a higher reaction mass efficiency. Benchmarking with the batch process, the amount of solvent is substantially reduced leading to a reduction in the size of the downstream equipment, wastes and energy consumption per unit of product. It results in a value for the process mass intensity and for the environmental impact factor half fraction of the parameters of the batch process ≈4 and ≈3, respectively. The achieved results are presented graphically in Figure 28.

Figure 28. Graphical representation of the results of the environmental analysis: Process Mass Intensity, E_{factor}, Mass productivity

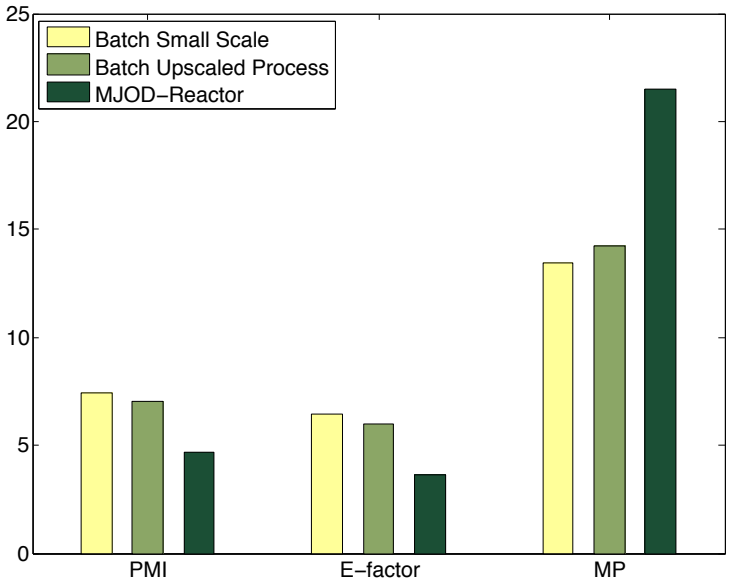

Clearly, wasted resources may have significant cost implications. For instance, a low atom economy metric greatly affects the cost of a synthesis. The agents involved are not used efficiently and incorporated into the product, purification and separation of the product might be required to remove by-products, reactants, reagents solvent, etc. and consequently the environmental, safety and health costs associated with the management of materials and post-treatment increase. New green chemistry processes will be introduced only if they can provide a payback quickly enough to be attractive in an economic sense. Thereafter an approximate economical evaluation of the process is reported in order to illustrate the added-value of the product and the economical and environmental benefits reached by the optimization of the process.

3.2. Economical analysis

One of the core principles of Chemical Engineering is the ability to take resources and raw materials adding value through their transformation into something more useful and hence more valuable products.[68]

The iodination reagent 1,3-diiodo-5,5-dimethylhydantoin **20** is a relative expensive reagent compared to the starting material, the substrate 5,5-dimethylhydantoin **21** and the iodinating reagent I-Cl**.**

The optimization of the production process allows determining the influence of processing technique and sequencing, equipment design and process variables in order to obtain an optimized atom economy and other environmental parameters, and thus the overall cost of the final process.[60, 63-64]

The cost-profit analysis here discussed is not exhaustive, because it gives no information about the utilities, the operating costs and the waste products treatment. Nevertheless, it gives a perception of the added value of the synthetized product, when compared to the cost of the starting materials, and the economical and environmental benefits reached by the optimization of the process. Table 19 reports the prices of the utilized reagents.

Table 19. Reagents prices

Compound	Price [a]	
DMH	7.32	€/100g
DIH	1426	€/100g
K_2CO_3	4.22	€/100g
95% I-Cl[b]	44	€/100g
99% I-Cl[c]	1294	€/100g
AcOEt	90	€/L

[a]The prices were retrived from the internet page http://www.sigmaaldrich.com. on January 30, 2014.
[b] Purity 95% I-Cl
[c] Purity 99.99% I-Cl

The stoichiometry of the transformation process set the material and heat flows for the process and ultimately the economy. The cost associated with the feedstock is determined by both its quantity and quality.

The iodinating reagent iodine monochloride is the most expensive and environmentally noxious compound used in the current process. The quantity of I-Cl was chosen to be 10% higher than the stoichiometric required one. Also the influence of the purity of such a reactant has been analysed. The benefit on the yield of the reaction performed with an I-Cl of higher purity (HP: 99.998% trace metals basis I-Cl vs LP: 95% reagent grade I-Cl) didn't justify the usage of such more expensive reagent.

The recovery and recycle of the unreacted iodine monochloride is subject of further development of the process in order to achieve an improved atom economy and a lower environmental impact.

The investigations of the process development were divided into three parts:

(1) Small-scale and up-scaled (10×) batch processes
(2) Transfer and development of the continuous flow process by means of the multi-jet oscillating disk (MJOD) flow reactor platform.
(3) Long time (8 h) run experiment using the MJOD flow reactor

Table 20 reports the total expenses for the reagents (the inputs) used and the commercial value of the obtained product (the output), separately for each phase.

During the first phase of the development, ≈300 g of DIH was produced (≈20 g in the small-scale (<1 g) batch and 280 g in the up-scaled (10×) batch reactor). The data show a rate of return around of 11 times the cost of the inputs (in details ≈8.5 for the small-scale and ≈11 for the up-scaled process) that corresponds to a profit of 980%.

The results obtained assessing and optimizing the flow process show a similar rate of return (rate of return of ≈11 times the costs of the inputs, profit of 975%). During these investigations ≈200 g of the target compound was synthetized.

The important benefits due to the continuous flow process are remarkable observing the data referred to the single optimized reaction of 8 hours performed with the MJOD flow reactor. 375 g of 1,3-diiodo-5,5-dimethylhydantoin were produced. The rate of return in this case was of 23 times the total cost of the starting materials (profit of 2175%), Figure 29.

Table 20. Amount of reagents used in the different phases of the developement

	Compound	Quantity			Cost [€]		
		1[a]	2[b]	3[c]	1[a]	2[b]	3[c]
	DMH	210g	160g	140g	15	12	10
	K_2CO_3	620g	480g	425g	27	20	18
	I-Cl	580g	445g	390g	255	195	172
	EtOAc	3.2L	1.25L	1.1L	98	38	34
$INPUT_{total\ costs}$					395	265	235
$OUTPUT_{total\ cost}$	DIH	300g	200g	375g	4280	2850	5345
PROFIT[d]					3885	2585	5110
%PROFIT[e]					980%	975%	2175%
Rate of Return[f]					10.86	10.73	22.84

[a]Batch process

[b]Short-time run flow process

[c] 8 hours run flow process

[d] $\text{PROFIT} = \text{OUTPUT}_{\text{total cost}} - \text{INPUT}_{\text{total cost}}$

[e] $\%\text{PROFIT} = \frac{\text{OUTPUT}_{\text{total cost}} - \text{INPUT}_{\text{total cost}}}{\text{INPUT}_{\text{total cost}}}$

[f] $\text{Rate of return} = \frac{\text{OUTPUT}_{\text{total cost}}}{\text{INPUT}_{\text{total cost}}}$

Figure 29. Rate of return for the different phases of the development. N=factor of return(Added value = N × Cost of input)

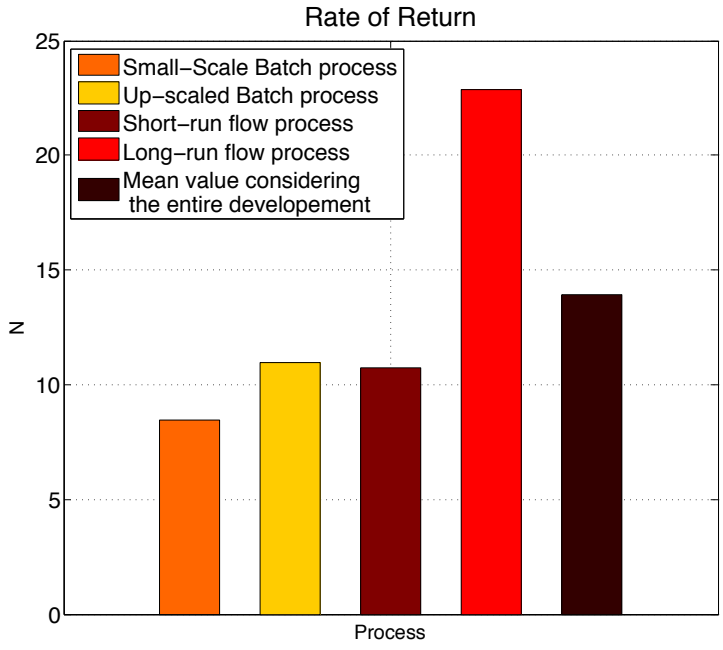

The extraordinary result reached by means of the flow reactor platform is just one of the benefits that the continuous process can bring. Some other aspects can have an indirect benign impact on cost and quality of a process.

Using the flow reactor, the reaction time is substantially reduced. When the reaction is run in batch mode it requires a long period of time (> 45 min) to achieve the desired conversion, leading to low-throughput per unit time. Performing the continuous flow process a drastic reduction of the required reaction time (< 9 min) was observed.

The flow reactor can run the same amount of reagents in less than half time (20 min) than the batch reactor. The productivity for the MJOD flow reactor was estimated to be 47 g h^{-1}. The volume of needed solvent is significantly reduced (50 mL of Ethyl Acetate for MJOD reactor vs 100mL for up-scaled batch process) leading to an higher process throughputs and to a reduction in size of the downstream equipment and in energy consumption per unit of product.

Pharmaceutical manufacturing extensively uses two methodologies to evaluate a process: quality by design (QbD) and contamination review question (CRQ).[69] QbD approach is facilitated by the use of the flow chemistry platform that allows continuous measurement and control of operating parameters as temperature and flow rates. The continuous platform enhances also the mixing and consequently the mass and heat transfer penalized by the low surface-to-volume ratio of the batch reactor. CQR methodology improves the product quality minimizing operational errors and operator exposure to chemical hazard. The MJOD reactor reduces significantly the risk since many operations are eliminated when compared to the set of operations required by the batch process. The additional unit operations, which have energy requirements in form of electricity, cooling water and supplementary reagents and expenses of manual labour are extremely reduced. During the batch process the product should be filtered, washed first with cold water and later with a mixture of cold water and thiosulfate. By means of the reactor it is possible to perform a semi-continuous filtration of the product concurrently washed by the reaction solvent, in a more uniformly way.

Economical benefits achieved applying flow reactor technology as lower raw material, solvent and energy usage results in a reduced environmental impact of the process.

4. Experimental

4.1. Chemicals, reagents and solvents.

All chemicals used herein were of analytical quality and were purchased from commercial supplier (Sigma-Aldrich, Italia and Norway) and used without further purification prior use.

- Product #: D161403 5,5-dimethyhydantoin [77-71-4]
- Product #: 208221 Iodine monochloride I-Cl [7790-99-0]
- Product #: 209619 Potassium carbonate K_2CO_3 [584-08-7]
- Product #: 72049 Sodium thiosulfate [7772-98-7]
- Product #: 33211N Ethyl acetate [141-78-6]

4.2. Instrumentation

4.2.1. Nuclear magnetic response ^{1}H NMR

The NMR spectra were recorded on a Bruker AV 400 (400 MHz) equipped with a 5 mm multinuclear probe with reverse detection was used to record ^{1}H-NMR spectra. 32 scans were acquired with an acquiring time of 5 seconds.

4.2.2. Gas chromatography – mass spectrometry GC-MS

Agilent 6890 Gas Cromatograph (GC) system equipped with a 30mt x 0.250mm HP-5MS GC column and an Agilent 5973 Mass Selective Detector (MSD) detector were used to record the GC-MS spectra of the antioxidant derivative.

4.2.3. Thermal Gravimetric Analysis TGA

Thass TGA XP-10, Gravimetric Sensitivity: 4700.4 units/mg

Method: 2 steps.

1: Iso at 27.9 °C for 10 min, Sample period: 0.5s

2: Scan from 27.9 °C to 900 °C at 5 °C/min, Sample period: 0.5s

(These data are given in the “Information” menù of the TGA file editor)

4.2.4. Infrared spectroscopy FTIR

Nicolet 380 FT-IR Diamond 30,000-200 cm^{-1}, Thermo Electron corporation , USA.

4.2.5. Electron spray ionization mass spectrometry ESI+ MS

Mass spectrometer: JMS-T100LC AccuTOF^{TM} from JEOL, USA, Inc. (Peabody, MA, USA). (Orthogonal accelerated time of flight single stage reflectron mass analyzer and a dual micro channel plate (MCP) detector).
DART source: DART-100 ion source from IonSense Inc. (Saugus, MA, USA).

An AccuTOF^{TM} JMS T100LC mass spectrometer from JEOL USA, Inc. (Peabody, MA, USA) that uses an orthogonal accelerated time of flight single stage reflectron mass analyzer and a dual micro channel plate (MCP) detector was used for mass spectrometric analyses. A DART-100 ion source from IonSense Inc. (Model nr DART 100, Saugus, MA, USA) was interfaced to the mass spectrometer inlet at a distance of 12 mm between the DART source exit and the cone MS-inlet. A detailed description of the instrumental settings/conditions is as follows; The DART ion source was operated with a temperature of 250 °C and a gas flow of 4.0 L/min.
The DART discharge needle voltage was set to +/-3,000 V and a perforated electrode voltage (electrode 1) of +/-150 V was applied. The grid voltage was set to 250 V.
The AccuTOF^{TM} mass spectrometer operated in the positive/negative mode at a resolving power of approximately 6000 FWHM. The atmospheric pressure interface conditions were as follow; Orifice 1 = +/-18 V, orifice 2 = +/- 3 V and ring lens = +/- 7 V. The temperature of orifice 1 was kept at 100 °C and the voltage of the ion guide (peak to peak voltage) was varied between 800 and 2500 V in order to apply transmission of ions of different *m*/*z* ratios. The spectra acquisition settings applied were as follows; acquisition 100-1000 *m*/*z*, spectral recording interval = 0.5 s, wait time = 0.03 ns and data sampling interval = 0.5 ns. A detector voltage of 2350 V was applied.

The samples were analysed as solutions in dichloromethane/methanol (~ 10 g mL^{-1}) and introduced to the DART gas stream by a glass capillary. Mass calibration and internal mass drift compensation was carried out using standard of known composition.

DART conditions:

DART discharge needle voltage: 3000 V
Electrode Voltage: 150 V
Gas: Helium
Gas flow: 4.0 mL/min
Gas temperature: 250 °C

MS conditions:

Ionization method: DART
Ionization mode: Positive/negative
Orifice1 Voltage: x V
Orifice2 Voltage: x V
Ring Lens Voltage: xV
Orifice1 Temperature: 100 °C
Ion Guide Peak Voltage: 800-2500 V
Detector Voltage: 2350 V
Acquisition range: 100-1000 m/z
Spectral recording interval: 0.5 s
Wait time: 0.03 ns
Data sampling interval: 0.5 ns

4.2.1. Computer software

Matlab

*MATLAB***,** version 8.1;The Mathwork, Inc.:Natick, MA, 2013

Sirius™

SIRIUS™, version 8.1; PRS as,:Bergen, NO, 2013

4.2.2. Multi-jet Oscillating Disk (MJOD) Flow Reactor

Multi-Jet Oscillating Disk (MJOD) flow reactor

Multi-jet oscillating disc (MJOD) flow reactor is a flow chemistry reactor platform developed for conducting continuous flow organic synthesis on millilitre scale rather than micro-scale.

The MJOD milli-reactor possesses further advantages compared to the micro flow reactor systems, which usually involve the mixing of substrate and reagents in a laminar flow in micro-sized channels.

The MJOD reactor rig was designed and developed with the goal to be a versatile reactor system usable for several types of organic reactions in continuous milli-scale (35-50 mL) and to be easily used for telescoped multi-step syntheses. Slurries of the substrate, the reagents or the catalysts can be used without clogging the channels, even thought feeding slurries to the reactor system remain a challenging task liquid-gas-solid multiphase reactions can easily be performed, with the reduction of the quantity of the phase transfer catalyst (PTC) or even in some cases to complete elimination of the PTC. This is a result of the enhanced mixing provided by the mechanical oscillator that ensures excellent mass and heat-transfer.

The MJOD flow reactor platform appears as an extremely flexible system, allowing building different reactor set-ups to provide diverse reactor lengths and reagent inlet patterns adapted for the particular requirement of various synthetic protocols.

The MJOJD reactor is composed of various parts (1) the reagents inlet section(s), (2) the reactor and heat exchanger section(s), (3) the outlet and pressure regulator section, and (4) the oscillator section.

The different units of standard dimensions (o.d. 40 mm) can be combined assembling the male and female joints, of which each unit is equipped, and using commercially available flange swing clamps (o.d. 50 mm as used for vacuum lines and fittings for oil vacuum pumps).

This particular design allows managing the residence time by prolonging or shortening the reactor body (concomitant or by regulate the pumping rate),

optimizing the mass-throughput and maintaining an accurate temperature control.

Each male joint is provided of four inlet channels, though which the reactant mixture is fed by means of pumps that are connected to reagent reservoirs. The inlets can be placed at different levels of the longitudinal direction of the reactor. Each reagent inlet is supplied with one-way valve in order to avoid back kick of the reaction mixture into the reagent feeding tubes, caused by the alternating pressure due to the oscillating movement of the piston. For the present investigation, the reactor was provided of one inlet at the bottom with only two of the inlet channels open.

The reaction mixture goes through the disk-jets with a small cross section <2 mm and enters into an area of larger diameter, the stainless steel tube ($\mathbf{d_{Re}}$: 12 mm, $\mathbf{d_{Ri}}$: 10 mm), which constitute the reactor body.

The decrease of the flow rate, due to this change of the cross section, leads to the formation of vortexes and movements in the mixture that enhance the interactions between the various reactants found in the reaction mixture.

Moreover, the mixing is improved by the oscillating movement of the oscillator that is composed of a large number of perforated disks (generally 60-100 four-jet disks) fixed in equal distances on a shaft (**h**: 1.3 mm), forming a multi-headed piston

The multi-jet disk ($\mathbf{d_D}$: 10 mm, **s**: 4 mm) is made of a polymer of high chemical, thermal and mechanical resistance (Teflon and Polyzene-containing polymers) and is perforated with four jets ($\mathbf{d_J}$: 1.00-1.30 mm), Figure 30.

The oscillator is also furnished with an electrical motor that can be regulated by adjustable direct current power supply for controlling the number of revolution and thus the frequency of the oscillators movements (amplitude : 0-25 mm, that is typically in a frequency range of 0-5 Hz).

The length of the piston corresponds to the reactor length plus the distance from the end of the reactor tube to the joining point of the cam wheel of the electrical motor.

The dimension of the ring is the same of the internal diameter of the reactor tube in order to form an annular reaction cavity.

The number of these cavities (**N-1**) can be changed varying the length of the piston and, consequently, the number of the rings used (**N**). Numerical value of the geometrical properties of the MJOD flow reactor used during the development are reported in Table 21.

The temperature control is provided by the circulation of heating or cooling fluids in an annular space between the reaction tube and another stainless steel tube ($\mathbf{d_{Ce}}$: 37 mm, $\mathbf{d_{Ci}}$: 33 mm) that surrounds it. This heating-cooling coat can be easily divided in different section, introducing and taking out the heat-transfer fluid at different locations, in order to obtain different temperature zones if the synthetic process requires several reactions to be carried out consequently in the reactor (telescoped multistep syntheses). Furthermore the specification for the reactor system support extreme temperatures, such as cryogenic and thermolysis condition.

In this investigation the temperature (< 10 °C) is controlled by means of cold water from the sink without the need of any additional refrigerating support units.

Figure 31 and 32 show the flow chart for the flow chemistry process using the MJOD reactor rig whereof vacuum filter unit was included allowing a fast separation of the reaction mixture and the precipitated target *N,N'*-diiodo-5,5-dimethylhydantoin.

The semi-continuous filtration of the product is performed by means of a glass-sinter funnel of 55 mm of diameter (Pyrex porosity grade 3).

Figure 30. Picture of the oscillator and perforated disks

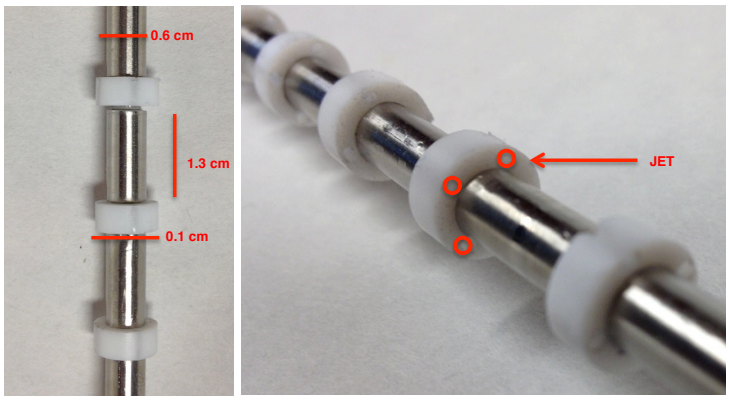

Figure 31. Picture of the multi-jet oscillating disk (MJOD) reactor system used in all of the flow experiments described in this thesis

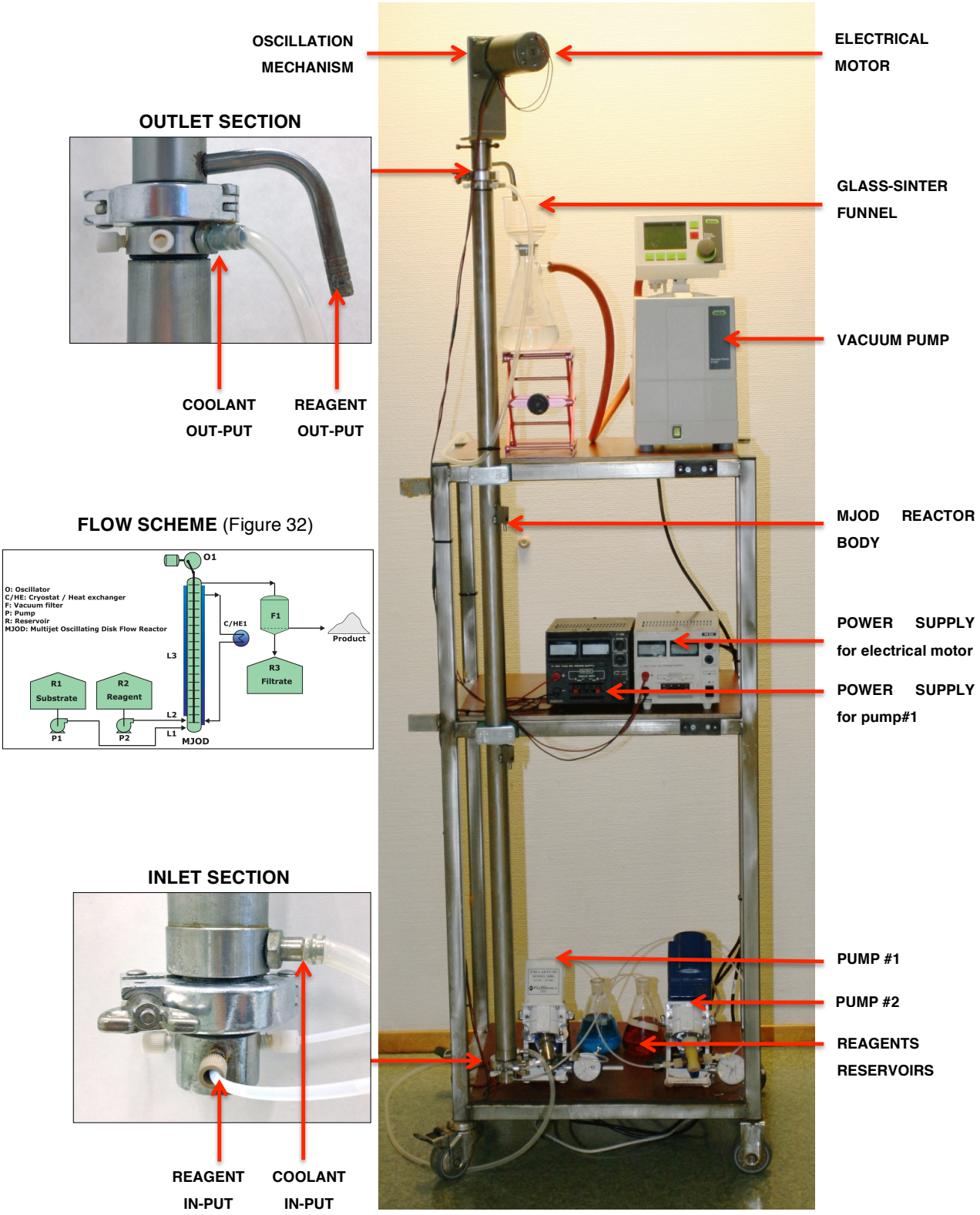

Figure 32. Flow scheme of the multi-jet oscillating disk (MJOD) reactor system used in all of the flow experiments described in this thesis.

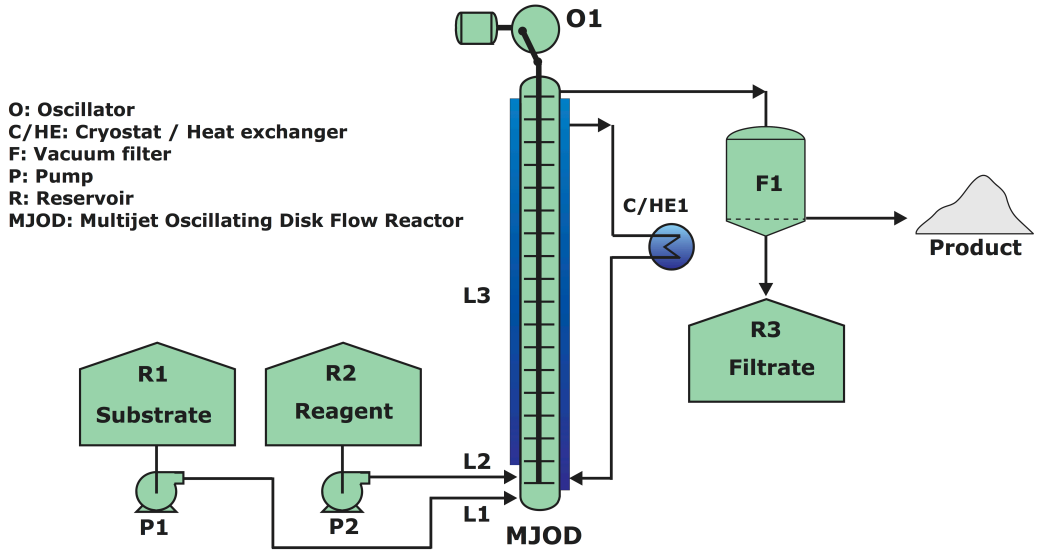

Table 21. Reactor dimensions

Length	**L**	1600	mm
External Reactor Diameter	$\mathbf{d_{Re}}$	12	mm
Internal Reactor Diameter	$\mathbf{d_{Ri}}$	10	mm
Internal Coat tube Diameter	$\mathbf{d_{Ce}}$	37	mm
External Coat tube Diameter	$\mathbf{d_{Ci}}$	33	mm
Disks Numbers	**N**	85	-
Disks Diameter	$\mathbf{d_D}$	10	mm
Disks Thickness	**s**	4	mm
Jets Diameter	$\mathbf{d_J}$	1:1.30	mm
Distance between disks	**h**	1.3	mm
Piston Diameter	$\mathbf{d_P}$	6	mm

The ratio of the internal reactor surface area to the net volume of the reactor $\mathbf{A \times V^{-1}_{net}}$ is a factor of paramount importance to define the heat exchange capabilities of the reactor. The following equations were used to determine the value of this parameter for the MJOD flow reactor used for all the flow experiments described in this thesis.

$$\mathbf{A} = 2 \times \pi \times \frac{\mathbf{d_{Ri}}}{2} \times \mathbf{L}$$

$$\mathbf{V_{net}} = \mathbf{V_{tot}} - \mathbf{V_{multi-jet\ disk}} - \mathbf{V_{piston\ shaft}}$$

where

$$\mathbf{V_{tot}} = \pi \times \frac{\mathbf{d_{Ri}}^2}{4} \times \mathbf{L}$$

$$\mathbf{V_{multi-jet\ disk}} = \pi \times \frac{\mathbf{d_D}^2}{4} \times \mathbf{s} \times \mathbf{N}$$

$$\mathbf{V_{piston\ shaft}} = \pi \times \frac{\mathbf{d_P}^2}{4} \times (\mathbf{L} - \mathbf{s} \times \mathbf{N})$$

Numerical calculations have been implemented using *MATLAB* version 8.1. In Appendix C, computations and numerical values are reported.

Figure 33 shows the flow rate [mL min^{-1}] as a function of the flow reactor residence time [min]. Modulating the revolution rate of the piston of the pump, the entire volume of the reactor can be filled during different times.

Figure 33. Requested flow to full off the volume of the reactor in a desired time

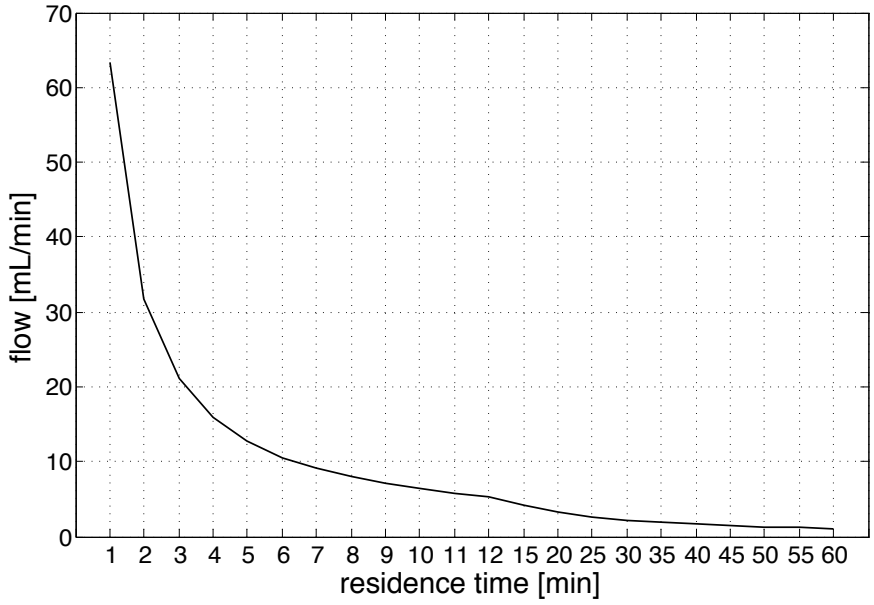

Support units

Pumps

Two different pumps were calibrated and used during the investigations. Appendix D provides computations and numerical values. Both of the pumps have the same working mechanism. A complete revolution of the piston in the precisely mated ceramic cylinder liner is required for each suction/discharge cycle. The flow rate is adjusted by turning a flow control knob, which moves the flow rate indicator along a fixed 20 unit scale linearly calibrated **10-0-10**. The **10** equals 100% flow rate in that direction, **0** equals zero flow. To improve the fine adjustment of the flow rates there is an additional indicator, which provides for 1000 discrete settings.

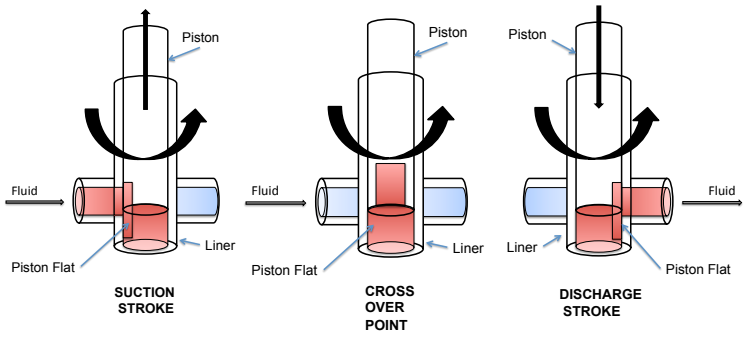

The differences between the two pumps concern the pump drive module and the pump head module. Pump#1 is a FMI LAB PUMP, Model QBG 24 VDC[70], provided with a stainless steel and ceramic head and an electrical control of stroke rate by voltage variation (in our experimentations settled at 24V). This pump has been used to feed the mixture of the **reservoir #1**, in order to avoid the possible oxidation of the metal due to the corrosive action of the iodine. Pump#2 is a FMI LAB PUMP, Model QG 20[71], provided with a ceramic head, which has been used to feed the I-Cl mixture from the **reservoir #2**. The range of flow rate for the two pump is different, as resulted from the calibration. The control of low flow rates with the QBG24 VDC pump, is difficult to manage. This fact requested to perform the reaction with two different amount of solvent for the two mixtures.

Vacuum pump

Vacuum Pump V-700, B·U·CHI Labortechnik AG,:Flawil, CH provided with a Vacuum Controller V-850, B·U·CHI Labortechnik AG,:Flawil, CH.

4.3. Batch synthetic procedure

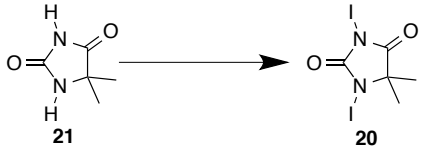

4.3.1. Method 1: Small scale DIH synthesis

DIH synthesis: Method 1

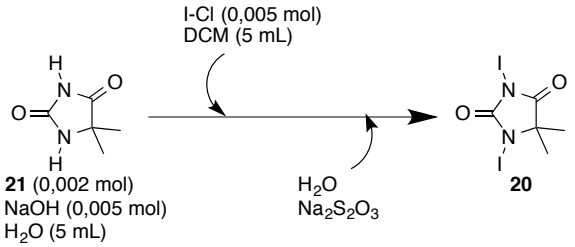

0.002 mol (0.6 g) of 5,5-dimethylhydantoin **21** and 0.005 mol (0.19 g) of sodium hydroxide were dissolved in 5 mL of cold water. It was then cooled to below 5° C in an ice bath. To this mixture, maintained in the ice bath, a solution of 0,005 mol (0.73 g) Iodine monochloride in 5 mL of Dichloro Methane (0.082 mol) previously prepared was added drop wise while stirring magnetically at the highest speed possible. After the completion of the drop wise addition, it was stirred at the same temperature for 15 min. At the end, the product was filtered off, washed with a mixture of water and sodium thiosulfate and dried under vacuum. The experiment was performed in the dark.

DIH synthesis: Method 2

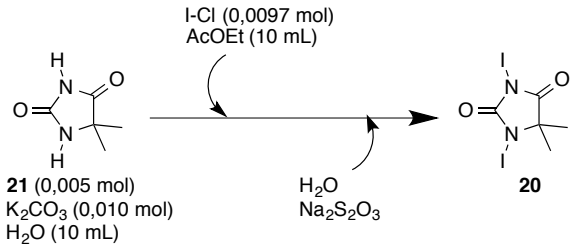

Optimized procedure

5 mmol (0.64 g) of 5,5-dimethylhydantoin **21** and 10 mmol (1.38 g) of Potassium carbonate were placed in a round bottom flask of 50 mL and dissolved in 10 mL of cold water. The reactor was then cooled to below 8° C in

an ice bath. To this mixture maintained in the ice bath a solution of 9.7 mmol (1.58 g) iodine monochloride in 10 mL ethyl acetate (0.125 mol) previously prepared was added drop wise while stirring magnetically at the highest speed possible. After the completion of the drop wise addition during 60 min, it was stirred at the same temperature for 40 minutes. At the end, the product was filtered off, washed with a mixture of water and thiosulfate and dried under vacuum. The experiment was performed in the dark.

Procedure used during the experimental design

5 mmol (0.64 g) of 5,5-dimethylhydantoin and (12, 15 or 18) mmol of Potassium carbonate were placed in a round bottom flask of 50 mL and dissolved in 10 mL of cold water. The reactor was then cooled to below 8° C in an ice bath. To this mixture maintained in the ice bath a solution of (12, 15 or 18) mmol iodine monochloride in 10 mL ethyl acetate previously prepared was added drop wise during 60 minutes while stirring magnetically at the highest speed possible. After the completion of the drop wise addition, it was stirred at the same temperature for 40 minutes. At the end, the product was filtered off, washed with a mixture of water and thiosulfate and dried under vacuum. The experiment was performed in the dark.

Imidazole iodination

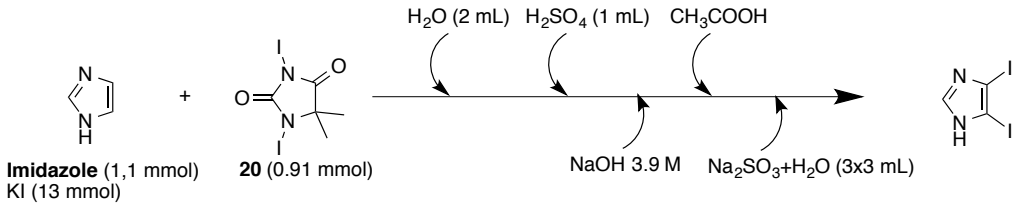

Imidazole (0.076 g, 1.1 mmol), KI (2.2 g, 13 mmol) and *N,N'*-diiodo-5,5-dimethylhydantoin (0.345 g, 0.91 mmol) were transferred to a round-bottom flask immersed in an ice- bath. Water (2 mL) was added and the heterogeneous mixture was stirred during the drop-wise addition of sulphuric acid (1 mL) over 1 min. After the addition, NaOH (3.9 M, 15 mL) was added. The resulting, milky solution was then neutralized (pH~6) with acetic acid, which

resulted in precipitation of the product. The crystals were filtered, washed multiple times with cold water and saturated Na_2SO_3 solution (3 x 3 mL) and allowed to air-dry to constant weight to give the product as creamy crystals.

4.3.2. Method 2: Up-scaled DIH synthesis

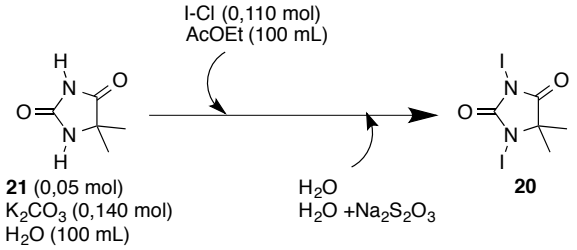

Optimized procedure

140 mmol (19.32 g) of Potassium carbonate were placed in a glass cylinder reactor (7.5 cm diameter) and dissolved in 100 mL of cold water. 50 mmol (6.4 g) of 5,5-dimethylhydantoin were added to the basic solution. The mixture was then cooled to below 5° C in an ice bath. To this mixture maintained in the ice bath a solution of 110 mmol (17.8 g) Iodine monochloride in 100 mL Ethyl Acetate previously prepared was added drop wise using a Q pump while stirring magnetically at the highest speed possible. After the completion of the drop wise addition during 30 minutes, the reactant mixture was stirred at the same temperature for 15 minutes. At the end, the product was filtered off, washed with cold water and then with a mixture of cold water and thiosulfate, filtered again and dried. The experiment was performed in the dark.

Procedure used during the experimental design

(140, 150, or 160) mmol of Potassium carbonate were placed in a glass cylinder reactor (7.5 cm diameter) and dissolved in 100 mL of cold water. 50 mmol (6.4 g) of 5,5-dimethylhydantoin were added to the basic solution. The mixture was then cooled to below 10° C in an ice bath. To this mixture maintained in the ice bath a solution of (100, 110 or 120) mmol Iodine monochloride in 100 mL Ethyl Acetate previously prepared was added drop wise using a Q pump while stirring magnetically (stirrer diameter 3.5 cm) at the highest speed possible. After the completion of the drop wise addition

during (30, 60, 90 or 120) min , the reactant mixture was stirred at the same temperature for (1, 15, 30, 60, 90, 180 or 270) minutes. At the end, the product was filtered off, washed with cold water and then with a mixture of cold water and thiosulfate, filtered again and dried at room temperature for 10 hours.
The experiment was performed in the dark.

4.4. Continuous flow chemistry process

Reaction

Optimized Procedure

The experiment was conducted in the following way: two different reservoirs were prepared, **mix#1** containing a mixture of substrate (DMH **21**: 50 mmol), base (K_2CO_3: 140 mmol) and water (100 mL) and **mix#2** containing the iodinating reagent (I-Cl: 110 mmol) and solvent (AcOEt: 50 mL). The substrate was added after preparing the aqueous basic solution in order to preserve it from the heat generation that occurred dissolving potassium carbonate in water. The reaction was started by pumping the substrate and the reagent using a calculate flow rate, whereof the product was collected at the output section. The oscillating speed of the piston was kept of 100 rpm. The mixture from the **reservoir#1** was pumped into the reactor with a flow rate of 4.69 mL min^{-1}, twice as fast as the pump that feeds the mixture stored in the **reservoir#2** (2.34 mL min^{-1}) in order to maintain the desired residence time of 9 min. Then the feeding of the reagent and of the substrate was terminated at the same time, a pure reaction medium (EtOAc) was pumped with a rate corresponding to $\mathbf{r_{solvent}} = \mathbf{r_{mix\#1}} + \mathbf{r_{mix\#2}}$. In this way, the flow rate (and thus the residence time) was kept constant throughout the entire experimental run. The reaction was conducted at a temperature of 8° C by mean of cold water as coolant in the coat of the reactor.

Procedure used during the introductory experiments

The experiments were conducted in the following way: two different reservoirs were prepared, **mix#1** containing a mixture of substrate (DMH **21**: 50 mmol), base (K_2CO_3: 140 mmol) and water (100 mL) and **mix#2** containing the

iodinating reagent (I-Cl: 110 mmol) and solvent (AcOEt: 50 mL or 100 mL). The substrate was added after preparing the aqueous basic solution in order to to preserve it from the heat generation that occurred dissolving potassium carbonate in water. The reaction was started by pumping the substrate and the reagent using a calculate flow rate, whereof the product was collected at the output section. The oscillating speed of the piston was kept of (0 10 70 100 130) rpm during the entire reaction.

The mixture from the **reservoir#1** was pumped into the reactor with a flow rate of (10.55, 7.03, 5.63, 4.69 or 3.51) mL min^{-1} , twice as fast as the pump that feeds the mixture stored in the **reservoir#2** (5.27, 3.51, 2.81, 2.35 or 1.75) mL min^{-1} in order to maintain the desired residence time of (4, 6, 7.5, 9 or 12) minutes. Then the feeding of the reagent and of the substrate was terminated at the same time, a pure reaction medium (EtOAc) was pumped with a rate corresponding to $\mathbf{r_{solvent} = r_{mix\#1} + r_{mix\#2}}$. In this way, the flow rate (and thus the residence time) was kept constant throughout the entire experimental run. The reaction was conducted at a temperature of 8° C by mean of cold water as coolant in the coat of the reactor.

Long time run process procedure

The experiments was conducted in the following way: two different reservoirs were prepared, **mix#1** containing a mixture of substrate (DMH **21**: 1.1 mol, 140 g), base (K_2CO_3: 3.1 mol , 425 g) and water (2.2) and **mix#2** containing the iodinating reagent (I-Cl: 2.4 mol 392 g) and solvent (EtOAc: 1.1 L). In particular, the substrate was added after preparing the aqueous basic solution in order to preserve it from the heat generation that occurred dissolving potassium carbonate in water. **Mix#2** was prepared in different steps to preserve the iodinating agent from degradation. The reaction was started by pumping the substrate and the reagent using a calculate flow rate, whereof the product was collected at the output section. The oscillating speed of the piston was kept of 100 rpm during the entire reaction. The mixture from the **reservoir#1** was pumped into the reactor with a flow rate of 4.69 mL min^{-1}, twice as fast as the pump that feeds the mixture stored in the **reservoir#2** (2.35 mL min^{-1}) in order

to maintain the desired residence time of 9 minutes. Then the feeding of the reagent and of the substrate was terminated at the same time, and pure reaction medium (EtOAc) was pumped for 30 minutes with a rate corresponding to $\mathbf{r_{solvent} = r_{mix\#1} + r_{mix\#2}}$ to collect the residual product. The flow rate (and thus the residence time) was kept constant throughout the entire experimental run. The reaction was conducted at a temperature of 8° C by mean of cold water as coolant in the coat of the reactor.

Work up

Quenching of the reaction mixture

The product was quenched with cold water while it was coming out from the reactor. After collecting all the precipitate, the same work-up performed for the product of the Batch process was performed. The product was filtered washed with cold water and afterwards with a mixture of cold water and thiosulfate. This kind of work-up showed a lot of drawbacks associated to a loss both in terms of quality and quantity of the obtained product (experiments #1, #2, #3 Table 9). The obtained product was dried at room temperature for 10 hours and then weighted.

Paper filtration

A continuous vacuum filtration of the product has been performed on to a paper filter (experiments #4 Table 9). The pores of the paper filter, usually utilized in the work up of the product obtained with the batch process, resulted too big to collect the product obtained with the flow reactor. The enhanced mixing might cause a shift of the particle-size distribution towards lower diameters. The obtained product was dried at room temperature for 10 hours and then weighted.

Glass-sinter funnel filtration

The technic chosen was to perform a continuous filtration onto a fiberglass filter (diameter 6 cm), using a vacuum pump set at 650 mbar. The obtained product was dried at room temperature for 10 hours and then weighted.

5. Conclusion

A green and cost effective process for the synthesis of the 1,3-diiodo-5,5-dimethylhydantoin was designed, investigated and optimized by means of statistical experimental design and multivariate regression.

Small scale (<1 g) and up-scaled (10×) batch processes were investigated by using multivariate mathematical and statistical methods, methodology also known as chemometrics.

Both of the batch processes were successfully optimized to provide high yields, ≈80% and ≈65%, respectively.

The stoichiometry of the process revealed an atom economy of 84%. Process mass intensity and environmental factor of the batch processes were PMI ≈7 and $\mathbf{E_{factor}}$ of ≈6, respectively. The reaction mass efficiency for the small-scale batch process resulted to be lower than the up-scaled one (62% vs 78%) probably due to higher relative excess of iodinating reagent and mass transfer issues.

The optimized batch process was transferred to the flow reactor platform multi-jet oscillating disk (MJOD) flow reactor, which offers an enhanced mixing and temperature control. These factors were seen as improved efficiency of the process, in terms of yield and reaction time. The continuous process showed a productivity of about 47 g h^{-1} (90% yield), at low energy and environmental costs through efficient mass and heat transfer and an efficient semi-continuous filtration of the product.

The process mass intensity (≈4) and the $\mathbf{E_{factor}}$ (≈3.5) resulted to be halved if compared to the values of the batch process.

During the process development and optimization ≈875 g of 1,3-diiodo-5,5-dimethylhydantoin of high quality were produced. Some of the synthetized compound was successfully used in test reaction as the di-iodination of imidazole. 300 g were produced using the batch process, 200 g assessing and developing the flow process and 375 g during one experiment of 8 hours by means of the multi-jet oscillating disk platform.

References

1. Sparks, K. J., In *Encyclopedia Britannica 2001 book of the year*.

2. Akdag, A.; Okur, S.; McKee, M. L.; Worley, S. D., The stabilities of *N*-Cl bonds in biocidal materials. *J Chem Theory Comput* **2006,** *2* (3), 879-884.

3. Worley, S. D.; Williams, D. E., Halamine Water Disinfectants. *Crit Rev Env Contr* **1988,** *18* (2), 133-175.

4. Worley, S. D.; Chen, Y.; Wang, J. W.; Wu, R.; Cho, U.; Broughton, R. M.; Kim, J.; Wei, C. I.; Williams, J. F.; Chen, J.; Li, Y., Novel *N*-halamine siloxane monomers and polymers for preparing biocidal coatings. *Surf Coat Int Pt B-C* **2005,** *88* (2), 83-156.

5. Metcalf, R. L., Insect Control. In *Ullmann's Encyclopedia of Industrial Chemistry*, Wiley-VCH Verlag GmbH & Co. KGaA: 2000.

6. Kukhar, V. P.; Soloshonok, V. A., *Fluorine-Containing Amino Acids, Synhesis and Properties*. John Wiley & Sons: Chichester, 1995.

7. Moore, S. L.; Payne, D. N., Types of Antimicrobial Agents. In *Russell, Hugo & Ayliffe's Principles and Practice of Disinfection, Preservation & Sterilization*, Blackwell Publishing Ltd: 2008; pp 8-97.

8. Beal, M.; Linak, E., *Chemical Economics Handbook Marketing Research Report: Chlorine/Sodium Hydroxide*. 2011.

9. Glauser, J., *Chemical Economics Handbook Marketing Research Report: Bromine*. 2009.

10. Kosjek, T.; Heath, E., Halogenated Heterocycles as Pharmaceuticals. In *Halogenated Heterocycles*, Iskra, J., Ed. Springer Berlin Heidelberg: 2012; Vol. 27, pp 219-246.

11. (a) Straub, J. O., Integrated Environ Assess Manag 6. 540-566; (b) Isanbor, C.; O'Hagan, D., Fluorine in medicinal chemistry: A review of anti-cancer agents. *J Fluorine Chem* **2006,** *127* (3), 303-319.

12. Andersson, M. I.; MacGowan, A. P., Development of the quinolones. *Journal of Antimicrobial Chemotherapy* **2003,** *51* (suppl 1), 1-11.

13. W.O., L. T. L. W. D. A. F., *Principles of medicinal chemistry*. 4th ed.; Philadelphia, 1955.

14. Banks, R. E., Fluorine chemistry at the millennium 'Fascinated by fluorine'. *J Fluorine Chem* **1999,** *100* (1-2), 175-175.

15. Herrera-Rodriguez, L. N.; Meyer, H. P.; Robins, K. T.; Khan, F., Perspectives on biotechnological halogenation Part II: Prospecting for future biohalogenases. *Chim Oggi* **2011,** *29* (6), 47-49.

16. Knight, J. C.; Edwards, P. G.; Paisey, S. J., Fluorinated contrast agents for magnetic resonance imaging; a review of recent developments. *RSC Advances* **2011,** *1* (8), 1415-1425.

17. Boldon, S.; Stenhagen, I. S. R.; Moore, J. E.; Luthra, S. K.; Gouverneur, V., Supported Synthesis of Halogenated Organic Compounds. *Synthesis-Stuttgart* **2011,** (24), 3929-3953.

18. Jiang, Z. X.; Liu, X.; Jeong, E. K.; Yu, Y. B., Symmetry-Guided Design and Fluorous Synthesis of a Stable and Rapidly Excreted Imaging Tracer for (19)F MRI. *Angew Chem Int Edit* **2009,** *48* (26), 4755-4758.

19. Priebe, H.; Aukrust, A.; Bjørsvik, H. R.; Tønseth, C. P.; Wiggen, U. N., Stability of the X-ray contrast agent iodixanol=3,3′ ,5,5′ -tetrakis(2,3-dihydroxypropylcarbamoyl)-2,2′ ,4,4′ ,6,6′ -hexaiodo-N,N′ -(2-hydroxypropane-1,3-diyl)-diacetanilide towards acid, base, oxygen, heat and light. *Journal of Clinical Pharmacy and Therapeutics* **1999,** *24* (3), 227-235.

20. France, S.; Weatherwax, A.; Lectka, T., Recent developments in catalytic, asymmetric alpha-halogenation: A new frontier in asymmetric catalysis. *Eur J Org Chem* **2005,** (3), 475-479.

21. (a) Gu, L. Q.; Lu, T.; Zhang, M. Y.; Tou, L. J.; Zhang, Y. G., Efficient Oxidative Chlorination of Aromatics on Saturated Sodium Chloride Solution. *Adv Synth Catal* **2013,** *355* (6), 1077-1082; (b) Hojati, S. F.; Gholizadeh, M.; Haghdoust, M.; Shafiezadeh, F., 1,3-Dichloro-5,5-dimethylhydantoin as a Novel and Efficient Homogeneous Catalyst in Biginelli Reaction. *B Korean Chem Soc* **2010,** *31* (11), 3238-3240.

22. Iranpoor, N.; Firouzabadi, H.; Shaterian, H. R., Catalytic and chemoselective deprotection of S,S- and S,O-acetals and ketals in the presence of their O,O-analogs with electrophilic halogens under neutral conditions. *Tetrahedron Lett* **2003,** *44* (25), 4769-4773.

23. Lamani, M.; Prabhu, K. R., NIS-Catalyzed Reactions: Amidation of Acetophenones and Oxidative Amination of Propiophenones. *Chem-Eur J* **2012,** *18* (46), 14638-14642.

24. Guo, R. N.; Cai, X. F.; Shi, L.; Ye, Z. S.; Chen, M. W.; Zhou, Y. G., An efficient route to chiral N-heterocycles bearing a C-F stereogenic center via asymmetric hydrogenation of fluorinated isoquinolines. *Chem Commun* **2013,** *49* (76), 8537-8539.

25. Zhang, H. H., Production and application of 1, 3-dibromo-5, 5-dimethylhydantoin. **2013,** *42* (3), 6.

26. (a) Sandtorv, A. H.; Bjørsvik, H. R., Fast Halogenation of Some N-Heterocycles by Means of N,N-Dihalo-5,5-dimethylhydantoin. *Adv Synth Catal* **2013,** *355* (2-3), 499-507; (b) Chaikovskii, V. K.; Filimonov, V. D.; Funk, A. A.; Skorokhodov, V. I.; Ogorodnikov, V. D., 1,3-diiodo-5,5-dimethylhydantoin - An efficient reagent for iodination of aromatic compounds. *Russ J Org Chem+* **2007,** *43* (9), 1291-1296.

27. De Luca, L., Naturally occurring and synthetic imidazoles: Their chemistry and their biological activities. *Curr Med Chem* **2006,** *13* (1), 1-23.

28. (a) Crabtree, R. H., NHC ligands versus cyclopentadienyls and phosphines as spectator ligands in organometallic catalysis. *Journal of Organometallic Chemistry* **2005,** *690* (24–

25), 5451-5457; (b) Herrmann, W. A., N-Heterocyclische Carbene: ein neues Konzept in der metallorganischen Katalyse. *Angewandte Chemie* **2002,** *114* (8), 1342-1363.

29. Iida, S.; Ohmura, R.; Togo, H., Direct oxidative conversion of alkyl halides into nitriles with molecular iodine and 1,3-diiodo-5,5-dimethylhydantoin in aq ammonia. *Tetrahedron* **2009,** *65* (31), 6257-6262.

30. Filimonov, V. D.; Krasnokutskaya, E. A.; Poleshchuk, O. K.; Lesina, Y. A.; Chaikovskii, V. K., Electronic structures and reactivities of iodinating agents in the gas phase and in solutions: a density functional study. *Russ Chem B+* **2006,** *55* (8), 1328-1336.

31. Chaikovskii, V. K.; Filimonov, V. D.; Funk, A. A., Evaluation of the Reactivity and Regioselectivity of Superelectrophilic Iodinating Systems. *Russ J Org Chem+* **2009,** *45* (9), 1349-1352.

32. http://www.sigmaaldrich.com. (Date: January 30, 2014).

33. (a) Pesti, J., Continuous Processes: Go with the Flow! *Org Process Res Dev* **2012,** *16* (5), 843-843; (b) Roberge, D., Microreactor Technology: A Revolution for the Fine Chemical and Pharmaceutical Industries? *Chemical engineering & technology* **2005,** *28* (3), 318-323; (c) Sleveland, D.; Bjørsvik, H.-R., Synthesis of Phenylboronic Acids in Continuous Flow by Means of a Multijet Oscillating Disc Reactor System Operating at Cryogenic Temperatures. *Org Process Res Dev* **2012,** *16* (5), 1121-1130; (d) Wirth, T. T., *Microreactors in organic synthesis and catalysis*. 2008; (e) Nagy, K. D.; Jensen, K. F., Micro Reaction Technology in Organic Synthesis. Von Charlotte Wiles und Paul Watts. *Angewandte Chemie* **2012,** *124* (7), 1548-1549; (f) Geyer, K., *Synlett* **2009,** *15*, 2382; (g) Brivio, M., *Lab on a chip* **2006,** *6*, 329; (h) Watts, P., *Chemical Society reviews* **2005,** *34*, 235.

34. Anderson, N. G., Using Continuous Processes to Increase Production. *Org Process Res Dev* **2012,** *16* (5), 852-869.

35. Liguori, L.; Bjørsvik, H.-R., Multijet Oscillating Disc Millireactor: A Novel Approach for Continuous Flow Organic Synthesis. *Org Process Res Dev* **2011,** *15* (5), 997-1009.

36. Orazi, O. O.; Corral, A.; Bertorello, H. E., N-Iodohydantoins. II.1,2 Iodinations with 1,3-Diiodo-5,5-dimethylhydantoin. *The Journal of Organic Chemistry* **1965,** *30* (4), 1101-1104.

37. Gottardi, W., Reaction of N-Bromo-Compounds with Iodine - Convenient Synthesis of N-Iodo Compounds. *Monatsh Chem* **1975,** *106* (4), 1019-1025.

38. Kodama, H.; Katsuhira, T.; Hino, T.; Takagi, K.; Seo, A. Preparation of 1,3-diiodohydantoins. JP2002030072A, 2002.

39. Inoue, K.; Hanamura, Y.; Miyazawa, T. Production or storage method of 1,3-diiodohydantoin compounds without free iodine. WO2007026766A1, 2007.

40. Elnagar, H. Y.; Peters, B. C.; Spielman, E. E.; Thomas, D. H. Process for producing N-halogenated hydantoins. US20060036099A1, 2006.

41. Protocol to the Vienna Convention on Substances that Deplete the Ozone Layer (Montreal Protocol). Canada, E., Ed. 2006.

42. Carbon tetrachloride. http://www.epa.gov/ttn/atw/hlthef/carbonte.html (accessed 30 January 2014).

43. (a) Brereton, R. G., Chemometrics : Data Analysis for the laboratory and Chemical Plant. In *Chemometrics*, John Wiley & Sons, Ltd: 2003; pp i-xiv; (b) Henrion, R.; Henrion, G., Chemometrics. In *Ullmann's Encyclopedia of Industrial Chemistry*, Wiley-VCH Verlag GmbH & Co. KGaA: 2000.

44. Brown, S., Chemometrics. In *Encyclopedia of Statistical Sciences*, John Wiley & Sons, Inc.: 2004.

45. (a) Liang, Y. Z., *Chemometrics and intelligent laboratory systems* **1996,** *32*, 1-10; (b) Vanden Branden, K., Robustness properties of a robust PLS regression method. *Analytica Chimica Acta* **2004,** *515*, 229-241; (c) Rousseeuw, P. J., Least median of squares regression. *J. Am. Statist. Assoc.* **1984,** *79*, 871-880; (d) Croux, C.; Haesbroeck, G., Principal component analysis based on robust estimators of the covariance or correlation matrix: influence functions and efficiencies. *Biometrika* **2000,** *87* (3), 603-618.

46. (a) Box, G. E. P., 1978; (b) Montgomery, D. C. D. C., *Design and Analysis of Experiments (7th Edition)*. 1991; (c) Box, G. E. P., 1987; (d) Myers, R. H., *Response Surface Methodology : Process and Product Optimization Using Designed Experiments*. 1995.

47. (a) Montgomery, D. C., *Introduction to Linear Regression Analysis*. 1982; (b) Draper, N. R. N. R.; Smith, H. H., *Applied regression analysis*. 1981.

48. Golshan, A.; Beyad, Y.; Maeder, M., Chemometrics and data fitting. *Journal of Chemometrics* **2013,** *27* (9), 260-261.

49. Ishikawa, K., *Guide to Quality Control*. 2nd ed.; Japan, 1991.

50. Forryan, C. L.; Compton, R. G., Studies of the electrochemical reduction of 4-nitrophenol in dimethylformamide: evidence for a change in mechanism with temperature. *Phys Chem Chem Phys* **2003,** *5* (19), 4226-4230.

51. Schultz, H.; Bauer, G.; Schachl, E.; Hagedorn, F.; Schmittinger, P., Potassium Compounds. In *Ullmann's Encyclopedia of Industrial Chemistry*, Wiley-VCH Verlag GmbH & Co. KGaA: 2000.

52. Malinowski, E. R. H., D. G. , *Factor Analysis in Chemistry.* New York, 2002.

53. (a) Kirschning, A., Chemistry in flow systems. *Beilstein Journal of Organic Chemistry* **2009,** *5*, 15; (b) Watts, P.; Haswell, S. J., The application of micro reactors for organic synthesis. *Chemical Society Reviews* **2005,** *34* (3), 235-246.

54. (a) Ritter, S. K. S., GREEN CHEMISTRY. *Chemical & engineering news* **2001,** *79* (29), 27-34; (b) Mitic, A.; Heintz, S.; Ringborg, R. H.; Bodla, V.; Woodley, J. M.; Gernaey, K. V., Applications, benefits and challenges of flow chemistry. *Chim. Oggi* **2013,** *31* (5), 4-8; (c)

Pastre, J. C.; Browne, D. L.; Ley, S. V., Flow chemistry syntheses of natural products. *Chemical Society Reviews* **2013,** *42* (23), 8849-8869.

55. http://sfxeu09.hosted.exlibrisgroup.com/sfx_ubb?sid=achs&genre=simple.

56. Ratner, D. M.; RatnerThese authors contributed equ, D. M. D. M.; Murphy, E. R. E.; Jhunjhunwala, M. M.; Snyder, D. A. D.; Jensen, K. F. K.; Seeberger, P. H. P., Microreactor-based reaction optimization in organic chemistry glycosylation as a challenge. *Chemical communications (London. 1996)* **2005,** *5* (5), 578.

57. Harvey, A. P.; Mackley, M. R.; Stonestreet, P., Operation and Optimization of an Oscillatory Flow Continuous Reactor. *Industrial & engineering chemistry research* **2001,** *40* (23), 5371-5377.

58. (a) Djerassi, C.; Lenk, C. T., Alpha-Iodoketones .2. Reaction of Enol Acetates with N-Iodosuccinimide. *J Am Chem Soc* **1953,** *75* (14), 3493-3495; (b) Djerassi, C.; Grossman, J.; Thomas, G. H., Alpha-Iodoketones .4. The Reaction of N-Iodosuccinimide with Enol Acetates of Delta-4-3-Ketosteroids. *J Am Chem Soc* **1955,** *77* (14), 3826-3829.

59. Eissen, M.; Metzger, J. O., Environmental performance metrics for daily use in synthetic chemistry. *Chem-Eur J* **2002,** *8* (16), 3580-3585.

60. Agency., U. S. E. P. "Green Chemistry". (accessed 2011-03-23).

61. (a) Poliakoff, M.; Fitzpatrick, J. M.; Farren, T. R.; Anastas, P. T., Green chemistry: Science and politics of change. *Science* **2002,** *297* (5582), 807-810; (b) Ritter, S. K., Green chemistry. *Chemical & Engineering News* **2001,** *79* (29), 27-34; (c) Hamley, P.; Poliakoff, M., Green chemistry: the next industrial revolution? *Tce* **2001,** (721), 24-27; (d) Anastas, P. T.; Warner, J. C.; Kirchhoff, M. M., Green chemistry: Practicing environmentally benign chemistry. *Abstr Pap Am Chem S* **2002,** *223*, U6-U6.

62. (a) Warner, J. C.; Cannon, A. S.; Dye, K. M., Green chemistry. *Environ Impact Asses* **2004,** *24* (7-8), 775-799; (b) Agency, U. S. E. P. "The 12 Principles of Green Chemistry". (accessed 2006-07-31).

63. Sorrel, S. R. Report of the BARRIERS project. http://www.sussex.ac.uk/spru/environment/reserch/barriers.html.

64. Jimenez-Gonzalez, C.; Ponder, C. S.; Broxterman, Q. B.; Manley, J. B., Using the Right Green Yardstick: Why Process Mass intensity Is Used in the Pharmaceutical Industry To Drive More Sustainable Processes. *Org Process Res Dev* **2011,** *15* (4), 912-917.

65. (a) Bennett, M. J., P., *Sustainable Measures*. Greenleaf Publishing, Ltd.: Sheffield, South Yorkshire, UK,, 1999; (b) 1999; (c) Constable, D. J. C.; Curzons, A. D. A.; Cunningham, V. L. V., Metrics to ???green??? chemistry???which are the best? *Green chemistry* **2002,** *4* (6), 521-527; (d) Curzons, A. D. A.; Mortimer, D. N. D.; Constable, D. N. D. J. C.; Cunningham, V. L. V., *Green chemistry* **2001,** *3* (1), 1-6; (e) dos Santos, L. M. F.; Constable, D. J. C.; Curzons, A. D. A.; Freitas dos Santos, A. D. L. M.; Geen, G. R. G.; Kitteringham, J. J.; Smith, P. P.; Hannah, R. E. R.; McGuire, M. A. M.; Webb, R. L. M.; Yu, M. M.; Hayler, J. D. J.; Richardson, J. E. J., Green chemistry measures for process research and development. *Green chemistry* **2001,** *3* (1), 7-9; (f) Henderson, R.; Dunn, P. J., *Green Chemistry Metrics Green Chemistry in*

the Pharmaceutical Industry. 2010; (g) http://sfxeu09.hosted.exlibrisgroup.com/sfx_ubb?sid=achs&genre=simple&stitle=Corporate Environmental Performance 2000&date=1999&volume=1. 1999; Vol. 1; (h) Hessel, V. V.; Hardt, S. S.; Löwe, H. H., *Chemical Micro Process Engineering*. 2005; (i) Lapkin, A., *Green Chemistry Metrics*. 2008; (j) 2003; (k) Sheldon, R. A., *Chemtech* **1994,** *24*, 38; (l) Sheldon, R. A. R., The E Factor: fifteen years on. *Green chemistry* **2007,** *9* (12), 1273.

66. Constable, D. J. C.; Curzons, A. D.; Cunningham, V. L., Metrics to 'green' chemistry - which are the best? *Green Chemistry* **2002,** *4* (6), 521-527.

67. http://sfxeu09.hosted.exlibrisgroup.com/sfx_ubb?sid=achs&genre=simple&aulast=&date=2008. 2008.

68. Deddis, C. R., *Process Economics* Vol. IV.

69. (a) Calabrese, G. S.; Pissavini, S., From batch to continuous flow processing in chemicals manufacturing. *AIChE Journal* **2011,** *57* (4), 828-834; (b) Newberger, S., *Pharmaceutical engineering* **2008,** *28* (6), 32-42.

70. FMI LAB PUMP, M. Q. V., Fluid Metering, Inc.: Syoset, NY, USA.

71. FMI LAB PUMP, M. Q., Fluid Metering, Inc.: Syoset, NY, USA.

Appendix

A. MATLAB program for the statistical design and optimization for the small-scale batch process

```
%% SMALL-SCALE BATCH REACTOR
%% EXPERIMENTAL DESIGN AND MULTIVARIATE REGRESSION

%% DATA
z1=[1.656 2.070 2.484];                    % K2CO3 quantity [g]
z2=[1.948 2.435 2.922];                    % I-Cl quantity  [g]

% Each of the experimental variables was scaled to facilitate the
%calculation of the regression coefficients (Beta)

for i = 1:3
x1(i)=(z1(i)-(z1(1)+0.5*(z1(3)-z1(1))))/(z1(3)-(z1(1)+0.5*(z1(3)-
z1(1))));
end
x1=[x1]

for i = 1:3
x2(i)=(z2(i)-(z2(1)+0.5*(z2(3)-z2(1))))/(z2(3)-(z2(1)+0.5*(z2(3)-
z2(1))));
end
x2=[x2]

%% RESPONSES
%Yield
y=[55.47; 68.47; 18.57; 67.57; 81.86; 79.42]; %Resa DIH [%]
yi=[ 42.25; 53.24; 0; 70.38; 61.45; 77.93]; %Resa Diiodo-Imidazole [%]
y1=[y yi];
yzeros=[81.86; 79.42]; % Central experiment of the design responses
yzerosi=[61.45; 77.93];% Central experiment of the design responses

%% SPAN CHECK
%check if the selected experimental levels represent a sufficient span
to
%provide significant variations in the responses, considering the
three
%experiments #1 where (x1, x2)= [-1 -1 ],#2 where (x1, x2)= [0 0], #3
where (x1, x2 )= [1 1]
% FIGURE 2
figure2=figure('Color',[1 1 1]);
ycheck=[y(1) locatecentral(2) y(4)];
 axes1=               axes('Parent',figure2,'Color',[1               1
```

```
1],'YGrid','on','XTickLabel',{'','1','5','4',''},'XTick',[0  1  2  3  4
],'XGrid','on','FontSize',18);
 xlim(axes1,[0 4]);
 ylim(axes1,[50 85]);
 xlabel('Experiment #','FontSize',17);
 ylabel('Yield %','FontSize',17);
box(axes1,'on');
hold(axes1,'all');
bar1=bar(ycheck,'BarWidth',0.4,'Parent',axes1)
set(bar1,'FaceColor',[1 0.4 0]);
title('SPAN CHECK - Small Scale Batch Process')
% FIGURE 3
figure1 = figure('Color',[1 1 1]);
axes1=axes('Parent',figure1,'Color',[111],'YGrid','on','XTickLabel',{'
','[- -]','[+ -]','[- +]','[+ +]','[0 0]','[0 0]',''},'XTick',[0 1 2 3
4 5 6 7],'XGrid','on','FontSize',17);
xlim(axes1,[0 7]);
ylim(axes1,[0 100]);
xlabel('Experiment #','FontSize',15);
ylabel('Yield %','FontSize',15);
box(axes1,'on');
hold(axes1,'all');
bar1=bar(y1,'BarWidth',0.6,'Parent',axes1);
set(bar1(1),'FaceColor',[1 0.4 0],'DisplayName','DIH-Synthesis');
set(bar1(2),'FaceColor',[0.039    0.14    0.41],'DisplayName','Imidazole
Iodination');
title('EXPERIMENTAL DESIGN - Batch Small Scale Process ')
legend(axes1,'show');

%% STATISTICAL ANALYSIS
%ALL THE EXPERIMENTS
%1-MEASURES OF CENTRAL TENDENCY
%GEOMETRIC MEAN, MEAN, MEDIAN, MODE
locate =[geomean(y) mean(y) median(y) mode(y)]
locatei =[geomean(yi) mean(yi) median(yi) mode(yi)]
%2-MEASURES OF DISPERSION
%MEAN ABSOLUTE DEVIATION, STANDARD DEVIATION, VARIANCE
stats=[mad(y) std(y) var(y)]
statsi=[mad(yi) std(yi) var(yi)]
%CENTRAL EXPERIMENTS
%1-MEASURES OF CENTRAL TENDENCY
%GEOMETRIC MEAN, MEAN, MEDIAN, MODE
locatecentral     =[geomean(yzeros)     mean(yzeros)     median(yzeros)
mode(yzeros)]
locatecentrali    =[geomean(yzerosi)    mean(yzerosi)    median(yzerosi)
```

```
mode(yzerosi)]
%2-MEASURES OF DISPERSION
%MEAN ABSOLUTE DEVIATION, STANDARD DEVIATION, VARIANCE
statscentral=[mad(yzeros) std(yzeros) var(yzeros)]
statscentrali=[mad(yzerosi) std(yzerosi) var(yzerosi)]

%% MULTIVARIATE REGRESSION
%% Design Matrix Construction
D = fracfact('b a ba');
%Column used to calculate the average response.
run=2^2+2;
I=ones(run,1);
%central experiments
numbercentralexp=2;
Zeros=zeros(numbercentralexp,3);
%% MODEL MATRIX
X1=[D;Zeros];
X=[I,X1]
k2co3=X(:,2);
icl=X(:,3);
%% DISPERSION MATRIX
DIAG=X'*X;
DispersionMatrix=(X.'*X)^(-1);
%% REGRESSION COEFFICIENTS
robustbeta = robustfit(X1,y)
b=regress(y,X)                                %REGRESSION COEFFICIENTS
%%REGRESSION COEFFICIENTS
% DIMETHYLHYDANTOIN IODINATION
% FIGURE 4
figure3=figure('Color',[1 1 1]);
axes1          =          axes('Parent',figure3,'Color',[1          1
1],'YGrid','on','XTickLabel',{'','b1','b2','b12', ''},'XTick',[0 1 2 3
4],'XGrid','on','FontSize',18);
  b1=[b(2:end,1)];
  xlim(axes1,[0 4]);
 ylim(axes1,[-15 20]);
 xlabel('regression coefficient','FontSize',17);
 ylabel('value','FontSize',17);
box(axes1,'on')
hold(axes1,'all');
bar2=bar(b1,'BarWidth',0.2,'Parent',axes1);
set(bar2,'FaceColor',[1 0.4 0]);
title('REGRESSION     COEFFICIENTS     -     Small     Scale     Batch
Process','FontSize',17)
% Normal Probability Plot
```

```
figure4 = figure('Color',[1 1 1]);
b1=[b(2:end,1)]
axes1 = axes('Parent',figure4,'FontSize',18);
xlim(axes1,[-10 2]);
ylim(axes1,[0 1]);
box(axes1,'on');
hold(axes1,'all');
pb1=probplot(b1)
xlabel('Probability','FontSize',17);
ylabel('b','FontSize',17);
title('Probability Plot for Normal Distribution - Dimethylhydantoin
Iodination','FontSize',17
%IMIDAZOLE IODINATION
figure5=figure('Color',[1 1 1]);
axes1          =          axes('Parent',figure5,'Color',[1          1
1],'YGrid','on','XTickLabel',{'','b1','b2','b12', ''},'XTick',[0 1 2 3
4],'XGrid','on','FontSize',18);
b1i=[bi(2:end,1)]
xlim(axes1,[0 4]);
 ylim(axes1,[-10 25]);
 xlabel('regression coefficient','FontSize',17);
 ylabel('value','FontSize',17);
box(axes1,'on');
hold(axes1,'all');
bar2=bar(b1i,'BarWidth',0.2,'Parent',axes1);
set(bar2,'FaceColor',[0.039 0.14 0.41]);
title('REGRESSION COEFFICIENTS - Imidazole Iodination', 'FontSize',17)
% Normal Probability Plot
figure6 = figure('Color',[1 1 1]);
b1i=[bi(2:end,1)]
axes1 = axes('Parent',figure6,'FontSize',15);
xlim(axes1,[-10 2]);
ylim(axes1,[0 1]);
box(axes1,'on');
hold(axes1,'all');
pb1=probplot(b1i)
xlabel('Probability','FontSize',17);
ylabel('b','FontSize',17);
title('Probability   Plot   for   Normal   Distribution   -   Imidazole
Iodination','FontSize',17)
%STANDARD ERROR for the regression coefficients are the square root of
the
%diagonal of the variance-covariance matrix, V
se = sqrt(diag(V))
```

```
%% RESPONSE SURFACE MODEL AND CONTOUR PLOT WITHIN MODEL LIMITS
x1fit = min(k2co3):0.01:max(k2co3);
x2fit = min(icl):0.01:max(icl);
[X1FIT,X2FIT] = meshgrid(x1fit,x2fit);
% RESPONCE SURFACE MODEL
% FIGURE 5
figure7=figure('Color',[1 1 1]);
% DMH IODINATION
subplot(1,2,1)
YFIT1 = b(1) + b(2)*X1FIT + b(3)*X2FIT + b(4)*X1FIT.*X2FIT;
f=mesh(X1FIT,X2FIT,YFIT1)
xlabel('K_2CO_3','FontSize',17)
ylabel('I-Cl','FontSize',17)
zlabel('Yield %  ','FontSize',17)
title ('y_2','FontSize',18)
% IMIDAZOLE IODINATION
subplot(1,2,2)
YFIT1i = bi(1) + bi(2)*X1FIT + bi(3)*X2FIT + bi(4)*X1FIT.*X2FIT;
f= mesh(X1FIT,X2FIT,YFIT1i)
xlabel('K_2CO_3','FontSize',17)
ylabel('I-Cl','FontSize',17)
zlabel('Yield %  ','FontSize',17)
title ('y_6','FontSize',18)
view(50,10)
% CONTOUR PLOT
% FIGURE 6
figure8=figure('Color',[1 1 1]);
% DMH IODINATION
axes1         =         subplot(1,2,1,'Parent',figure8,'YTickLabel',{'-
1','0','+1'},'YTick',[0            100            200],'XTickLabel',{'-
1','0','+1'},'XTick',[0 100 200],'Layer','top','FontSize',17);
xlim(axes1,[-0.1 201]);
ylim(axes1,[-0.1 201]);
box(axes1,'on');
hold(axes1,'all');
xlabel('x_1','FontSize',17);
ylabel('x_2','FontSize',17);
title (' y_2','FontSize',18)
[c,h]=contour(YFIT1,20,'LineWidth',1.5)
    clabel(c)
% IMIDAZOLE IODINATION
axes2         =         subplot(1,2,2,'Parent',figure8,'YTickLabel',{'-
1','0','+1'},'YTick',[0            100            200],'XTickLabel',{'-
1','0','+1'},'XTick',[0 100 200],'Layer','top');
xlim(axes2,[-0.1 201]);
```

```
ylim(axes2,[-0.1 201]);
box(axes2,'on');
hold(axes2,'all');
xlabel('x_1','FontSize',17);
ylabel('x_2','FontSize',17);
title ('y_6','FontSize',18)
[c,h]=contour(YFIT1i,20,'LineWidth',1.5')
    clabel(c)
%% RESPONSE SURFACE MODEL AND CONTOUR PLOT EXTRAPOLATION
x1fite = -2:0.005:2;
x2fite = -2:0.005:2;
[X1FIT,X2FIT] = meshgrid(x1fite,x2fite);
YFIT1e    =    beta(1)    +    beta(2)*X1FIT    +    beta(3)*X2FIT    +
beta(4)*X1FIT.*X2FIT;
% FIGURE 8
figure9=figure('Color',[1 1 1]);
axes1           =           axes('Parent',figure9,'YTickLabel',{'-2','-
1','0','+1','+2'},'YTick',[0  200  400  600  800],'XTickLabel',{'-2','-
1','0','+1','+2'},'XTick',[0           200           400           600
800],'Layer','top','FontSize',17);
xlim(axes1,[-0.1 801]);
ylim(axes1,[-0.1 801]);
box(axes1,'on');
hold(axes1,'all');
[c,h]=contour(YFIT1e,20,'LineWidth',1.5)
    clabel(c)
xlabel('K_2CO_3','FontSize',17)
ylabel('I-Cl','FontSize',17)
title ('Model Extrapolation','FontSize',18)
%% EXPERIMENTS WITH DIFFERENT SOLVENT VOLUMES FOR THE DMH IODINATION
% FIGURE 7
figure10=figure('Color',[1 1 1]);
ydil=[60.77 locatecentral(2) 51.84];
%Create axes
axes7=axes('Parent',figure10,'Color',[111],'YGrid','on','XTickLabel',{
'','7.5','10','12.5',''},'XTick',[0123 4],'XGrid','on','FontSize',17);
 xlim(axes7,[0 4]);
 ylim(axes7,[50 85]);
 xlabel('Volume [mL]','FontSize',12);
 ylabel('Yield %','FontSize',12);
box(axes7,'on');
hold(axes7,'all');
bar1=bar(ydil,'BarWidth',0.3,'Parent',axes7)
set(bar1,'FaceColor',[1 0.4 0]);
title('Different Reaction Volumes')
```

B. MATLAB program for the statistical design and optimization for the up-scaled (10×) batch process

```
%% UP-SCALED BATCH REACTOR
%% EXPERIMENTAL DESIGN AND MULTIVARIATE REGRESSION
 %DATA

z1=[19.32 20.70 22.08];             % K2CO3 quantity [g]
z2=[16.23 17.86 19.48];             % I-Cl quantity [g]
z3=[60 90 120];                     % Addition Time [min]

% Each of the experimental variables was scaled to facilitate the
%calculation of the regression coefficients (Beta)

for i = 1:3
x1(i)=(z1(i)-(z1(1)+0.5*(z1(3)-z1(1))))/(z1(3)-(z1(1)+0.5*(z1(3)-
z1(1))));
end
x1=[x1]

for i = 1:3
x2(i)=(z2(i)-(z2(1)+0.5*(z2(3)-z2(1))))/(z2(3)-(z2(1)+0.5*(z2(3)-
z2(1))));
end
x2=[x2]

for i = 1:3
x3(i)=(z3(i)-(z3(1)+0.5*(z3(3)-z3(1))))/(z3(3)-(z3(1)+0.5*(z3(3)-
z3(1))));
end
x3=[x3]

%% RESPONSES
%Yield of the dimethylhydantoin iodination
% Rese DMH Iodination [%]
y=[62.54;  41.23;  51.92;  41.98;  20.85;  16.94;  38.53;  55.49;  58.25;
55.88 ; 59.49];
% Experiment in the center of the experimental domain responses[%]
yzeros=[58.25; 55.88 ; 59.49];
[m1,n1]=size(y);
% FIGURE 9
figure1 = figure('Color',[1 1 1]);
axes1           =           axes('Parent',figure1,'Color',[1           1
1],'YGrid','on','XTickLabel',{'','1','2','3','4','5','6','7','8','9','
10','11',''},...
```

```
    'XTick',[0    1    2    3    4    5    6    7    8    9    10    11
12],'XGrid','on','FontSize',18);
 xlim(axes1,[0 12]);
 ylim(axes1,[0 70]);
 xlabel('Experiment #','FontSize',17);
 ylabel('Yield %','FontSize',17);
box(axes1,'on');
hold(axes1,'all');
bar1=bar(y,'BarWidth',0.4,'Parent',axes1);
set(bar1(1),'FaceColor',[1       0.8       0],'DisplayName','Imidazole
Iodination');
title('EXPERIMENTAL DESIGN Up-Scaled Batch Process ')

%% STATISTICAL ANALYSIS
 %ALL THE EXPERIMENTS
%1-- MEASURES OF CENTRAL TENDENCY
%GEOMETRIC MEAN, MEAN, MEDIAN, MODE
locate =[geomean(y) mean(y) median(y) mode(y)]
%2--MEASURES OF DISPERSION
%MEAN ABSOLUTE DEVIATION, STANDARD DEVIATION, VARIANCE
stats=[mad(y) std(y) var(y)]
%CENTRAL EXPERIMENTS
%1-- MEASURES OF CENTRAL TENDENCY
%GEOMETRIC MEAN, MEAN, MEDIAN, MODE
locatecentral     =[geomean(yzeros)     mean(yzeros)     median(yzeros)
mode(yzeros)]
%2--MEASURES OF DISPERSION
%MEAN ABSOLUTE DEVIATION, STANDARD DEVIATION, VARIANCE
statscentral=[mad(yzeros) std(yzeros) var(yzeros)]
% MULTIVARIATE REGRESSION
%% Design Matrix Construction
D = fracfact('c b a cb ca ba cba');
%Column used to calculate the average response.
run=2^3+3;
I=ones(run,1);
%central experiments
numbercentralexp=3;
Zeros=zeros(numbercentralexp,7);
%% MODEL MATRIX
X1=[D;Zeros];
X=[I,X1]
%% DISPERSION MATRIX
DIAG=X'*X;
DispersionMatrix=(X.'*X)^(-1);
```

```
k2co3=X(:,2)
icl=X(:,3)
tadd=X(:,4)
%% REGRESSION COEFFICIENTS
robustbeta = robustfit(X1,y)
b=regress(y,X)
[robustbeta,stats] = robustfit(X,y);
stats.w'
% DIMETHYLHYDANTOIN IODINATION
% FIGURE 10
figure5=figure('Color',[1 1 1]);
axes1           =           axes('Parent',figure5,'Color',[1           1
1],'YGrid','on','XTickLabel',{'','b1','b2','b3','b12','b13','b23','b12
3', ''},...
    'XTick',[0 1 2 3 4 5 6 7 8],'XGrid','on','FontSize',18);
b1= b(2:8)
xlim(axes1,[0 8]);
 ylim(axes1,[-10 10]);
 xlabel('Regression Coefficient','FontSize',17);
 ylabel('Value','FontSize',17);
box(axes1,'on');
hold(axes1,'all');
bar2=bar(b1,'BarWidth',0.4,'Parent',axes1);
set(bar2,'FaceColor',[1 0.8 0]);
title('REGRESSION COEFFICIENTS Up-Scaled Batch Process','FontSize',17)
% Normal Probability Plot
figure6 = figure('Color',[1 1 1]);
b1=[b(2:end,1)]
axes1 = axes('Parent',figure6,'FontSize',18);
xlim(axes1,[-10 2]);
ylim(axes1,[0 1]);
box(axes1,'on');
hold(axes1,'all');
pb1=probplot(b1)
xlabel('Probability','FontSize',17);
ylabel('b','FontSize',17);
title('Probability Plot for Normal Distribution','FontSize',18)
%STANDARD ERROR for the regression coefficients are the square root of
the diagonal of the variance-covariance matrix, V
[beta,sigma,E,V] = mvregress(X,y);
beta;
sigma;
E;
V;
se = sqrt(diag(V))
```

```
%%confidence limit of the estimated parameters
Y=y.^2;
SST=sum(Y(:,end));                %Total sum of squares
SSR=b'*X'*X*b;                    %Residual sum of squares
SSE= SST-SSR;                     %Sum of squares errors of prediction
s2=SSE/1
dof= m1-8                              %degrees of freedom = number of
experiments used to estimate 11 model parameters
ErrorVariance=SSE/dof;            %Error variance
Vi=ErrorVariance/m1
StandardError=sqrt(Vi)
tcrit=2.571 ;                        %critical t-value at the 95% level
for five degrees of freedom
ConfidenceLimit= tcrit*StandardError
%% RESPONSE SURFACE MODEL AND CONTOUR PLOT WITHIN MODEL LIMITS
x1fit = min(k2co3):0.01:max(k2co3);
x2fit = min(icl):0.01:max(icl);
x3fit = min(tadd):0.01:max(tadd);
% RESPONCE SURFACE MODEL
% FIGURE 11
figure7 = figure('Color',[1 1 1]);
%x1 vs x2
subplot(1,3,1)
[X1FIT,X2FIT] = meshgrid(x1fit,x2fit);
YFIT1 = b(1) + b(2)*X1FIT + b(3)*X2FIT + b(5)*X1FIT.*X2FIT;
f= mesh(X1FIT,X2FIT,YFIT1)
xlabel('x_1','FontSize',17)
ylabel('x_2','FontSize',17)
zlabel('Yield %','FontSize',17)
title ('K_2CO_3  vs  I-Cl','FontSize',18)
view(50,10)
%x1 vs x3
subplot(1,3,2)
[X1FIT,X3FIT] = meshgrid(x1fit,x3fit);
YFIT2 = b(1) + b(2)*X1FIT + b(4)*X3FIT + b(6)*X1FIT.*X3FIT;
f= mesh(X1FIT,X3FIT,YFIT2)
xlabel('x_1','FontSize',17)
ylabel('x_3','FontSize',17)
zlabel('Yield %','FontSize',17)
title ('K_2CO_3  vs  t_a_d_d','FontSize',18)
view(50,10)
%x2 vs x3
subplot(1,3,3)
[X2FIT,X3FIT] = meshgrid(x2fit,x3fit);
YFIT3 = b(1) + b(3)*X2FIT + b(4)*X3FIT + b(7)*X2FIT.*X3FIT;
```

```
f= mesh(X1FIT,X3FIT,YFIT3)
xlabel('x_2','FontSize',17)
ylabel('x_3','FontSize',17)
zlabel('Yield %','FontSize',17)
title ('I-Cl  vs  t_a_d_d','FontSize',18)
view(50,10)
% CONTOUR PLOT
% FIGURE 12
figure8 = figure('Color',[1 1 1]);
% x1 vs x2
subplot1=subplot(1,3,1,'Parent',figure8,'YTickLabel',{'-
1','0','+1',},'YTick',[0           100           200],'XTickLabel',{'-
1','0','+1'},'XTick',[0 100 200],'Layer','top','FontSize',18);
xlim(subplot1,[-0.1 201]);
ylim(subplot1,[-0.1 201]);
box(subplot1,'on');
hold(subplot1,'all');
xlabel('x_1','FontSize',17);
ylabel('x_2','FontSize',17);
title ('K_2CO_3  vs  I-Cl','FontSize',18)
[c,h]=contour(YFIT1,20,'LineWidth',1.5)
    clabel(c)
% x1 vs x3
subplot2=subplot(1,3,2,'Parent',figure8,'YTickLabel',{'-
1','0','+1',},'YTick',[0           100           200],'XTickLabel',{'-
1','0','+1'},'XTick',[0 100 200],'Layer','top','FontSize',18);
xlim(subplot2,[-0.1 201]);
ylim(subplot2,[-0.1 201]);
box(subplot2,'on');
hold(subplot2,'all');
xlabel('x_1','FontSize',17);
ylabel('x_3','FontSize',17);
title ('K_2CO_3  vs  t_a_d_d','FontSize',18)
[c,h]=contour(YFIT2,20,'LineWidth',1.5)
    clabel(c)
% x2 vs x3
subplot3=subplot(1,3,3,'Parent',figure8,'YTickLabel',{'-
1','0','+1',},'YTick',[0           100           200],'XTickLabel',{'-
1','0','+1'},'XTick',[0 100 200],'Layer','top','FontSize',18);
xlim(subplot3,[-0.1 201]);
ylim(subplot3,[-0.1 201]);
box(subplot3,'on');
hold(subplot3,'all');
xlabel('x_2','FontSize',17);
ylabel('x_3','FontSize',17);
```

```
title ('I-Cl  vs  t_a_d_d','FontSize',18)
[c,h]=contour(YFIT3,20,'LineWidth',1.5)
    clabel(c)
%% RESPONSE SURFACE MODEL AND CONTOUR PLOT EXTRAPOLATION
x1fit = -2:0.005:2;
x2fit = -2:0.005:2;
x3fit = -2:0.005:2;

[X1FIT,X2FIT] = meshgrid(x1fit,x2fit);
 YFIT1 = b(1) + b(2)*X1FIT + b(3)*X2FIT + b(5)*X1FIT.*X2FIT;
[X1FIT,X3FIT] = meshgrid(x1fit,x3fit);
 YFIT2 = b(1) + b(2)*X1FIT + b(4)*X3FIT + b(6)*X1FIT.*X3FIT;
[X2FIT,X3FIT] = meshgrid(x2fit,x3fit);
 YFIT3 = b(1) + b(3)*X2FIT + b(4)*X3FIT + b(7)*X2FIT.*X3FIT;
% FIGURE 13
figure9 = figure('Color',[1 1 1]);
% x1 vs x2
subplot1=subplot(1,3,1,'Parent',figure9,'YTickLabel',{'-2','-
1','0','+1','+2'},'YTick',[0  200  400  600  800],'XTickLabel',{'-2','-
1','0','+1','+2'},'XTick',[0           200           400           600
800],'Layer','top','FontSize',18);
xlim(subplot1,[-0.1 801]);
ylim(subplot1,[-0.1 801]);
box(subplot1,'on');
hold(subplot1,'all');
xlabel('x_1','FontSize',17);
ylabel('x_2','FontSize',17);
title ('K_2CO_3  vs  I-Cl','FontSize',18)
[c,h]=contour(YFIT1,20,'LineWidth',1.5)
    clabel(c)
% x1 vs x3
subplot2=subplot(1,3,2,'Parent',figure9,'YTickLabel',{'-2','-
1','0','+1','+2'},'YTick',[0  200  400  600  800],'XTickLabel',{'-2','-
1','0','+1','+2'},'XTick',[0           200           400           600
800],'Layer','top','FontSize',18);
xlim(subplot2,[-0.1 801]);
ylim(subplot2,[-0.1 801]);
box(subplot2,'on');
hold(subplot2,'all');
xlabel('x_1','FontSize',17)
ylabel('x_3','FontSize',17)
title ('K_2CO_3  vs  t_a_d_d','FontSize',18)
[c,h]=contour(YFIT2,20,'LineWidth',1.5)
    clabel(c)
% x2 vs x3
```

```
subplot3=subplot(1,3,3,'Parent',figure9,'YTickLabel',{'-2','-
1','0','+1','+2'},'YTick',[0  200  400  600  800],'XTickLabel',{'-2','-
1','0','+1','+2'},'XTick',[0           200           400           600
800],'Layer','top','FontSize',18);
xlim(subplot3,[-0.1 801]);
ylim(subplot3,[-0.1 801]);
box(subplot3,'on');
hold(subplot3,'all');
xlabel('x_2','FontSize',17);
ylabel('x_3','FontSize',17);
title ('I-Cl  vs  t_a_d_d','FontSize',18)
[c,h]=contour(YFIT3,20,'LineWidth',1.5)
    clabel(c)
%% Further extrapolation
x2fit = -2.5:0.005:2.5;
x3fit = -2.5:0.005:2.5;
[X2FIT,X3FIT] = meshgrid(x2fit,x3fit);
YFIT3 = b(1) + b(3)*X2FIT + b(4)*X3FIT + b(7)*X2FIT.*X3FIT;
% FIGURE 15
figure10=figure('Color',[1 1 1]);
subplot3=axes('Parent',figure10,'YTickLabel',{'-2.5','-2','-
1','0','+1','+2','+2,5'},'YTick',[0    100    300    500    700    900
1000],'XTickLabel',{'-2.5','-2','-1','0','+1','+2','+2,5'},'XTick',[0
100 300 500 700 900 1000],'Layer','top','FontSize',18);
xlim(subplot3,[-0.1 1001]);
ylim(subplot3,[-0.1 1001]);
box(subplot3,'on');
hold(subplot3,'all');
xlabel('x_2','FontSize',17);
ylabel('x_3','FontSize',17);
title ('I-Cl  vs  t_a_d_d','FontSize',18)
[c,h]=contour(YFIT3,20,'LineWidth',1.5)
    clabel(c)
```

C. MATLAB program for calculation of flow reactor parameters

```
%% REACTOR SIZING
%DATA
L=1600;                 %[mm] length
D=10;                   %[mm] Internal diameter
r=D/2;                  %[mm] Internal radius
N=85;                   %[]   Discs Numbers
s=4;                    %[mm] Discs Thickness
d=1.3;                  %[mm] Distance between discs
dp=6;                   %[mm] Piston diameter
rp=dp/2;                %[mm] Piston radius
```

```
% Internal reactor surface area
A= 2*pi*r^2*L;
% Volume
Vtot= pi*r^2*L;          %[mm^3] Total Volume
Vdisc= pi*r^2*s;         %[mm^3] Disc Volume
Vtotdisc=Vdisc*N;        %[mm^3] Total discs Volume
lp=L-s*N;                %[mm^3] Piston length
Vp= pi*rp^2*lp;          %[mm^3] Total piston Volume

Vnet=Vtot-Vtotdisc-Vp;   %[mm^3] Total Volume Available
Vnetl=Vel*1e-3;          %[ml]   Units conversion

VrmixWhite=Vnetl*2/3;       %[ml] Volume of reservoir#1
VrmixBlu=Vnetl/3;           %[ml] Volume of reservoir#2
time=[1 2 3 4 4.5 5 6 6.5 8 9 10 15 20 25 30 35 40 45 50 55 60];
%[min]

flow=[];
flow=Vnet./time       %[ml/min] flow setted with each pump
flow1=[];
flow1=VrmixWhite./time     %[ml/min] flow setted with pump#1
flow2=[];
flow2=VrmixBlu./time       %[ml/min] flow setted with pump#2
%table
n=length(time)
% FIGURE
plot(flow)
for i= 1:1:n
       dat(i,:)=[time(i), flow1(i), flow2(i), values1(i), values2(i)];
end
f2 = figure('Position',[200 200 400 150]);
cnames = {'Time [min]','Flow#1 [ml/min]','Flow#2 [ml/min]','SetPump#
```

D. MATLAB PROGRAM for the flow rate calibration of feeding pumps

Pump#1

```
% Pump#1 : CALIBRATION CURVE
V1= 5;     %[ml]
set1=[ 0.7 1.7 2.7 3.7 4.7 5.7 6.7 7.7 8.7 9.7 10.7];   %[%]
t1=[5.12 1.8 1.41 0.7 0.51 0.47 0.35 0.31 0.28 0.25];  %[min]
f1=V1./t1
fl1=[0 f1]
% interpolation
xifl1=flow1;
```

```
x=0:0.1:20;
pp=pchip(fl1,set1);
values1=fnval(pp,xifl1);
curve=fnval(x,pp);
figure(1)
plot(set1,fl1,curve,x);
```

Pump#2

```
% Pump#2 : CALIBRATION CURVE
V= 10 ;     %[ml]
set2=[ 0 1 2 3 4 5 6 7 8 9 10];   %[%]
t2=[16.05 8.51 5.58 4.05 3.11 2.55 2.06 1.7 1.52 1.44];  %[min]
f2=V./t2
fl2=[0 f2]
% interpolation
xifl2=flow2;
x=0:0.1:7;
pp=pchip(fl2,set2);
values2=fnval(pp,xifl2);
curve=fnval(x,pp);
figure(3)
plot(set2,fl2,curve,x);
```

E. MATLAB program for graphical presentation of results from flow short-run experiments

```
%% DIFFERENT RESDENCE TIME
yield=[33.72 57.7 51.66 58.72 53.99];
time= [4 6 7.5 9 12],
%% CENTRAL EXPERIMENT RESIDENCE TIME=9 [MIN]
ycentral=[58.72 59.51 61.27 56.74 58.95];
%% STATISTICAL PARAMETERS
locate     =[geomean(ycentral)     mean(ycentral)     median(ycentral)
mode(ycentral)];
stats=[mad(ycentral) std(ycentral) var(ycentral)];
% FIGURE 17
figure1 = figure('Color',[1 1 1]);
axes1          =          axes('Parent',figure1,'Color',[1          1
1],'YGrid','on','XTickLabel',{'','4','6','9','12',''},...
    'XTick',[0 1 2 3 4 5 ],'XGrid','on','FontSize',12);
 xlim(axes1,[0 5]);
 ylim(axes1,[0 70]);
 ylabel('Yield %','FontSize',12);
box(axes1,'on');
hold(axes1,'all');
bar1=bar(time,'BarWidth',0.3,'Parent',axes1);
```

```
set(bar1(1),'FaceColor',[0.6 0 0]);
title('Residence Time Variation - MJOD Reactor ','FontSize',17)
E=[stats(3) stats(3) stats(3) stats(3)];
errorbar(time,E,'xk', 'LineWidth',2)
% Remove NaN values and warn
nanMask1 = isnan(xdata1(:)) | isnan(ydata1(:));
if any(nanMask1)
    warning('GeneratedCode:IgnoringNaNs', ...
        'Data points with NaN coordinates will be ignored.');
    xdata1(nanMask1) = [];
    ydata1(nanMask1) = [];
end
% Find x values for plotting the fit based on xlim
axesLimits1 = xlim(axes1);
xplot1 = linspace(axesLimits1(1), axesLimits1(2));
fitResults1 = polyfit(xdata1, ydata1, 2);
% Evaluate polynomial
yplot1 = polyval(fitResults1, xplot1);
% Plot the fit
fitLine1            =            plot(xplot1,yplot1,'k','DisplayName','
quadratic','Parent',axes1,...
    'Tag','quadratic',...
    'LineWidth',1);
%% FURTHER EXPERIMENTS : MODEL EVALUATION
% MODEL SHORT TIME EVALUATION: Residence time 9 [min], DMH 50[mmol],
I-Cl
%110[mmol], K2CO3 140[mmol], H2O 100[mL]
% x = [4min 6min 7.5min 9min 9min 9min 9min 9min 25∞C 100EtOAc IClHP
I3CL 12min 0V 10V 5V 15V 7.5 min]
  y = [33.72  57.71  56.49  58.72  59.51  61.27  56.74  58.95  18.98  65.45
56.50 NaN 53.99 9.84 60.33 59.01 74.33 71.19 51.66]
%% COMPARISONS
% Create figure
% FIGURE 19
figure1 = figure('Color',[1 1 1]);
%% ICl
% Create subplot
subplot1                                                                =
subplot(1,3,1,'Parent',figure1,'XTickLabel',{'','LP(rif)','HP',''},'Fo
ntSize',15);
Icl=[locate(2) y(11)]
xlim(subplot1,[0 3]);
ylim(subplot1,[0 70]);
box(subplot1,'on');
hold(subplot1,'all');
```

```
% Create xlabel
xlabel('I-Cl Quality','FontSize',12);
% Create ylabel
ylabel('Yield %','FontSize',12);
title('I-Cl Quality Effect','FontSize',17)
% Create stem
bar1=bar(Icl,'BarWidth',0.3,'Parent',subplot1);
set(bar1(1),'FaceColor',[0.6 0 0]);
E=[stats(3) stats(3)];
errorbar(Icl,E,'xk', 'LineWidth',2)
%% DILUITION
% Create subplot
subplot2     =     subplot(1,3,2,'Parent',figure1,'XTickLabel',{'','50
(rif)','100 ','100', ''},'FontSize',15);
EtOAc=[locate(2) y(10) 62.18]
xlim(subplot2,[0 4]);
ylim(subplot2,[0 70]);
box(subplot2,'on');
hold(subplot2,'all');
% Create xlabel
xlabel('EtOAc Volume [mL] ','FontSize',12);
% Create ylabel
ylabel('Yield','FontSize',12);
title('EtOAc Volume Effect','FontSize',17)
% Create stem
bar1=bar(EtOAc,'BarWidth',0.3,'Parent',subplot2);
set(bar1(1),'FaceColor',[0.6 0 0]);
E=[stats(3) stats(3) stats(3)];
errorbar(EtOAc,E,'xk', 'LineWidth',2)
%% REACTION TEMPERATURE
% Create subplot
subplot3                                                              =
subplot(1,3,3,'Parent',figure1,'XTickLabel',{'','5(rif)','25[        ∞
C]',''},'FontSize',15);
T=[locate(2) y(9)]
xlim(subplot3,[0 3]);
ylim(subplot3,[0 70]);
box(subplot3,'on');
hold(subplot3,'all');
% Create xlabel
xlabel('Temperature [∞C]','FontSize',12);
% Create ylabel
ylabel('Yield %','FontSize',12);
title('Temperature Effect','FontSize',17)
% Create stem
```

```
bar1=bar(T,'BarWidth',0.3,'Parent',subplot3);
set(bar1(1),'FaceColor',[0.6 0 0]);
E=[stats(3) stats(3)];
errorbar(T,E,'xk', 'LineWidth',2)
% FIGURE 18
%% RESIDENCE TIME 7.5
figure5=figure ('Color', [1 1 1])
axes4                                                                    =
axes('Parent',figure5,'XTickLabel',{'','9(rif)','7.5','7.5',''},'XTick
',[0 1 2 3 4],'FontSize',15);
sette=[locate(2) y(3) y(19) ]
xlim(axes4,[0 4]);
ylim(axes4,[0 65]);
box(axes4,'on');
hold(axes4,'all');
% Create xlabel
    xlabel('Residence Time [min]','FontSize',12);
% Create ylabel
ylabel('Yield %','FontSize',12);
title('Residence Time Effect ','FontSize',17)
% Create stem
bar1=bar(sette,'BarWidth',0.3,'Parent',axes4);
set(bar1(1),'FaceColor',[0.6 0 0]);
E=[stats(3) stats(3) stats(3) ];
errorbar(sette,E,'xk', 'LineWidth',2)
% FIGURE 20
%% PISTON SPEED
%different speeds: comparison of the reaction yield
figure4= figure ('Color', [1 1 1])
axes4                                                                    =
axes('Parent',figure4,'XTickLabel',{'','0','10','70','100','130(rif)',
''},'XTick',[0 1 2 3 4 5],'FontSize',15);
med=(y(17)+y(18))/2;
speed=[y(14) y(16) y(15) med locate(2)];
xlim(axes4,[0 6]);
ylim(axes4,[0 80]);
box(axes4,'on');
hold(axes4,'all');
xlabel('Piston Speed [rpm]','FontSize',12);
ylabel('Yield %','FontSize',12);
title('Piston Speed Effect ','FontSize',17)
bar1=bar(speed,'BarWidth',0.3,'Parent',axes4);
set(bar1(1),'FaceColor',[0.6 0 0]);
E=[stats(3) stats(3) stats(3) stats(3) stats(3)];
errorbar(speed,E,'xk', 'LineWidth',2)
```

```
% Best Experiment repetition
figure3= figure ('Color', [1 1 1])
axes2                                                                    =
axes('Parent',figure3,'XTickLabel',{'','#15','#16',''},'XTick',[0  1  2
3],'FontSize',15);
speed15v=[y(17) y(18)];
xlim(axes2,[0 3]);
ylim(axes2,[0 80]);
box(axes2,'on');
hold(axes2,'all');
xlabel('Piston Speed 100 [rpm]','FontSize',12);
ylabel('Yield [%]','FontSize',12);
bar1=bar(speed15v,'BarWidth',0.3,'Parent',axes2);
set(bar1(1),'FaceColor',[0.6 0 0]);
E=[stats(3) stats(3)];
errorbar(speed15v,E,'xk', 'LineWidth',2)
```

F. MATLAB program for evaluation of set-values for the long time run experiment with the MJOD flow reactor

```
%reaction condition MJOD-reactor long time
time= [6 8 10]*60;                                    %[min]
V=63.33;                                        %[mL]
tr=9;                                           %[min]
flow=V/tr;                                      %[mL/min]
Vsingolareazione1=150;                          %[mL]
Vsingolareazione2=200;                          %[mL]
tsingolareazione1=Vsingolareazione1/flow;       %[min]
tsingolareazione2=Vsingolareazione2/flow;       %[min]
N1=time./tsingolareazione1                       %[-]
N2=time./tsingolareazione2                       %[-]
TheoricalY=18.9;                                %[g]
MeanY1=0.5902;
MeanY2=0.6381;
EffY1=TheoricalY*MeanY1                         %[g]
EffY2=TheoricalY*MeanY2                         %[g]
% Expected product during 8 h
P8h1=EffY1*N1
P8h2=EffY2*N2
% Prediction With oscillating speed 100 [rpm], taking into account the
% benefit reached during the screening phase
Y15V1=0.7276*TheoricalY
one=Y15V1-EffY1
two=one*EffY2/EffY1
Y15V2=EffY2+two
```

```
Y=Y15V2/TheoricalY
P8h1p=Y15V1*N1
P8h2p=Y15V2*N2
```

G. MATLAB program for calculation of environmental parameters

```
%environmental analysis
%DATA
%a*DMH + 2 b*icl + c*H2o + e*AcOEt + f*K2CO3 = p*DIH + w
%a*x + 2.2*b*z + s1 + s2 + base = p*y + w
%molecular weights
a=128.13;
b=162.35;
c=18;
e=98;
f=138;
p=379.5;
% masses involved calculation
molDMH=[0.005 0.05 0.05];
molICls=[0.01 0.10 0.10];
molICl=[0.015 0.11 0.11];
gEtOAc=[8.95 89.5 44.75];
gH2O=[10 100 100];
gK2CO3=[2.070 19.32 19.32];
gDMH=molDMH*a;
gICl=molICl*b;
TM=gDMH+gICl
gDIH=[1.532 12.385 17.05];
gDIHt=molDMH*p
Ww= TM + gEtOAc + gK2CO3 + gH2O - gDIH
W= TM + gEtOAc + gK2CO3 - gDIH
molDIH=[];
molDIH=gDIH./p;
%Preliminary Reaction-Level measures
AE=p/(a+2*b)
diff=((molICl-molICls)./(molICl));
E=gICl.*diff
phi=E./(TM-E)
AEexp=AE./(1+phi)
%Post-Process Reaction-Level Green Measures
yield=[];
yield=(molDIH./molDMH)*100
RME=AEexp.*yield
RME1=gDIH./TM
%Final Process-Level Green Measures
```

```
PMI=(TM + gEtOAc + gK2CO3)./gDIHt
Efactor=PMI-1
MP=100./PMI
PMIw=(TM + gEtOAc + gK2CO3 + gH2O)./gDIHt
Efactorw=PMIw-1
MPw=100./PMIw
PARAMETERS=[PMI;Efactor;MP];
% FIGURE 28
%% PMI
% Create figure
figure1 = figure('Color',[1 1 1]);
%% ICl
% Create subplot
subplot1                                                                =
subplot(1,3,1,'Parent',figure1,'XTickLabel',{'','BSS','BUS','MJOD',''}
,'XTick',[0 1 2 3 4]);
xlim(subplot1,[0 4]);
ylim(subplot1,[0 10]);
box(subplot1,'on');
hold(subplot1,'all');
% Create xlabel
xlabel('Phase of the Development');
% Create ylabel
ylabel('PMI');
% Create stem
stem(PMI,'Marker','.');
%% MP
% Create subplot
subplot2                                                                =
subplot(1,3,2,'Parent',figure1,'XTickLabel',{'','BSS','BUS','MJOD',''}
,'XTick',[0 1 2 3 4]);
xlim(subplot2,[0 4]);
ylim(subplot2,[0 25]);
box(subplot2,'on');
hold(subplot2,'all');
% Create xlabel
xlabel('Phase of the Development');
% Create ylabel
ylabel('MP');
% Create stem
stem(MP, 'Marker', '.');
%% Efactor
% Create subplot
subplot3                                                                =
subplot(1,3,3,'Parent',figure1,'XTickLabel',{'','BSS','BUS','MJOD',''}
```

```
,'XTick',[0 1 2 3 4]);
xlim(subplot3,[0 4]);
ylim(subplot3,[0 10]);
box(subplot3,'on');
hold(subplot3,'all');
% Create xlabel
xlabel('Phase of the Development');
% Create ylabel
ylabel('E-factor');
% Create stem
stem(Efactor,'Marker','.');
%%figure
% Create figure
figure1 = figure( 'Color',[1 1 1]);
% Create axes
axes1 = axes('Parent',figure1,'XTickLabel',{'PMI','E-factor','MP'},...
    'XTick',[1 2 3],...
    'CLim',[1 3]);
box(axes1,'on');
hold(axes1,'all');
% Create multiple lines using matrix input to bar
bar1 = bar(PARAMETERS,'BarWidth',0.6,'Parent',axes1);
set(bar1(1),'DisplayName','Batch Small Scale');
set(bar1(2),'DisplayName','Batch Upscaled Process');
set(bar1(3),'DisplayName','MJOD-Reactor');
% Create legend
legend1 = legend(axes1,'show');
```

H. MATLAB program for economical calculation

```
%ECONOMICAL ANALYSIS
%DATA
%[DMH I-Cl K2CO3 EtOAc DIH]
prices=[0.0732 0.44 0.0422 0.09 14.26];     %euro/g

%numero reazioni=[Small-scale batch   Up-scaled batch   FlowEperiments
8hFlow]
numeroreaction=[19 30 25 22];
grDMH=[0.64; 6.4; 6.4; 6.4];
grICl=[2.43; 17.8; 17.8; 17.8];
grK2CO3=[2.07; 19.32; 19.32; 19.32];
mLEtOAc=[10; 100; 50; 50];
gDIH=[17 280 200 375];
quantity=[grDMH grICl grK2CO3 mLEtOAc];
```

```
tot1=diag(grDMH*numeroreaction);
tot2=diag(grICl*numeroreaction);
tot3=diag(grK2CO3*numeroreaction);
tot4=diag(mLEtOAc*numeroreaction);
totA=[tot1 tot2 tot3 tot4]
productvalue=gDIH*prices(5)
for i= 1:4

tot1(i)=tot1(i)*prices(1)+tot2(i)*prices(2)+tot3(i)*prices(3)+tot4(i)*
prices(4);
end
tot=[tot1]
for i = 1:4
x1(i)=productvalue(i)/tot(i)
end
xa=[x1];
x=[xa; xa]
% FIGURE 29
figure1 = figure('Color',[1 1 1]);
axes1           =           axes('Parent',figure1,'Color',[1           1
1],'YGrid','on','XTickLabel',{'','',''},'XTick',[0      1      2      3
],'XGrid','on','FontSize',17);
 xlim(axes1,[0.5 1.5]);
 ylim(axes1,[0 20]);
 xlabel('Process','FontSize',15);
 ylabel('Times*Input_C_o_s_t','FontSize',15);
box(axes1,'on');
hold(axes1,'all');
bar1=bar(x,'BarWidth',0.6,'Parent',axes1);
set(bar1(1),'FaceColor',[1   0.4   0],'DisplayName','Small-Scale   Batch
process');
set(bar1(2),'FaceColor',[1    0.8    0],'DisplayName','Up-scaled    Batch
process');
set(bar3(3),'FaceColor',[0.6    0    0],'DisplayName','Short-run    Flow
process');
set(bar4(4),'FaceColor',[0.3     0.4     0],'DisplayName','8[h]     Flow
process');
title('RATE OF RETURN ')
legend(axes1,'show');
```

I. Thermal gravimetric analysis TGA Spectrum

Thermal Analysis

date: 16/07/2013 15:30:32

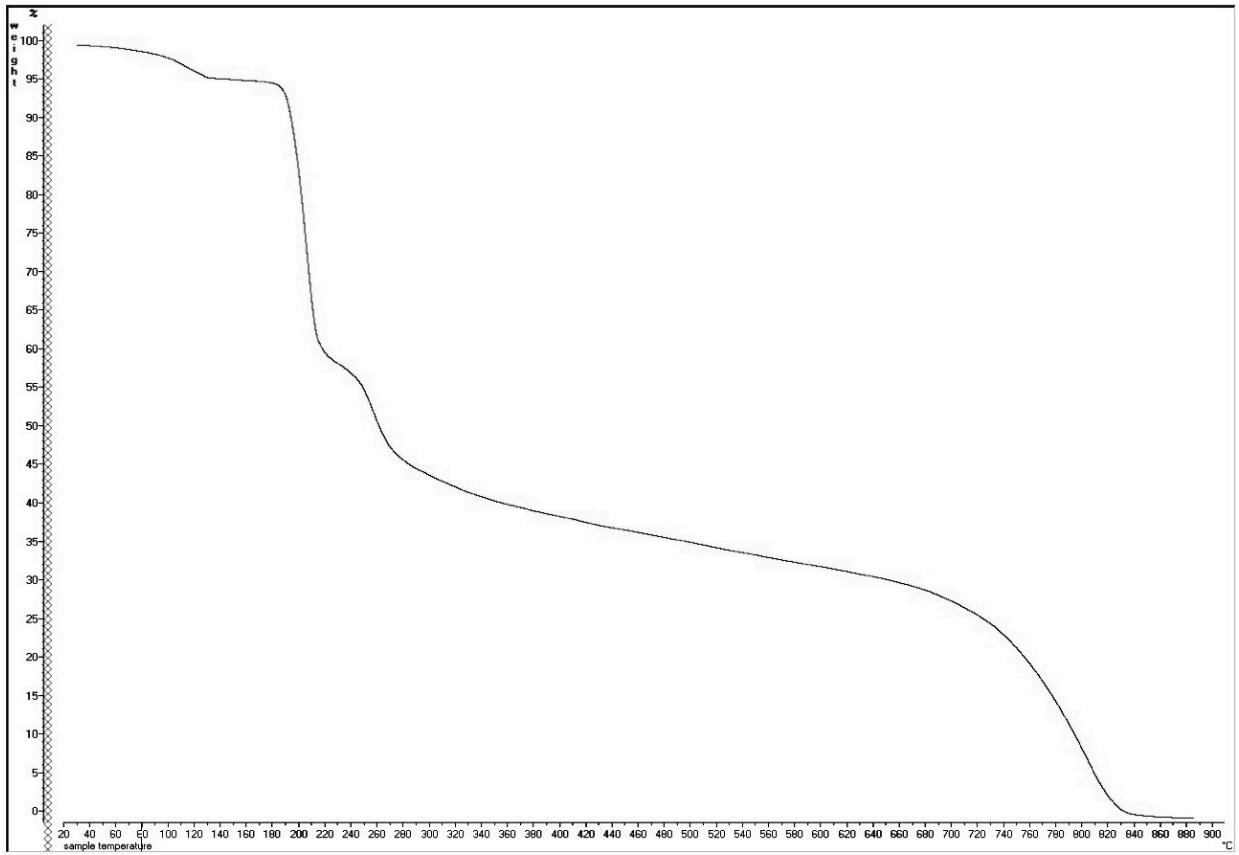

File Name: NIH_15-7.xpd
Run Date: 16/07/2013 12:55:33
Sample ID: NIH_15-7-13
Sample Weight: 15.986 mg
Method Title:
Method Information:

This method contains 2 steps.
1: Iso at 28°C for 10 min, Sample period: 0.5s
2: Scan from 28 to 900°C at 5°C/min, Sample period: 0.5s

J. Infrared spectroscopy FTIR Spectra

1,3-diiodo-5,5-dimethylhydantoin

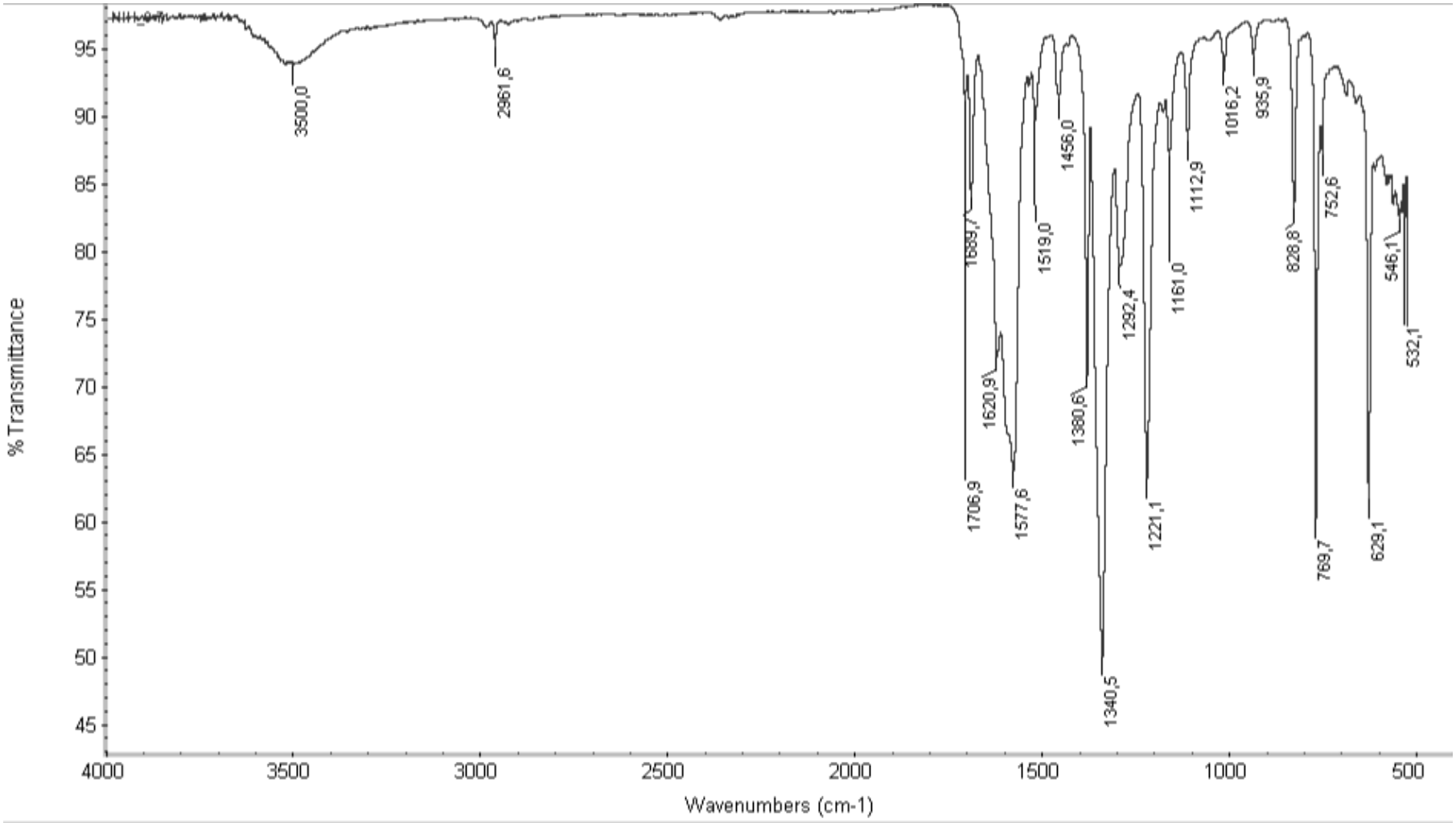

5,5-dimethylhydantoin and 1,3-diiodo-5,5-dimethylhydantoin

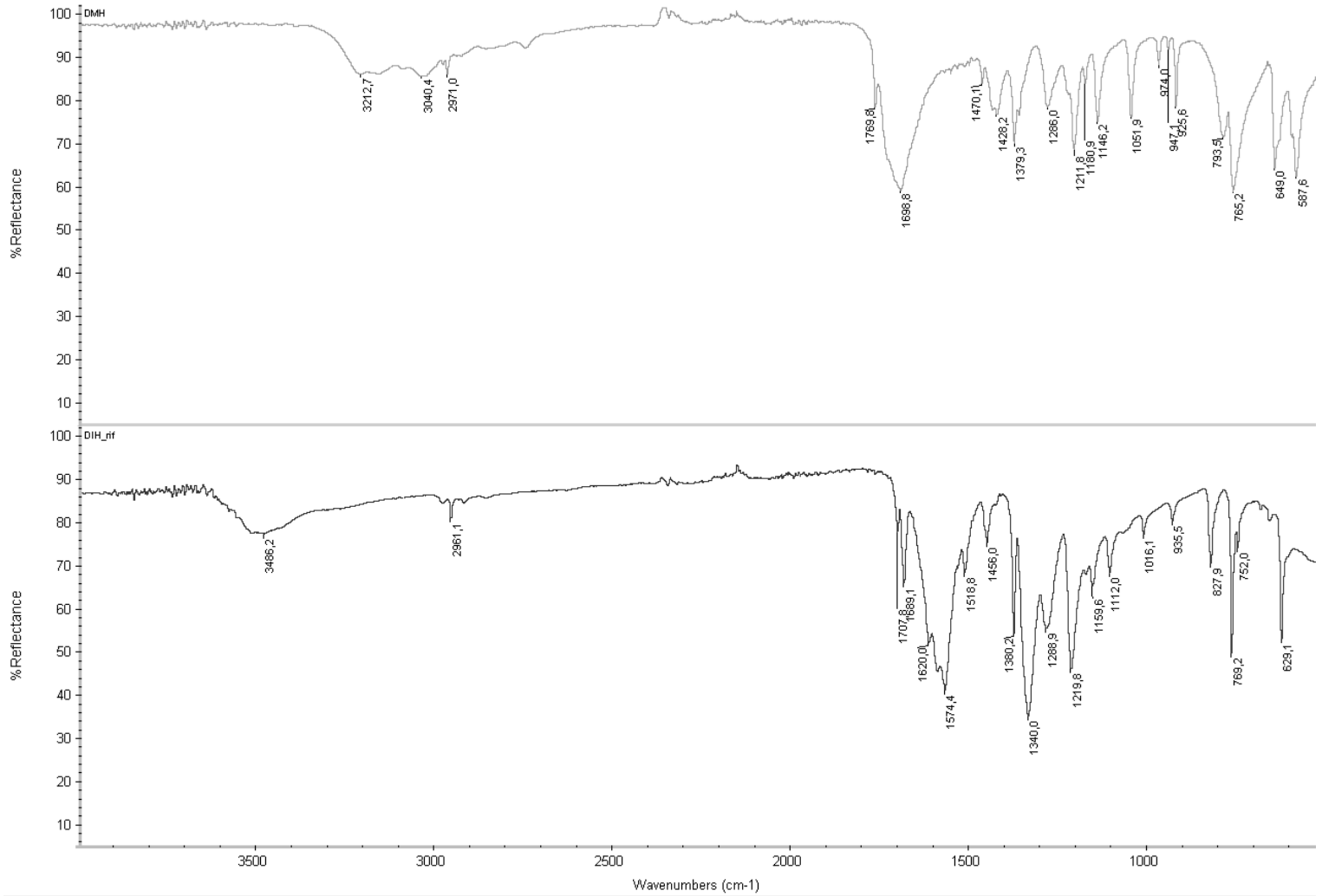

1,3-diiodo-5,5-dimethylhydantoin produced during the Batch processes and with the MJOD reactor

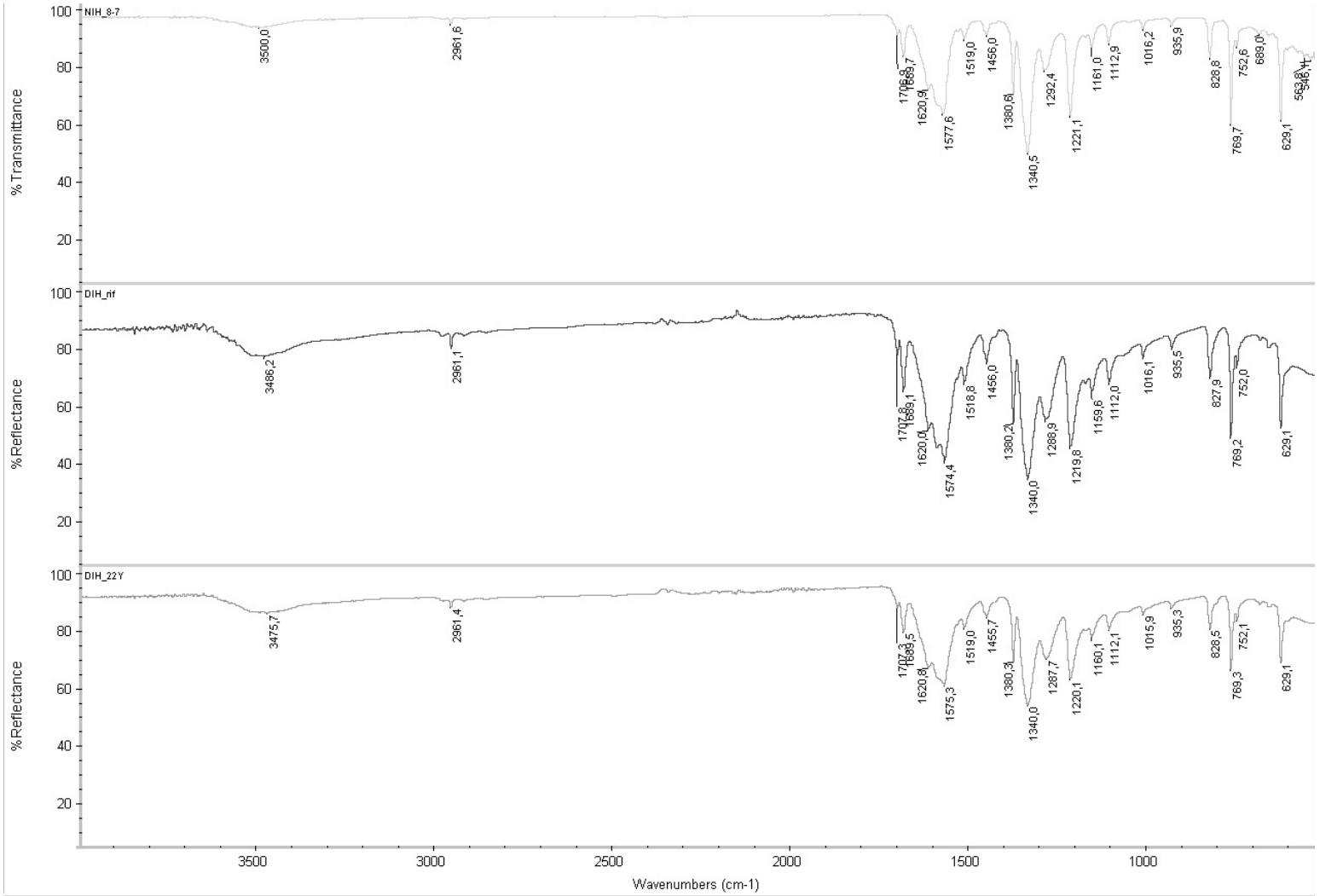

K. Nuclear magnetic response $^{-1}$H NMR spectrum

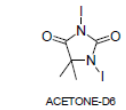

L. Electron spray ionization mass spectrometry ESI+MS Spectrum

Acq. Data Name: MartaFerreri110314_DIH_DART+_2
Internal Sample Id:
Ionization Mode: ESI+ | Orifice1 Volt Sweep: 40V | Spec. Record Interval: 0.8[s]
MS Calibration Name: PEG_ESI+_1000 | Acquired m/z Range: 100.0..1000.0 | Ring Lens Volt: 20[V]
Time of Maximum: 0.192[min]
Reduction History: Determine m/z[Peak Detect[Centroid,50,Area];Correct Base[5.0%]];Average(MS[1] 0.187..0.210)-1.0*Average(MS[1] 0.090..0.133);Correct Base[5.0%]
Experiment Date/Time: 3/11/2014 14:25:07 | Operator Name: Accutof